Adsorption of Volatile and Perfluorinated Compounds from Groundwaters using Granular Activated Carbon

by

David M Kempisty
B.S. Environmental Engineering, Michigan Technological University, 1996
M.S. Environmental Engineering & Management, Air Force Institute of Technology, 2006

A thesis submitted to the
Faculty of the Graduate School of the
University of Colorado in partial fulfillment
of the requirements for the degree of
Doctor of Philosophy
Department of Civil, Environmental and Architectural Engineering
2014

This thesis entitled:
Adsorption of Volatile and Perfluorinated Compounds from Groundwaters Using Granular Activated Carbon

written by David M. Kempisty
has been approved for the
Department of Civil, Environmental and Architectural Engineering

R. Scott Summers (chair)

Karl G. Linden

Fernando L. Rosario-Ortiz

Joann Silverstein

Detlef R. U. Knappe

Date:

The final copy of this thesis has been examined by the signatories, and we find that both the content and the form meet acceptable presentation standards of scholarly work in the above mentioned discipline.

ABSTRACT

Kempisty, David M. (Ph.D. Civil Engineering)

Adsorption of Volatile and Perfluorinated Compounds from Groundwaters Using Granular Activated Carbon

Thesis directed by R. Scott Summers, Professor, Department of Civil, Environmental and Architectural Engineering, University of Colorado at Boulder

The removal of organic contaminants in drinking water processes can be accomplished with a variety of technologies. In particular, the use of granular activated carbon (GAC) has been cited as the best available technology for the removal of 51 of 54 regulated organic contaminants (CFR, 1994). The citation of best available technology is due to GAC's ability to meet today's regulatory standards. The U.S. Environmental Protection Agency is currently considering reducing the maximum contaminant level for a group of up to 16 carcinogenic volatile organic compounds (cVOC). Additionally, another set of organic compounds, perfluorinated alkyl acids (PFAAs), are attracting regulatory attention due to their ubiquitous presence in the environment and persistent, bioaccumulative and toxic properties. Using a variety of groundwaters, this thesis attempts to address whether GAC is a viable treatment technology to meet lower standards for cVOCs or new standards for PFAAs. Waters containing different background matrices of dissolved organic matter (DOM) spiked with low concentrations of cVOCs (0.1 – 50 μg/L) or already containing trace concentrations of PFAAs (16 - 690 ng/L) were treated with GAC using bench-scale flow-through adsorbers. Scale-up

work was accomplished to correlate bench-scale results to full-scale for both groups of compounds.

GAC adsorption capacity for cVOCs was negatively affected by competition in two forms: co-solute competition and DOM competition. Co-solute competition was strongly affected by the similarity in adsorptivites between co-solutes. Grouping co-solutes by their Freundlich adsorption coefficients, co-solutes with similar adsorptivites were found to affect capacity 4-5x more than co-solutes with dissimilar adsorptivites. Output from the Pore and Surface Diffusion Model (PSDM) supported this. DOM negatively affected GAC adsorption capacity for cVOCs to a greater extent. Bed volumes to 10% breakthrough were reduced by an average of 28% when comparing the low-TOC end member water (TOC: 0.3 mg/L) against organic-free water. Larger differences were observed for waters with higher TOC concentrations. Regressions to predict 10% breakthrough were applied to 22 breakthrough curves from four different groundwaters with concentrations of 1,2 dichloroethane (1,2 DCA) spanning 2.5 orders of magnitude. Correlations considered various DOM characteristics as measured by fluorescence, UV spectroscopy, and size exclusion chromatography. The best predictors of bed volumes to 10% breakthrough were Peak C / UV_{340} * 1,2 DCA concentration ($R^2 = 0.82$, n = 22) and Peak C / UV excitation * 1,2 DCA concentration ($R^2 = 0.82$, n = 22). Avoiding the cost and expertise required for fluorescence analysis, a correlation was developed using only UV_{254} absorbance and 1,2 DCA concentration ($R^2 = 0.74$, n = 22). The RSSCT over-predicted GAC capacity for cVOCs by a factor of 1.4 – 2.4. The fouling index (FI) proposed by Corwin (Corwin and Summers, 2010) provided mixed results to correct over-capacity predictions of the RSSCT. Two of four FIs obtained using the 95% CI about a regression developed by Kennedy contained the full-scale capacity (Kennedy, 2013). A correlation relating the ratio of

the influent target organic concentration to TOC concentration was developed during this effort. Results were satisfying; all four FIs obtained using the 95% CI contained the targeted full-scale capacity breakthrough curve.

The effective use of GAC for the removal of PFAAs from groundwater was demonstrated. GAC efficiency was not affected with increasing EBCT indicative of negligible DOM pre-loading occurring as a function of adsorber depth. The RSSCT over-predicted full-scale GAC capacity for PFAA by a factor of 1.7. Scale-up efforts used three independent correlations; all regressions overcorrected RSSCT capacities. Variable full-scale influent concentrations, and unequal influent concentrations between the RSSCT and the full-scale adsorber, are believed to be responsible for scale-up difficulty. CURs were calculated for 20 breakthrough curves from both RSSCT and full-scale adsorbers. The 4 carbon-chained PFBA is the only compound where GAC treatment is in the transition range between practical and unfeasible; seven other PFAA compounds met thresholds for feasibility and GAC treatment should be considered practical.

DEDICATION

To she who writes love on her arms…

ACKNOWLEDGEMENTS

The opportunity provided by the U.S. Air Force to attend a university of my choosing for my PhD was an incredible one. Deciding where and with whom to study was a difficult decision but I don't know that I could have chosen any better than Dr. Scott Summers at the University of Colorado. Scott is a gifted teacher, pragmatic advisor, and a friend who understands the important things in life, specifically family. Thank you for all the solid counsel both professionally and personally.

Entering into the academic world after 15 years in the Air Force makes for a difficult transition. The entire Summers' lab group made that transition much easier with eager assistance and helping hands reacquainting me with lab techniques and academic concepts learned long ago but not frequently used. Special thanks to Dr. Anthony Kennedy and Dr. Julie Korak for all the discussion, insight, and direction with adsorption and fluorescence and so much more. Thank you also to Dorothy Noble, Hyeongki Lee, Leigh Gilmore, Dr. Yaal Lester, Dr. Dave Wagner and the entire crew of CU contemporaries that made each day at CU more enjoyable.

Thanks to all those that served on my committee throughout this process especially Dr. Detlef Knappe and Dr. Fernando Rosario-Ortiz. The prompt and personal attention Detlef provided made him feel more like a second advisor than a geographically separated one. And Fernando, with his dual connection to all things pertaining to environmental organic chemistry and 1.5-year old toddlers, I thank him for our thorough discussions in both arenas.

Regarding toddlers, now full-fledged ruffians, Cameron Piper and Jack Finn have been and continue to be wonderful. Thank you for always enthusiastically greeting Poppy and making me feel like a conquering hero after a difficult day in the RSSCT battlefield. May we enjoy many more days drinking Ultrapure water together.

To my wife and the mother of my children, Carrie: two big thank you's and an I love you. Your continual support and encouragement were always uplifting but moreso, the peace of mind knowing you were taking care of Cameron and Jack was invaluable. You with 101 daily dynamic tasks and me with one large PhD dissertation; I often thought that I was the one with the easier task. A cord of three strands is not easily broken; thank you for being such a great member of our team.

TABLE OF CONTENTS

LIST OF TABLES

LIST OF FIGURES

Chapter 1 Introduction

1.1 Motivation

In March of 2010, then administrator of the U.S. Environmental Protection Agency (EPA), Lisa Jackson, announced that group regulation of contaminants would be explored further to reduce costs of monitoring and improve the protection of the public drinking water systems (EPA, 2010). Group regulation currently occurs for the contaminant classes of disinfection byproducts (e.g., total trihalomethanes and halo acetic acids) and radionuclides (e.g., gross alpha and gross beta). The first group of chemicals to be considered for inclusion in group regulation is carcinogenic volatile organic compounds (cVOCs). Additionally, the congressional mandated 6-year review of Safe Drinking Water Act regulations is considering lowering the maximum contaminant level of eight currently regulated cVOCs. At the same time, under the Contaminant Candidate List 3 (CCL3), eight unregulated cVOCs are being considered for regulatory oversight. These announcements led to a variety of questions. From a toxicological standpoint, are all cVOCs equally weighted? Analytically, are singular or multiple methods available to quantify cVOCs to proposed limits? What is the prevalence of single and multi-cVOC impacted waters and do multi-solute waters behave differently than single solute waters? Finally, from a technological standpoint, is there a viable feasible treatment technology available to meet sub-part-per-billion concentrations. A large portion of this work focuses on the treatment aspect of cVOCs from an adsorption perspective; specifically the use of granular activated carbon (GAC) to remove carcinogenic VOCs from groundwater in the presence of other dissolved organic matter (DOM).

Carcinogenic VOCs found in the environment are generally from anthropogenic sources; there are no significant sources of these compounds found native in the environment. The carcinogenic VOCs selected in this effort are all currently regulated under the Safe Drinking Water Act (e.g., 1,2 dichloroethane (1,2 DCA), carbon tetrachloride (CT), and trichloroethylene (TCE)) or are being considered for regulation and on the current contaminant candidate list (e.g., 1,1 dichloroethane (1,1 DCA)).

1,1 Dichloroethane is a chemical intermediate used in the manufacturing sector and is found in paint removers and as a component in gasoline. 1,2 DCA is chemical intermediate used extensively in the production of plastics and soaps, and as a solvent, and was formerly used in the United States as a fumigant. Carbon tetrachloride is a powerful solvent used in the production of asphalt, chlorinated rubber, and various gums and rosins. It is used as a cleaning agent for a variety of mechanical and electrical equipment and is used in the production of nylon. Trichloroethylene is used in a variety of processes including production and/or cleaning aspects of the plastics, jewelry, automobile, plumbing, textile, paper, glass, and printing industries. The carcinogenic classification of these chemicals are listed in Table 1.1.

Table 1.1 Carcinogenic Classification of Volatile Compounds

cVOC	US EPA Carcinogen Classification (U.S. EPA Integrated Risk Information System)
1,1 Dichloroethane	C - Possible Human Carcinogen
1,2 Dichloroethane	B2 - Probable Human Carcinogen
Carbon tetrachloride	B2 - Probable Human Carcinogen
Trichloroethylene	2A - Suspected Human Carcinogen*

* International Agency for Research on Cancer classification

Best available technologies (BAT) for the removal of cVOCs from water sources are listed in the SDWA. In 2009, an EPA Feasibility Support document reviewed BATs to

determine the potential to achieve concentrations based on new estimated quantitation levels and/or health effects information. GAC was identified as the BAT for 6 of 8 currently regulated cVOCs; the exceptions being dichloromethane and vinyl chloride (EPA, 2009). The EPA report used existing studies to make their conclusions, however, much of the work was done at high concentrations (>1 mg/L). For the eight unregulated cVOCs, GAC was identified as a potential BAT at an AWWA Treatment Workshop but due to limited existing data further studies were recommended (AWWA, 2011b). Determining GAC's ability to remove one or more cVOCs at µg/L and sub-µg/L concentrations from source water containing DOM was an objective of this research.

Perfluoroalkyl acids (PFAAs) are a class of chemicals consisting of a chain of carbon atoms with attached fluorine atoms. The chemical structure of these compounds provides some unique properties including fire resistance and the ability to repel both oil and water. Due to these properties PFAAs can be found in a variety of consumer and industrial products including food packaging, stain repellants, non-stick cookware, lubricants, paints, and fire-fighting foams and have been identified in the environment around the world (Focazio et al., 2008; Kim et al., 2007; Loos et al., 2009). Adverse health effects have been linked with exposure and uptake of PFAAs to include total cholesterol, glucose metabolism, body mass index, thyroid function, infertility, uric acid, lowered immune response to vaccinations and attention deficit/hyperactive disorder (Grandjean et al., 2012; Saikat et al., 2013). Due to these potential health effects and their persistence in human tissue PFAAs are being investigated for regulation (Rahman et al., 2014). Considering PFAAs resistance to degradation in the environment, its relatively high water solubility, and wide-spread detection in waters around the world, determining adequate treatment technologies is timely and prudent. Conventional water treatment technologies have not shown

the ability to substantially remove PFAAs from water (Rahman et al., 2014). Determining GAC's ability to remove PFAAs at ng/L concentrations from source water containing DOM was a second area of research focus.

1.2 Research Objectives and Hypothesis

The overall objective of this effort is to evaluate GAC's ability to remove low concentrations of cVOCs and PFAAs from groundwater. For cVOCs, the degree of GAC adsorption capacity reduction attributable to the presence of other cVOCs and/or DOM is evaluated. Multiple cVOCs have been identified in occurrence studies. The degree to which multiple solutes affect GAC capacity is evaluated with single-solute, bi-solute and tri-solute columns. Groundwater DOM is generally lower in total organic carbon (TOC) content and different in character than a surface water DOM. Studies were carried out to delineate GAC capacity reductions in different groundwaters, a surface water, and in an organic-free water. Scale-up of bench scale results to accurately predict full-scale adsorber performance is of paramount importance if the benefits of the bench-scale adsorbers are to be truly realized. These objectives are addressed in the hypotheses below:

- H-1; GAC capacity for cVOCs is negatively affected by competition from both dissolved organic matter in groundwaters and co-solutes.
- H-2; Characteristics of dissolved organic matter, other than concentration, can be used to predict cVOC adsorption.
- H-3; Bench-scale breakthrough results can be scaled up to predict full-scale adsorber performance.

Early evidence suggests that adsorption with activated carbon may have success as an effective treatment of PFAA impacted waters. Treating both long- and short-chain PFAAs in

groundwater using GAC was explored in this effort. Scale-up of bench-scale results to a full-scale adsorber that operated for 4.8 years was also investigated. The following hypothesis addresses this objective.

- H-4; Adsorption of perfluoroalkyl acids from a groundwater using GAC behaves in a similar manner to cVOC adsorption.

1.3 Scope

The main focus of this effort was on GAC adsorption of cVOCs in natural waters at environmentally relevant concentrations spanning 2.5 orders of magnitude from 0.1 µg/L to 50 µg/L. The cVOCs investigated are all currently regulated under the Safe Drinking Water Act (e.g. 1,2 DCA, carbon tetrachloride, and TCE) or are being considered for regulation and on the current CCL3 (e.g. 1,1 DCA). The cVOCs selected are representative of weak (1,1 DCA and 1,2 DCA), moderate (carbon tetrachloride) and strong (TCE) adsorbing compounds. The source of water for the majority of this study involved groundwater, however for comparison purposes, one surface water and lab-grade organic-free water were included. The rapid small-scale column test (RSSCT) was used simulate full-scale adsorber performance. The RSSCT is designed maintaining similitude with the governing full-scale mass transfer mechanisms. Using GAC with a smaller particle size, RSSCT results can be obtained in a fraction of the time with a smaller volume of water as compared to full- or pilot- scale experimental set-ups. Scale-up of RSSCT results to full-scale adsorber performance was accomplished with existing and new methodologies. Empty bed contact times (EBCTs) of 7.5 minutes and 15 minutes were used to represent using GAC in either a filter-adsorber or post-filter configuration, respectively.

Another focus of this research was assessing the adsorption behavior of PFAAs in groundwaters and making comparisons to cVOC adsorption. The effect of EBCT and the

adsorption capacity associated with GAC particle size were investigated. Carbon use rates were determined for eight different PFAAs at two different EBCTs in both bench-scale and full-scale set-ups. RSSCT results were compared to a full-scale adsorber that operated for 4.8 years and scale-up methodologies were employed. Data is presented from three different EBCTs of 7.5 minutes, 13 minutes, and 26 minutes.

1.4 Thesis organization

This thesis is organized into seven chapters. Chapter 1 provides an introduction and overview. Chapter 2 is dedicated to methodology and is a thorough description of the materials and methods employed throughout this effort. Each subsequent chapter has a smaller materials and methods section, but for the detail required to duplicate any part of this research, Chapter 2 should be consulted. Significant review of the current literature is not included in Chapter 2 but instead apportioned to the later topical chapters so as to create more stand-alone, publishable products. Chapters 3 through 6 are stand-alone chapters each addressing one hypothesis: Chapter 3: Adsorption Competition; Chapter 4: Effect of DOM on 1,2 DCA Adsorption in Groundwaters; Chapter 5: Scale-Up of RSSCT Results to Predict Full-scale Adsorber Performance; Chapter 6: Adsorption of Perfluoroalkyl Acids. Chapter 7 summarizes the findings of the entire effort in the context of the hypotheses discussed above and identifies potential future research initiatives in this subject area. Finally an appendix is included which contains raw data and tables and figures not shown in the body of the thesis.

Chapter 2 Materials and Methods

This chapter is a description of the materials and methods employed throughout this research effort. Each subsequent chapter has a smaller, more concise, materials and methods section but if any portion of this research is meant to be duplicated, this chapter should be consulted.

2.1 Materials

2.1.1 Waters

Four different groundwaters and one surface water were used in the course of this effort. The water quality parameters and designations are shown in Table 2.1.

Table 2.1 Water designations and quality parameters for source waters (four groundwaters, one surface water, and lab-grade deionized water)

Water Designation	Source	pH	TOC (mg/L)	UVA_{254} (cm^{-1})	SUVA (L/mg-m)
CO GW I	GW	7.0	0.3	0.004	1.48
CO GW II	GW	7.8	1.5	0.020	1.35
dilCO GW II	GW	8.2	0.8	0.012	1.53
OH GW	GW	7.8	1.0	0.016	1.55
BEM	SW	6.8	1.5	0.038	2.53
DI Water	DI	6.8	0.1	0.004	-

The first Colorado groundwater (GW) source, designated CO GW I, was collected from a privately-owned 170' deep well in 4-mile canyon in Boulder county, Colorado. After transported to the laboratory, water was aerated via mechanical mixing for at least 30 minutes to oxygenate the water and promote precipitation of dissolved iron in the water. The GW was also allowed to equilibrate with the atmosphere for a period of at least two days but not longer than 7

days before filtered through a 5 μm polypropylene cartridge filter (Culligan Sediment Cartridges; Model P5-145358) and placed into a high density polyethylene (HDPE) storage drum until needed for experimental use.

The second and third GWs came for another site in Boulder County, Colorado where water was extracted from two 600' deep wells in the Laramie-Fox Hills aquifer. This source provided two different groundwaters for this effort: CO GW II and dilCO II. CO GW II was "as-received" from the wellhead. Diluted CO GW II (dilCO II) was made by combining CO GW II with CO GW II that had passed through a bed of GAC to remove DOM. A 25 mm column of GAC with an EBCT of 8.1 minutes was used to remove DOM from the raw CO GW II. Approximately 140L of water was processed in this manner. The TOC of the processed water was measured to ensure DOM breakthrough had not occurred in the pretreatment GAC bed. The CO GW II and the GAC-treated CO GW II were combined to reduce the TOC from the original 1.5 mg/L in CO GW II to 0.8 mg/L in the dilCO II water. Blended in this manner allowed the desired TOC concentration to be achieved but still maintained the same inorganic content as CO GW II.

The fourth groundwater is an Ohio GW, designated OH GW, and was collected from the Greater Cincinnati Water Works' Bolton Treatment Plant, well #6, in Butler County, Ohio. The OH GW uses the Great Miami Aquifer as its source. The well was always turned on at least 24 hours prior to collecting water for the experiments. OH water was stored at 4°C in a cold room until needed.

The surface water, designated BEM, was collected from the Big Elk Meadows Water Association in Larimer County, Colorado. Water is drawn from Mirror Lake, a low alkalinity source with high TOC (~10-16 mg/L; depending upon season) and processed through a 25 μm

cartridge filter (DGD-7525-20, Pentek Inc., Uppers Saddle River, NJ) before being transported back to the laboratory. In the laboratory the water was processed though a low-pressure reverse osmosis membrane (FILMTEC LE-4040, Dow Chemical Co., Midland, MI). The RO system was run in batch mode; permeate was discharged to a laboratory sink and retentate was recirulated back to the feed water. RO operating parameters were kept constant: feed pressure was 690kPa and a flow rate of 45 L/min was maintained. Permeate flow rates were consistent at approximately 6 L/min. This was continued until the feed water had a conductivity of approximately 600 μS, which equated to a TOC of approximately 75 mg/L. The concentrated BEM extract was then coagulated using aluminum sulfate (~100 mg/L, Macron Fine Chemicals, Avantor Performance Materials, Center Valley, PA) and filtered through a 0.45 μm cartridge filter (Memtrex MNY941CGS, General Electric, Fairfield, CT). Coagulation and filtration reduced the TOC concentration in the BEM concentrate to about 50 mg/L. BEM concentrate was then combined with DI water to achieve a TOC concentration in the product water of 1.5 mg/L The DI water was obtained from a Barnstead Nanopure ultrapure water system (ThermoScientific; Series 2113 by Thermo Fisher Scientific Inc, Waltham, MA). This DI water was both the dilution water for the BEM and the organic-free background matrix for other experimental work discussed in later chapters.

2.1.2 Adsorbents

Norit GAC 400 granular activated carbon from CabotNorit was used for the majority of this research. Norit GAC 400 is virgin bituminous-based GAC and is representative of a range of bituminous-based GACs. The log-mean diameter of the as-received GAC was 0.92 mm (12 x 40 US Standard Sieve). The density of the GAC was determined to be 470 kg/m^3. Characteristics and pore size distribution for Norit GAC 400 is provided in Table 2.2.

Table 2.2 Norit GAC 400 Characteristics and Pore Size Distribution

Base Material	U.S. Sieve Size	Iodine # (mg/g)	Apparent bed density (g/cm^3)	Size Distribution (nm)	Specific Volume (mL/g)	Percentage
Reagglomerated Virgin Bituminious	12 x 40	>1000	0.47	Micropore (<2)	0.39	49.4%
				Mesopore (2-50)	0.13	16.4%
				Macropore (>50)	0.27	34.2%

An additional carbon, Calgon F600, was used in the PFAA portion of this effort. Calgon F600 is an agglomerated bituminous GAC with an apparent bed density of 630 kg/m^3. The log-mean diameter of the as-received F600 was 0.92 mm (12 x 40 US Standard Sieve). Characteristics and pore size distributions are provided in Table 2.3.

Table 2.3 Calgon F600 GAC Characteristics and Pore Size Distribution

Base Material	U.S. Sieve Size	Iodine # (mg/g)	Apparent bed density (g/cm^3)	Size Distribution	Specific Volume (mL/g)	Percentage
Reagglomerated Virgin Bituminious	12 x 40	850	0.63	Adsorption pores (<10nm)	0.32	19.8%
				Transport pores (>10nm)	1.3	80.2%

2.1.3 Adsorbates

Carcinogenic volatile organic compounds were obtained from Sigma Aldrich of St Louis, MO. All cVOCs were *analytical standard* grade and in neat form. For the PFAA portion of this research, water received from the source was already impacted with PFAAs; the water was treated "as-received" with no addition of adsorbates.

cVOCs selected were representative of a range of applicable adsorptivities; two compounds can be classified as weakly adsorbing (1,1 DCA and 1,2 DCA), one compound is

moderately adsorbing (carbon tetrachloride) and one compound is considered to be strongly adsorbing (TCE). Table 2.4 details properties of the compounds used in this effort.

After receiving in neat form, cVOC stock solutions were prepared in 500 mL volumetric flasks at concentrations ranging from 200 µg/mL to 600 µg/mL. Attention was given not to approach a compound's solubility limit. In reality, this was only a consideration with carbon tetrachloride whose solubility is approximately 800 µg/mL. Volumetric flasks were placed on a stir plate for at least 6 hours but not more than 12 hours and then transferred into 2 mL amber gas chromatography vials with zero headspace. Vials containing stock cVOCs were stored at 4°C until needed.

Table 2.4 Properties of adsorbates used in cVOC research

cVOC	Molar Mass g/mol	Molar Volume cm3/mol	Dimensionless Henry's Constant (@10°C; 1 atm)	Freundlich K $(\mu g/g)/(L/\mu g)^{1/n}$	Freundlich 1/n	Solubility (mg/L)	log K_{ow}
1,1 Dichloroethane	99.0	84.2	0.160	64.6	0.706	5040	1.79
1,2 Dichloroethane	99.0	78.2	0.039	129	0.533	8600	1.98
Carbon Tetrachloride	153.8	96.5	0.634	387	0.594	800	2.83
Trichloroethylene	131.4	89.7	0.230	1180	0.484	1280	2.61

2.1.4 Rapid Small-Scale Column Materials

Wetted components used in the experimental set-up consisted of polytetrafluoroethylene (PTFE or Teflon), HDPE, polyvinylidene fluoride (PVDF), ceramic, stainless steel and glass. Either 11 mm glass columns with Teflon caps or 4.76 mm ID Teflon tubing was used as column material. Tubing was either Teflon or stainless steel ¼" OD tubing (Nalgene 890 FEP by Thermo Fisher Scientific Inc, Waltham, MA). Two different pumps were used in this effort. PTFE diaphragm pumps (drive: model # 77521; head: model# 7090-62; Cole-Parmer, Vernon Hills, IL) were used for the majority of the cVOC research effort. Positive displacement pumps

(drive: model # QG50; head: model # RH1-CKC-LF, Fluid Metering Incorporated, Syosset, NY) were used for the PFAA research. The FMI pump was used in limited cVOC experiments. Although an accurate flow rate was able to be maintained, the pump head repeatedly seized causing damage to the ceramic piston and requiring costly repair. Therefore the Cole-Parmer product was found to be superior and used for the majority of experimental set-ups. Other materials used included glass wool pre-filters and 22 L glass carboys to deliver and collect influent and effluent water. The glass wool pre-filters were used both as a support media for the GAC and, in another location of the experimental set-up, as a pre-filter to remove any particulate matter than might cause an increase to pressure inside the column.

2.2 Methods

2.2.1 Total Organic Carbon / Ultraviolet Absorbance /Ferrous and Total Iron / pH / Conductivity / Alkalinity

A Shimadzu TOC-V CSH analyzer (Shimadzu Corp, Kyoto, Japan) using high temperature combustion/non-purgeable organic carbon procedures in accordance with EPA method 415.3 was used for measurement of TOC. Samples were adjusted to a pH < 2 with 6N HCl prior to TOC analysis. Ultraviolet adsorption measurements were measured from 200 nm to 600 nm on a Cary spectrophotometer (Varian Cary Bio 100, Agilent Technologies). A quartz cell with 1 cm path length held the sample contents during analysis. Ferrous and Total Iron was measured with a Hach DR/4000 Spectrophotometer (Hach Company, Loveland, CO) using methods 8146 and 8008, respectively. pH was measured on a Denver Instrument pH meter (Model 220, Denver Instrument, Bohemia, NY) in accordance with American Public Health Association Standard Method (APHA-SM) 4500-H^+. Conductivity was measured using a Hanna portable conductivity meter (HI 991300, Hanna Instruments, Woonsocket, RI) in accordance

with APHA-SM 2510B. Alkalinity was measured using a Hach Digital Titrator (16900-01, Hach Company, Loveland, CO) in accordance with APHA-SM 2320.

2.2.2 Gas Chromatography/Mass Spectrometry

The EPA's Office of Research and Development in Cincinnati, OH performed sample analyses for cVOCs. The Water Supply and Water Resources Division, National Risk Management Research Laboratory used a split-less head space injection method (modified EPA method 524.3) on an Agilent 7890A gas chromatography unit paired with a 5975C mass spectrometer. QA, QC and calibration recommendations from EPA method 524.3 were followed. An 8-point calibration curve was used and a blank or check sample was run every ten samples. Method Reporting Limits were less than 37 ppt for all cVOCs used during experimentation. Duplicate and triplicate samples were collected for between 5% and 10% of the samples collected. Analytical error estimates are provided in the appendix.

2.2.3 High Performance Liquid Chromatography/Mass Spectrometer/Mass Spectrometer

For the PFAA portion of this research, samples were prepared and analyzed by the Colorado School of Mines with isotope dilution using direct injection with liquid chromatography (LC)/tandem mass spectrometry (MS/MS) on an AB Sciex 3200 (AB Sciex, Redwood City, CA). This method is detailed in a previous study (Guelfo and Higgins, 2013). 20% of samples were run in triplicate. Limits of quantification (LOQs) were 20 ng/L for all of the perfluorocarboxylic acids (PFCA), and 10 ng/L for all of the perfluorosulfonic acids (PFSA).

2.2.4 Size Exclusion Chromatography

SEC utilized an Agilent 1220 High-Performance Liquid Chromatography instrument with a Protein Pack column (PT WAT 084-601; Waters Corporation). An Agilent diode array was

used to measure UV_{254} absorbance. The mobile phase included the following buffers: sodium monobasic phosphate (NaH_2PO_4; 0.0024 M), sodium diabasic phosphate ($NaHPO_4$; 0.0016M), and sodium sulfate (Na_2SO_4; 0.025 M). The calibration curve ($R^2 = 0.96$) was generated using polystyrene sulfonates with MWs ranging from 210 to 17,000 Da. Sample conductivities were adjusted prior to analysis to 4.6 – 4.8 mS with the addition of concentrated mobile phase. A 100 µL injection volume was used in the SEC protocol. MWs (both weight-averaged and number-averaged) were determined inputting the sample elution time into the standard curve regression equation.

2.2.5 Fluorescence

Fluorescence analysis was conducted using a Horbia spectrofluorometer (Fluoromax-4, John Yvon Horiba Corporation). Lamp scans and cuvette checks were performed prior to analysis. Excitation wavelengths were from 240 nm to 450 nm in 10 nm increments with a 5 nm slit width. Emission wavelengths were integrated over 0.25 seconds and measured from 300 nm to 560 nm in 2 nm increments with a 5 nm slit width. Fluorescence intensities were measured in the (signal to reference) ratio mode. Instrument specific signal and reference detector correction factors were applied. Inner filtering effects were accounted for using sample UV absorbance data. Raman normalization (excitation: 350 nm; emission: 365 nm – 450 nm) accounted for Raman scattering by subtracting fluorescence observed in DI water blanks. First and second order Rayleigh scattering was removed through masking.

2.2.6 RSSCT Experimental Set-Up

The RSSCT experimental set-up was used extensively in this effort. Process variables including the EBCT and the size of the GAC particle were varied throughout the course of this

research but the overall design remained the same. Equations and fundamentals of the RSSCT are presented below first, followed by the methodology to physically set up the RSSCT.

RSSCTs are bench-scale experiments and use mass transfer relationships from the Diffused Flow Pore and Surface Diffusion Model and the principles of similitude to replicate full-scale adsorption phenomena but do so in a fraction of the time (Berrigan, 2004; Crittenden et al., 1986a; 1987). The mass transfer mechanisms addressed in the DFPSDM account for advection, axial diffusion and dispersion, intraparticle pore and surface diffusion, and mass transfer resistance in the bulk liquid phase (Crittenden et al., 1986a). Further discussion on these mechanisms and their respective mathematical equations and dimensionless numbers has been documented extensively elsewhere (Berrigan, 2004; Corwin, 2012; Crittenden et al., 1987; 1986a; Fotta, 2012; Kennedy, 2013; Mastropole, 2011; Summers et al., 1995). A table summarizing these mechanisms was prepared by Corwin and is presented in Table 2.5. Using GAC of a smaller size and maintaining similitude between the dimensionless parameters responsible for the mass transfer of the target organic in the full- and small-scale columns creates a small column (i.e. RSSCT) that behaves as a full sized column.

Table 2.5 Dimensionless numbers used in the Scaling of the RSSCT

Dimensionless Number	Equation	Used to Match
Pore solute distribution parameter	$Dg = \frac{\varepsilon_p(1-\varepsilon)}{\varepsilon}$	Local equilibrium
Stanton number	$St = \frac{2k_f \cdot L(1-\varepsilon)}{d_p \cdot v_f}$	Film mass transfer
Peclet number	$Pe = \frac{v_f \cdot L}{\varepsilon \cdot D_L\left[0.67 + 0.5\left(\frac{d_p \cdot v_f}{\varepsilon \cdot D_L}\right)^{1.2}\right]}$	Axial dispersion
Pore diffusion modulus	$Ed = \frac{4 \cdot L \cdot Dg \cdot D_L \cdot \varepsilon}{d_p^2 \cdot v_f \cdot \tau}$	Intraparticle mass transfer
ε_p = porosity of the particle ε = porosity of the bed k_f = film mass transfer coefficient L = length of the adsorber		v_f = filter approach velocity d_p = GAC particle diameter D_L = liquid diffusivity of adsorbate τ = tortuosity

Crittenden demonstrated that the ratio of the EBCTs of the small and the large columns could be represented by equation 2.1 (Crittenden et al., 1987):

$$\frac{EBCT_{SC}}{EBCT_{LC}} = \left[\frac{R_{SC}}{R_{LC}}\right]^2 * \left[\frac{D_{LC}}{D_{SC}}\right] \qquad (eqn.\ 2.1)$$

where SC and LC represent the small and large columns, respectively. D is the intraparticle diffusivity of the target organic and R is the radius of the GAC particle. Mathematically, it is the ratio of the GAC particle *sizes* that is important and often times, equation 2.1 is written in terms of the GAC *diameter*. Operationally this may be more convenient as sieve sizes and vendor literature often report GAC *diameter*. For consistency, the particle *radius* will continue to be used throughout this chapter.

Equation 2.2 represents the ratio of GAC particle sizes in large and small columns and is referred to as the scaling factor (SF).

$$SF = \frac{R_{LC}}{R_{SC}} \qquad (eqn.\ 2.2)$$

Empirically it has been shown that the intraparticle diffusivity can decrease with decreasing particle size (Sontheimer et al., 1988). This is due to an increasing tortuosity inside a smaller heterogeneous pore. If the intraparticle diffusivities are related to particle size raised to a diffusivity factor, X, then equation 2.3 can be substituted into equation 2.1 to provide equation 2.4, the RSSCT design equation.

$$\left[\frac{D_{SC}}{D_{LC}}\right] = \left[\frac{R_{SC}}{R_{LC}}\right]^{X} \qquad (eqn.\,2.3)$$

$$\frac{EBCT_{SC}}{EBCT_{LC}} = \left[\frac{R_{SC}}{R_{LC}}\right]^{2-X} \qquad (eqn.\,2.4)$$

Generally, one of two RSSCT designs has been used to simulate full-scale adsorbers. One is the constant diffusivity (CD) design and the other is the proportional diffusivity (PD) design. These designs differ in the scaling of the intraparticle diffusion of the target organic. If the intraparticle diffusivities are equal between the GAC sizes, X = 0 and the CD design equation is produced:

$$\frac{EBCT_{SC}}{EBCT_{LC}} = \left[\frac{R_{SC}}{R_{LC}}\right]^{2} \qquad (eqn.\,2.5)$$

If however, the intraparticle diffusivities are linearly proportional to the GAC size ratios, X = 1 and the PD design equation is produced:

$$\frac{EBCT_{SC}}{EBCT_{LC}} = \frac{R_{SC}}{R_{LC}} \qquad (eqn.\,2.6)$$

Although the CD- and PD-RSSCT designs have been the default for RSSCT experimental work, there is nothing keeping the diffusivity relationship strictly constant (X = 0) or strictly linear (X = 1). Mixed results for target organic breakthrough for both the CD- and PD-RSSCT have been reported (Berrigan, 2004; Corwin and Summers, 2010; EPA, 1996;

Henderson and Cannon, 2011; Kennedy, 2013; Knappe et al., 1997; Mastropole, 2011). The CD-RSSCT seems to predict initial breakthrough of the target organic better than the PD design, while the PD-RSSCT seems to more accurately predict full-scale breakthrough of DOM. Since this effort focuses to a great extent on the effect of groundwater DOM on target organic breakthrough, equation 2.6 and the PD-RSSCT design was used in this effort. Further justifying the use of the PD-RSSCT are the recently developed scaling equations to improve prediction of full-scale GAC capacity (Corwin and Summers, 2010; Kennedy, 2013).

Aside from the EBCT, the other critical design variable in the RSSCT is the hydraulic loading rate. Maintaining external mass transfer similitude between the large and small columns produces an RSSCT of equal length to the large column. This is not ideal, requiring a large volume of water and a high hydraulic loading rate in order to meet the design EBCT. To overcome this, the hydraulic loading rate of the RSSCT can be reduced to a point as long as the Peclet number is greater than or equal to the Peclet number of the large column and thereby ensuring dispersion in the RSSCT doesn't control mass transfer (Crittenden et al., 1987). The Peclet number is the rate of adsorbate transport by advection relative to axial dispersion. Summers demonstrated that maintaining a minimum Reynolds number would ensure internal mass transfer still controlled over external mass transfer and result in shorter PD-RSSCT column lengths (Summers et al., 1995). This adjusted hydraulic loading rate for the PD-RSSCT is represented by equation 2.7 (Summers et al., 1995):

$$v_{SC} = SF * v_{LC} * \left[\frac{Re_{SC,min}}{Re_{LC}}\right] \qquad (eqn. 2.7)$$

Re represents the Reynolds number and is a measure of turbulence in the adsorber. Re_{LC} is the turbulence in the large column and $Re_{SC,min}$ is the minimum turbulence required to

maintain dispersion the mechanical range and ensure that dispersion is not a dominant mechanism. Equations 2.8 and 2.9 were used to calculate Re numbers.

$$Re_{LC} = \frac{d_{p,LC} * v_{LC}}{\varepsilon * k_v} \qquad (eqn. 2.8)$$

$$Re_{SC,min} = \frac{500}{Sc} \qquad (eqn\ 2.9)$$

where $d_{p,LC}$ is the diameter of the GAC particle, v_{LC} is the hydraulic loading rate of the large column, ε is the bed porosity, k_v is the kinematic viscosity and Sc is the Schmidt number and relates fluid viscosity to the target organic bulk liquid diffusion coefficient. The Sc number was calculated with equation 2.10.

$$Sc = \frac{\mu}{D_W} \qquad (eqn. 2.10)$$

where μ is the dynamic viscosity and D_w is the diffusivity of the target organic in water. For this effort, D_w was determined using a small fictitious target organic with a molar volume of 105 cm^3/mol. A copy of the excel spreadsheet used to assist in the RSSCT design is included in the appendix.

Figure 2.1 shows the set-up of a generic RSSCT. The specific design and set-up of the RSSCT-PD was done in accordance with the EPA Manual for Bench- and Pilot-Scale Treatment Studies (EPA, 1996). Using a mortal and pestle, GAC was ground down to a desired U.S. Standard Sieve size of 100 x 200 (or 20 x 60 for the scale-up effort). An automated sieve shaker (Cenco-Meinzer 18480, Central Scientific Company, Chicago, IL) aided in this process. These sizes equate to log-mean diameters of 0.11 mm and 0.49 mm, respectively. Fines were decanted using DI water. The GAC was placed under vacuum for 24 hours or until no visible air bubbles could be seen when agitating the GAC beaker. Using a Pasteur pipette, GAC was transferred to a 4.76 mm ID Teflon column with 2 cm of glass wool inserted into the base to provide support

for the GAC media. For the scale-up work, a Teflon-capped 11 mm glass column (Ace Glass, Vineland, NJ) with 8 cm of 2 mm glass beads and wire screen to support GAC media was used. The ratio of column size to GAC diameter yielded aspect ratios of 44 and 23 for the 0.11 mm and 0.49 mm GAC particle-sized columns, respectively. These ratios are greater than 8 – 10 and thereby eliminate the concern of wall effects (i.e. short-circuiting of water around the media) (Knappe et al., 1999). Glass wool pre-filters were installed to remove any particulate matter from the influent water and avoid any pressure increases to the experimental set-up. Pre-filters were changed out every 7 – 14 days depending upon visual appearance. A stainless steel pressure dampener with pressure gauge was installed for each experimental set-up to avoid pulsing of the influent flow and to aid in detecting pressure increases occurring in the system. An estimate of experimental error for the RSSCT experimental was done by creating and operating two columns under identical conditions and examining results for any differences. Experimental output for the duplicate columns is provided in the appendix.

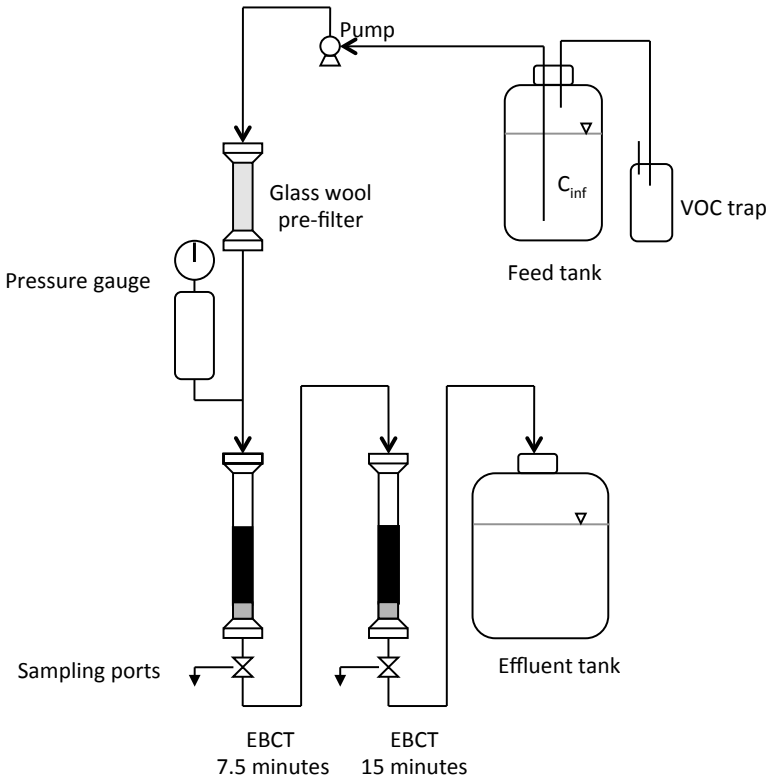

Figure 2.1 Experimental set-up of rapid small-scale column test (RSSCT)

Using stock solutions prepared previously, influent water was spiked to a desired concentration in 22 L glass carboys. A stainless steel stir rod was used to moderately mix the cVOCs into solution with care given not to introduce excessive amounts of air and cause unwanted volatilization. Due to the volatile nature of the contaminants of concern, VOC traps were incorporated into the experimental set-up and are shown in Figure 2.1. VOC traps were spiked at three times the concentration of the influent carboy; this has previously been shown to be an effective measure to minimize volatilization (Corwin, 2010; Fotta, 2012; Kennedy, 2013; Mastropole, 2011).

For each RSSCT, two columns were run in series each with a corresponding GAC mass to produce the desired EBCT for the particular experiment. EBCTs of 7.5, 13 and 15 minutes were designed and operated during this effort. In between the two columns a sampling valve could be installed to collect effluent samples at the shorter EBCT. As there was less pressure in

the shorter column, a needle valve was used to reduce the flow to obtain the correct EBCT. Samples collected after passing through both columns were representative of the longer EBCT. Influent and effluent samples were collected at least every 3 to 4 days, often times more frequently when target organic breakthrough was expected to be occurring. At the time of sampling, the volume of water collected in the effluent carboy was recorded to determine the cumulative throughput of the system.

RSSCT experiments using CO GW I experienced pressure build-up over time. This was thought be caused by the high hardness levels in the groundwater. To relieve pressure, backwashing of the GAC and acid washing of the RSSCT components occurred as needed. GAC would be removed from the column, placed in a 100 mL beaker containing effluent water, and mixed with a Pasteur pipette to simulate backwashing. The GAC would be repacked into the column. Less than 10% bed expansion was noted and would reduce further when the column returned to operation. Simultaneously when repacking the columns, an acid wash of the column tubing and components would be preformed. 6M HCl was added to DI water to achieve a pH of approximately two and recirculated through the RSSCT set-up (with the exception of the GAC and pressure dampener) for 6 – 12 hours. A tap water rinse followed by a DI water rinse was then carried out for a total of 2 more hours. Finally influent water was passed though the tubing for approximately 20 minutes before reassembling the RSSCT with the backwashed GAC. This process reduced pressures in the column from approximately 50-70 psi to approximately 20-30 psi but had to be repeated every other week and sometimes weekly.

2.2.7 Adsorption Modeling

Adsorption Design Software (AdDesignS) from Michigan Technological University provided the modeling capabilities for this effort (Hand and Mertz, 1999). AdDesignS offers

three different models to predict target organic removal using GAC. The Equilibrium Column Model (ECM) is ideally used to determine elution order of compounds in a multi-component mixture, predict the maximum effluent concentrations due to co-solute competition, and determine if some number of compounds in a mixture can neglected to simplify the required mathematic computations without significantly effecting results. The Constant Pattern Homogeneous Surface Diffusion Model (CPHSDM) is only for a single compound but because it can be solved using algebraic equations, avoids complex mathematical solutions. Due to its simplicity, the CPHSDM is ideally suited for early adsorber design. The Pore and Surface Diffusion model (PSDM) is a non-steady state fixed bed model using numerical methods to predicted adsorber performance. The PSDM requires a greater number of input variables (adsorbate characteristics, hydraulic operating parameters, equilibrium and kinetic properties of the target organic, etc) and more calculation time, but provides breakthrough capacity curves for each compound. For this effort, the PSDM was exclusively used.

The PSDM evaluates the 6 mechanisms to approximate GAC capacity in a fixed bed (Crittenden et al., 1986b). Externally, the model accounts for (1) advective flow, (2) axial dispersion and diffusion and (3) mass transfer across the film boundary layer. Internally, both (4) pore and (5) surface diffusion contributions to mass transfer inside GAC pores are addressed. Finally, an equation addressing (6) local equilibrium between the solute in the intraaggregate phase and the adsorbed phase is included. Using dimensionless parameters to create mass balances around the bulk and intraparticle phases, two partial differential equations are developed and linked using a coupling equation between the bulk and adsorbent phases assuming local equilibrium at the surface of the adsorbent (Hand and Mertz, 1999). Using orthogonal collocation, the partial differential equations are converted to ordinary differential equations and

solved using Gears Stiff Method (Hand and Mertz, 1999). Further development of the equations used to describe the mass transfer mechanisms and model mathematics are presented elsewhere by Crittenden and Hand (Crittenden et al., 1986a; 1980; Hand et al., 1989).

Input to the model was based upon normal operation parameters for GAC adsorbers. Corwin demonstrated that intraparticle diffusion is responsible for the majority of mass transfer control in typical water treatment plants (Corwin, 2012). This was confirmed with the hydrodynamics of the adsorber yielding a Biot number greater 50 (Corwin, 2010). The Biot number is the ratio of adsorbate transport by film mass transfer relative to intraparticle mass transfer. Other work has shown that in the presence of DOM, intraparticle diffusion is dominated by pore diffusion and surface diffusion can be considered negligible (Hand et al., 1989). Film mass transfer coefficients were calculated using the correlation of Gnielinski and liquid diffusion coefficients were calculated using the Hayduk and Laudie correlation (Gnielinski, 1978; Hayduk and Laudie, 1974).

Chapter 3 cVOC Adsorption: Competitive Effects of Co-solutes and DOM

3.1 Abstract

The EPA announced plans to regulate up to 16 carcinogenic VOCs (cVOC) as one group (EPA, 2011). Occurrence studies have demonstrated the presence of multiple VOCs co-existing in groundwaters in the United States (Rowe et al., 2007; Toccalino et al., 2010; Zogorski et al., 2006). The interaction between multiple cVOCs in a GAC adsorber can potentially result in earlier breakthrough of target organic and/or effluent concentrations exceeding influent concentrations. Both of these scenarios can have significant implications to treatment processes. The overall objective of this study is to understand the impact of co-solutes and DOM on cVOC breakthrough at low contaminant concentrations. Specifically, the impact of groundwater DOM on cVOC adsorption was evaluated. Competitive interactions between strong, moderate, and weak adsorbing cVOCs were also explored. Finally the utility of the pore and surface diffusion model (PSDM) was evaluated by comparing model output to experimental results.

Competition from both DOM and co-solutes was observed. GAC capacity measured in bed volumes to 50% breakthrough was reduced by 20% and 31% for the 7.5 minute and 15-minute EBCT columns when comparing background matrices of a natural water (TOC: 0.3 mg/L) to organic-free water. Greater capacity reductions were seen in a third, higher TOC water (TOC: 1.5 mg/L). Co-solute competition was observed but to a lesser extent. Grouping co-solutes by their Freundlich adsorption coefficients, co-solutes with similar adsorptivities were found to affect capacity 4-5x more than co-solutes with dissimilar adsorptivities. Displacement competition caused by both DOM and co-solutes was observed. Immediately after breakthrough,

columns with background matrices of DI had between 0% and 4% displacement, while DOM-containing columns exhibited greater displacement (6% - 17%). Co-solute competition occurred with 1,2 DCA solid-phase concentration reductions of 3-5% occurring in organic-free water after addition of TCE. Indicative of DOM competition, the displacement increased to 12–57% in a column with a natural water background matrix.

DOM is not considered in the PDSM, and therefore, the model was limited to analysis of single solute and co-solute interactions in organic-free water. The PSDM predicts the solid-phase concentration of a target organic before co-solute addition well (within ~8% of experimental results). The model was useful in elucidating the effects on capacity of weak, moderate, and strong co-solutes. Kinetically the model had difficulty predicting displacement as a function of throughput.

3.2 Introduction

About 105 million people in the United States – over 1/3 of the population - receive their drinking water from public systems that use groundwater as their source (Toccalino et al., 2010). Over 19% of the groundwater samples from 3,498 wells sampled in a USGS study contained VOCs at a concentration of 0.2 µg/L or greater (Zogorski et al., 2006). Of 98 aquifers investigated, 90 of them contained VOCs (EPA, 2011; Zogorski et al., 2006). Another study detected VOCs in 60% of 833 groundwater samples that are used as source water (Rowe et al., 2007; Toccalino et al., 2010; Zogorski et al., 2006). Often times multiple VOCs are found. One data query revealed 8%, 6%, 4%, and 22% of 335,000 samples had TCE co-occurring with 1,2 dichloroethane, 1,2 dichloropropane, PCE, and vinyl chloride, respectively (AWWA, 2011b; Toccalino et al., 2010). Admittedly the author notes that the data evaluated *samples* and not individual sources or systems, but the point is that co-occurrence of cVOCs in groundwater does

occur and investigation of cVOC competition between co-solutes deserves merit. If competition is causing displacement and concentrations greater than the influent appear in the effluent, regulatory compliance may be in jeopardy. If competition is causing capacity reductions, earlier initial breakthrough of contaminant will result in more frequent GAC change-outs. Both experimental and modeling work has been previously accomplished on multicomponent systems but not at the sub-µg/L concentration range and not specifically with cVOCs in groundwater.

The overall objective of this study is to understand the impact of co-solutes and DOM on cVOC adsorption at low contaminant concentrations. Using different groundwaters as the background matrix, the cVOC adsorption as a function of DOM type and concentration was evaluated. The effect of influent waters containing multiple cVOCs versus a single cVOC was explored. Finally, the ability of the pore and surface diffusion model to predict experimental observations was investigated.

3.3 Background

Competition can result in both reduced GAC capacity for target organics and scenarios were effluent concentrations exceed influent concentrations. Reduced capacity is due to sorption of other, non-target, organics. Hereafter the type of competition will be referred to as "DOM competition". Reduced capacity for target organics can also be affected by a co-solute; one co-solute will out-compete another resulting in reduced capacity for both co-solutes. For the remainder of this chapter, this type of competition will be referred to as "co-solute competition". Caused by both DOM and co-solutes, a third classification of competition occurs when the effluent concentration exceeds the influent concentration. This type of competition will be referred to as "displacement competition". The components responsible for displacement competition, DOM or a co-solute, are the same as the other two types of competition; however,

the observation of it in experimental results (C_{eff}/C_0 >1) and the experimental design to test for it are different, and therefore its separate category. Hereafter C_{eff}/C_0 will be referred to as C/C_0.

3.3.1 DOM competition

Reduced capacity for target organics in the presence of DOM has been demonstrated at higher TOC concentrations and/or in surface waters (Corwin, 2012; Hand et al., 1989; Jarvie et al., 2005; Kennedy, 2013; Sontheimer et al., 1988; Speth, 1991; Summers et al., 1989; Zogorski et al., 2006). DOM competitive effects were investigated with two different waters: organic-free deionized water and a low TOC (0.3 mg/L) Colorado groundwater. Single solute experiments with low cVOC concentrations were run in each water and capacity comparisons were made to discern the differences caused by the presence of DOM.

3.3.2 Co-solute competition

The adsorption of target organics can be impacted by the presence of other competing co-solutes. In this effort, both single solute and co-solute experiments were conducted in organic-free water and two different Colorado groundwaters. Breakthrough results from the single solute column were compared with the multi-component columns and capacity and kinetic differences were investigated. The PSDM was also used to predict single and co-solute behavior in the GAC column.

3.3.3 Displacement competition

One indicator of competition between adsorbates is the observation of effluent concentrations from a GAC adsorber exceeding influent concentrations. This phenomenon is called displacement and can occur when competing adsorbates (either DOM or another target organic) are introduced into an absorber. A weaker adsorbing compound will travel through an

adsorber faster than a more strongly adsorbing compound. When the stronger compound reaches further into the GAC bed, it will compete with the (previously adsorbed) weaker compound for an adsorption site and may displace the weaker compound. This results in an effluent containing both the mass of the influent and the mass of the displaced compound and results in an normalized effluent concentration (C/C_0) greater than 1. This phenomenon is also called the chromatographic effect.

Theoretically there is no difference between simultaneously introducing multiple chemicals into a column or introducing competing compounds step-wise. When chemicals are introduced simultaneously, separate mass transfer zones are established (e.g. MTZ1 and MTZ2). MTZ1 contains both contaminants but a portion of MTZ2 contains only the weaker absorbing (and faster traveling) compound. As MTZ1 moves through the column, the stronger absorbing contaminant may outcompete the weaker absorbing compound and cause desorption. When this occurs effluent concentrations can exceed influent concentrations and displacement is occurring. If competition is not occurring, displacement will not be observed.

Alternatively, when introduced subsequently one after another, the adsorber will be operated until a compound has exhausted the GAC bed capacity and has completely broken through. Then a second compound would be introduced to the adsorber. If competition is occurring, displacement of the first compound will be observed in the effluent as the second compound moves through the GAC bed. Concentrations of the second absorbing chemical can be incrementally increased until a displacement is observed. For this effort, both simultaneous and incremental cVOC loading were used to investigate displacement competition. The PSDM will be used to predict displacement with both cVOC delivery methods.

3.4 Materials and Methods

3.4.1 Materials

3.4.1.1 Waters

Groundwater was collected from two different groundwater sources in Colorado. The first Colorado groundwater (GW) source, designated CO GW I, was collected from a privately-owned 170 foot well in 4-mile canyon in Boulder County, CO. The second Colorado GW source, designated CO GW II, was from another site in Boulder County and extracted from two 600' deep wells in the Laramie-Fox Hills aquifer. Both waters were aerated via mechanical mixing for at least 30 minutes to oxygenate the water and promote precipitation of dissolved iron in the water. The GW was also allowed to equilibrate with the atmosphere for a period of at least 2 days but not longer than 7 days before filtered through a 5 μm polypropylene cartridge filter (Culligan Sediment Cartridges; Model P5-145358) and placed into a HDPE storage drum until needed for experimental use. Properties for the water are described in Table 2.1. Deionized water was obtained from a Barnstead Nanopure water purification unit by Thermo Fisher Scientific Inc.

3.4.1.2 Adsorbates

Carcinogenic volatile organic compounds were obtained from Sigma Aldrich of St Louis, MO. All cVOCs were *analytical standard* grade and in neat form. The cVOCs were selected to represent a range of applicable adsorbtivities; two compounds can be classified as weakly adsorbing (1,1 dichloroethane and 1,2 dichloroethane), one compound is moderately adsorbing (carbon tetrachloride) and one compound is considered to be strongly adsorbing (trichloroethylene). Table 2.4 provides properties of the compounds researched in this effort.

3.4.1.3 Adsorbents

Norit GAC 400 granular activated carbon from CabotNorit was used for this effort. Norit GAC 400 is virgin bituminous-based GAC and is representative of a range of bituminous-based GACs. The log-mean diameter of the as-received GAC was 0.92 mm (12 x 40 US Standard Sieve). The density of the GAC was determined to be 470 kg/m^3. Pore size distribution for Norit GAC 400 are given in Table 2.2.

3.4.2 Methods

3.4.2.1 Analytical QA/QC

The EPA's Office of Research and Development in Cincinnati, OH performed sample analyses for cVOCs. The Water Supply and Water Resources Division, National Risk Management Research Laboratory used a split-less head space injection method (modified EPA method 524.3) on an Agilent 7890A/5975c GC/MS for cVOC analyses. QA, QC and calibration recommendations from EPA method 524.3 were followed. An 8-point calibration curve was used and a blank or check sample was run every ten samples. Limits of detection for the cVOCs of interest are located in the appendix.

3.4.2.2 RSSCT set-up

The specific design and set-up of the RSSCT-PD was done in accordance with the EPA Manual for Bench- and Pilot-Scale Treatment Studies (EPA, 1996); for the sake of brevity a summary overview is provided here. RSSCTs used GAC 400 by Norit, a bituminuous coal based GAC. Using a mortal and pestle, GAC was ground down to a sieve size of 100 x 200 (US Standard Sieve Size) equating to a log-mean diameter of 0.11 mm. Fines were decanted using DI water. The GAC was placed under vacuum for 24 hours or until no visible air bubbles could be seen when agitating the GAC beaker. Using a Pasteur pipette, GAC was transferred to a 4.76

mm ID Teflon column with glass wool inserted into the base to provide support for the GAC media. The ratio of Teflon column size to GAC diameter provided an aspect ratio of 44 and thereby eliminated the concern of wall effects (i.e. short-circuiting of water around the media). Two columns were run in series: the first contained 0.76 g of GAC and the second contained 1.52 g of GAC. Operated at a flow rate of 2.0 mL/min produced equivalent full-scale EBCTs of 7.5 min and 15 min, respectively. Influent and effluent samples were collected 1 to 2 days.

3.4.2.3 Sample preparation and analysis

All samples were collected headspace free in 40 mL glass VOC vials. Samples were preserved to a pH <2 with 6N HCl. All attempts were made to complete analysis within 30 days of collection, although some samples exceeded this holding time. Analysis was conducted using a headspace methodology on a Agilent 7890A gas chromatography unit paired with a 5975C mass spectrometer. Method Reporting Limits were less than 37 ppt for all cVOCs discussed within this chapter.

3.4.2.4 Adsorption Modeling

Adsorption Design Software (AdDesignS) from Michigan Technological University provided the modeling capabilities for this effort (Hand and Mertz, 1999). Different models can be selected within the AdDesignS software but for this effort the Pore and Surface Diffusion model (PSDM) was exclusively used. The PSDM is a non-steady state fixed bed model using numerical methods to predicted adsorber performance. Additional discussion of variables input into the model is included in Chapter 2.

3.5 Results and Discussion

Displacement competition can be seen in Figure 3.1. The effluent concentration is normalized to the influent concentration and the operation time is expressed as throughput in bed

volumes, which is calculated as the ratio of operation time to EBCT. An RSSCT experiment was run with lab-grade organic-free deionized water. An initial concentration of 1,2 DCA of 5.0 μg/L was applied for 35.5 K bed volumes. At this point, the GAC capacity for 1,2 DCA had been exhausted (i.e. complete breakthrough). While continuing to add 1,2 DCA, TCE was introduced into the influent. The TCE concentration was increased three times and is represented by the open triangles in Figure 3.1. The effluent concentration is seen to exceed the influent concentration after addition of TCE. Normalized effluent concentrations of 1.2 or greater are observed when 1.0 μg/L and 3.0 μg/L of TCE were added to the influent. Data shown are from a column with an EBCT of 15 minutes; a 7.5 minute EBCT exhibited similar results. Similar displacements (C/C_0 ~1.2 - 1.4) have been seen in other bi-solute systems but with phenolic compounds at higher initial concentrations of 122 mg/L – 174 mg/L (Crittenden et al., 1980; Thacker et al., 1983).

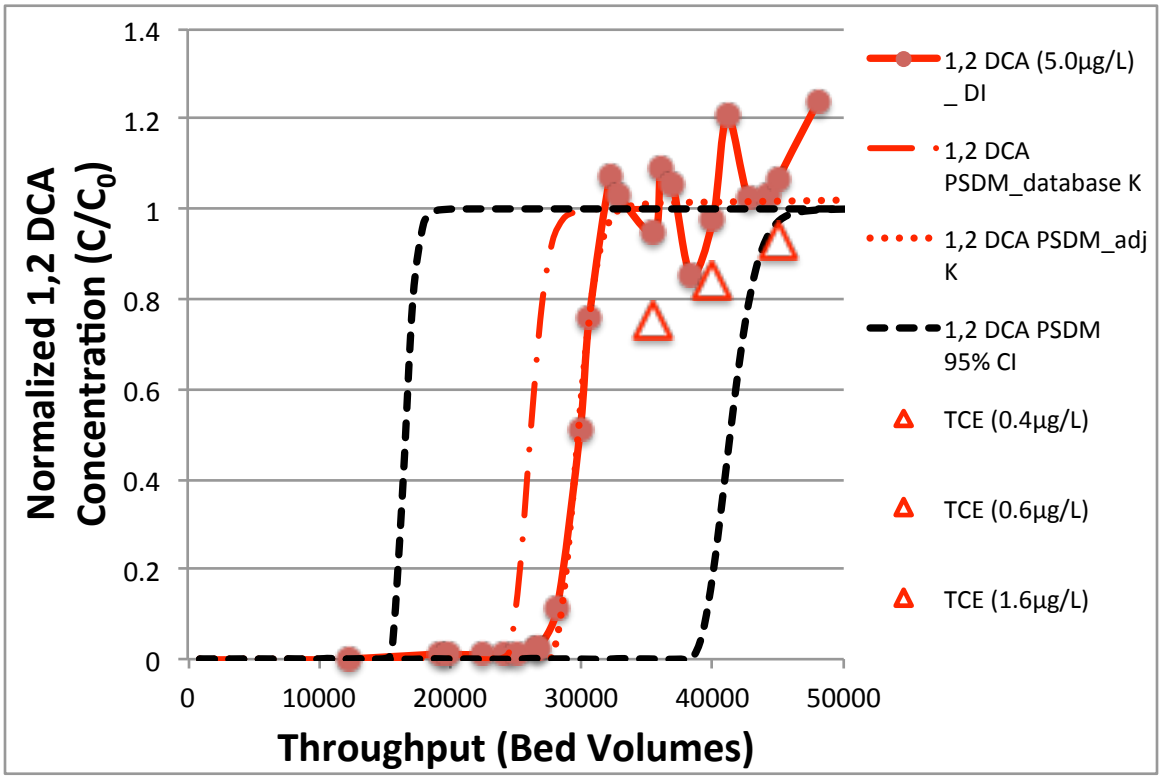

Figure 3.1 1,2 DCA Breakthrough a) observed experimentally in DI Water, b) predicted by PSDM with K_F value of 129 µg/g $(L/\mu g)^{1/n}$, c) predicted by PSDM with K_F value of 147 µg/g $(L/\mu g)^{1/n}$. 95% CI about database K_F noted by outside black dashed lines; EBCT: 15 minutes; Open triangles denote three increasing additions of TCE after 100% 1,2 DCA breakthrough: 0.4 µg/L, 0.6µg/L, and 1.6 µg/L.

Also shown in Figure 3.1 are output from two PSDM runs. The first line (dash-doted) uses a Freundlich K value of 129 µg/g $(L/\mu g)^{1/n}$ from the AdDesigns isotherm database (Speth and Miltner, 1990). This value underprediced the experimental capacity. The second line (dotted) uses a greater Freundlich K value of 147 µg/g*$(L/\mu g)^{1/n}$; this resulted in a better match to the experimental data. This adjusted K is value is 14% greater than the database value but well within the 95% confidence interval reported (81.8 – 204 µg/g*$(L/\mu g)^{1/n}$) (Speth and Miltner, 1990). The breakthrough using the 95% CI K values are shown with the black dashed lines. The discussion below will focus on the model output using the adjusted Freundlich K value.

There is a significant difference between the displacement observed in the experimental

DI column and the displacement predicted by the model. Almost no displacement is predicted by the model at an experimentally equivalent volume of water treated. When TCE addition in the model is carried out beyond the volume of water treated experimentally, displacement is observed. Figure 3.2 shows the displacement predicted when the run time is carried out to 1 x 10^6 bed volumes. Slight displacement competition ($C/C_o \sim 1.05$) is consistently observed indicating that the stronger adsorbing TCE is displacing the weaker 1,2 DCA. Displacement continues until TCE breakthrough occurs.

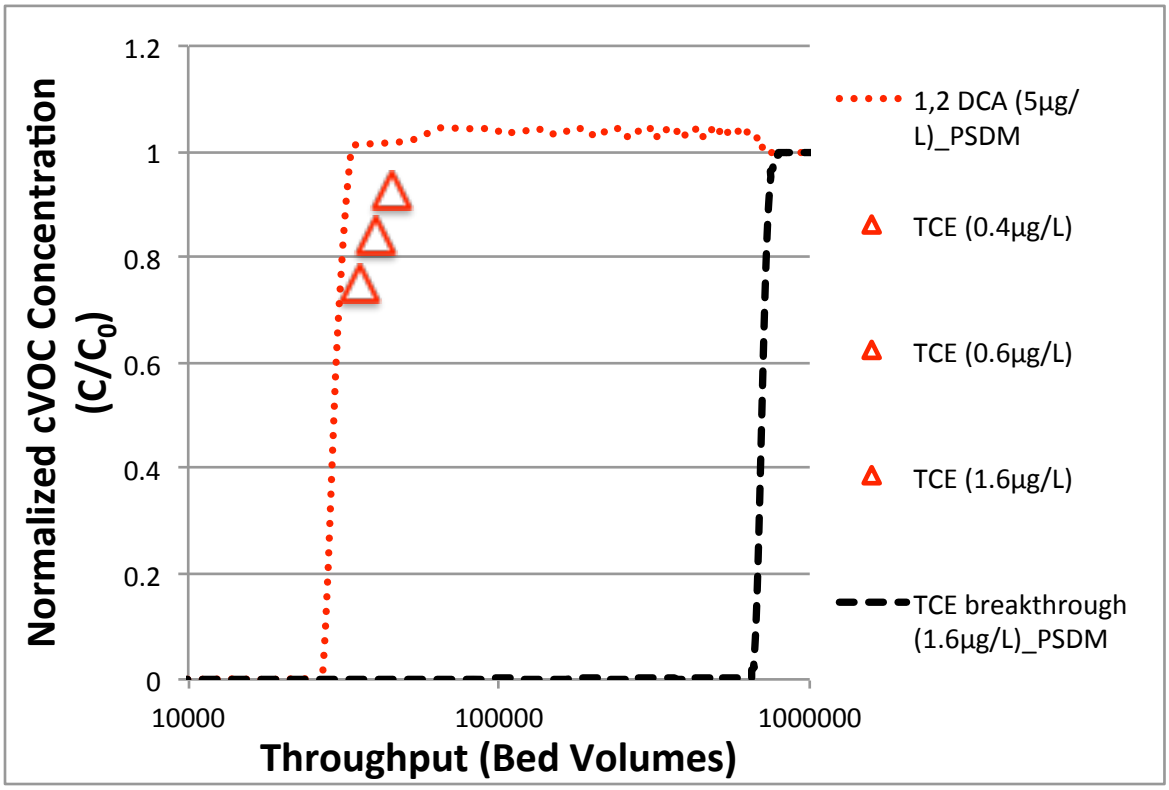

Figure 3.2 1,2 DCA Breakthrough predicted by PSDM when carried out to 1.0 x 10^6 bed volumes. . EBCT: 15 minutes. Open triangles denote three increasing additions of TCE after 100% 1,2 DCA breakthrough: 0.4 µg/L, 0.6µg/L, and 1.6 µg/L. Note the logarithmic x-axis scale.

Comparing the mass of 1,2 DCA-applied against the mass of 1,2 DCA-adsorbed is another way to observe displacement competition. This can be seen in Figure 3.3 and Figure 3.4 for the experimental and model runs, respectively. These figures are created by integrating the

area under the influent curve and above the effluent breakthrough curves to determine mass-applied and mass-adsorbed, respectively. For the experimental DI run, the mass of 1,2 DCA adsorbed after 1,2 DCA had completely broken through but before TCE was added into the influent was approximately 536 µg. Normalizing to the mass of GAC in the 15 minute column yields a solid-phase concentration (q) of 353 µg/g GAC. After TCE was added to the influent, the cumulative mass of 1,2 DCA adsorbed decreased to 521µg or 343µg/g GAC – a reduction of 3% over 13 K bed volumes. For the model run, the 1,2 DCA mass adsorbed decreases from 495 µg to 67 µg over approximately 760 K bed volumes. This equates to reduction in q from 326 µg/g GAC to 44 µg/g GAC; a reduction of 87%.

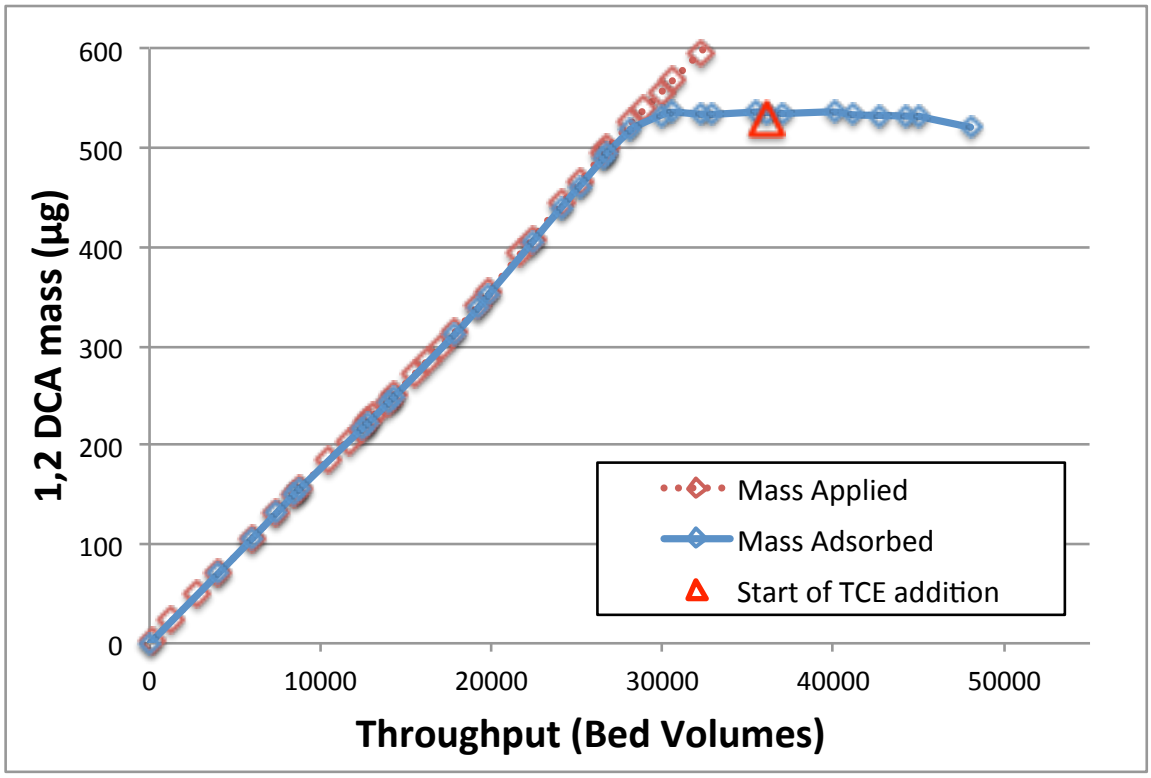

Figure 3.3 Experimental 1,2 DCA Mass (µg): Applied vs. Adsorbed showing displacement after addition of TCE. TCE addition began at ~36K bed volumes.

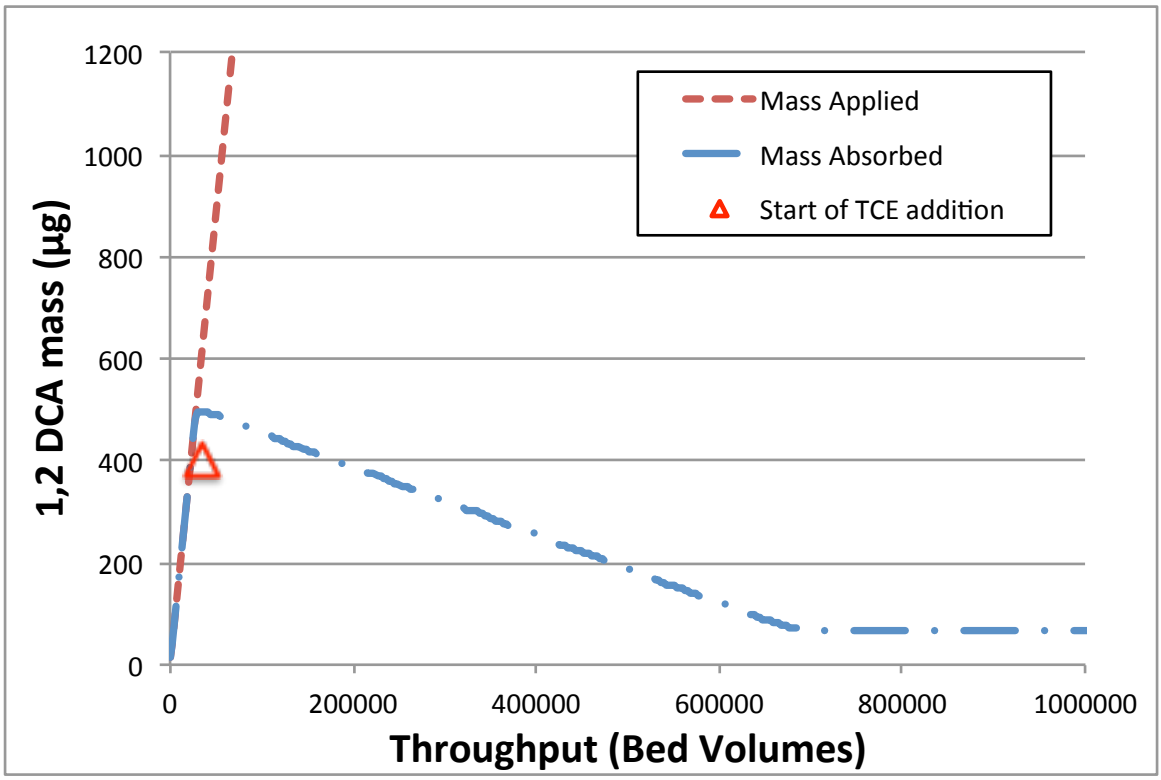

Figure 3.4 PSDM Predicted 1,2 DCA Mass (µg): Applied vs. Absorbed. TCE addition began at ~36K bedvolumes. Displacement continues for ~760K bed volumes after TCE addition; much slower than seen experimentally.

A comparison of the experimental DI RSSCT and the model run is presented in Table 3.1. The model well-predicts the solid-phase concentration of 1,2 DCA before TCE addition. Predictions from the model are within 8% of the experimental data. Comparing q after TCE addition is difficult because the number of bed volumes passed containing TCE in the experimental effort was only 13 K compared with over 900 K for the model run. Determining q for the model at 13 K bed volumes after TCE addition shows a negligible 0.6% decrease in q. To equate the 3% reduction of q seen in the experimental data required continuing the model run for 33 K bed volumes after TCE addition. The model predicts 1.5 times more throughput to have an equal 3% reduction in q seen experimentally.

Table 3.1 1,2 DCA Solid Phase Concentration: Experimental Observation vs. PSDM Prediction

Condition	q - 1,2 DCA solid-phase concentration *before* TCE addition (µg/g GAC)	q - 1,2 DCA solid-phase concentration *after* TCE addition (µg/g GAC)	bed volume difference (before/after TCE addition (K))	% reduction in solid-phase concentration
experimental	353	343	13	3%
model (run out to TCE BT)	326	44	760	87%
model (to match experimental throughput)	326	324	13	1%
model (to match experimental reduction in q)	326	316	33	3%

Overall, the PSDM predicts the solid-phase concentration of the target organic before co-solute addition well (within ~8% of experimental) but is kinetically limited after co-solute addition. Eventually displacement is predicted by the model but not in the timeframe seen experimentally. Previous efforts have had difficulty predicting accurate displacement kinetics of compounds with distinctly different adsorbtivities, as is the case with 1,2 DCA and TCE (Sontheimer et al., 1988). Merk theorized that diffusional resistance and mutual interference of diffusing co-solutes were responsible for the lack of kinetic agreement between different models and experimental data (Merk et al., 1981). Experimentally, the weaker co-solutes occupy lower energy sites on the GAC and become mobile more easily. Sontheimer offered that this creates a greater solid-phase concentration gradient for the weaker co-solute (1,2 DCA in this case) and faster internal mass transfer kinetics result (Sontheimer et al., 1988). This phenomenon is not captured in the PSDM. These findings suggest that caution should be applied when using the PSDM to predict the initial magnitude of displacement occurring in multi-solute scenarios.

The experimental set-up to compare GAC capacity in natural waters and organic free waters is provided in Table 3.2. For these experiments, an initial influent concentration of 1,2 DCA was applied to the column until breakthrough was achieved and then subsequent addition of TCE was initiated. Results from the 15 minute EBCT are shown in Figure 3.5. The organic-free scenarios discussed above are again shown. Earlier breakthrough of 1,2 DCA in the CO GW I (TOC: 0.3 mg/L) compared to the DI column is indicative of DOM competition. When comparing bed volumes to 50% breakthrough for the DI column, the CO GW I column exhibits a 31% and 20% capacity reduction for the 7.5 minute and 15 minute EBCTs, respectively. Making the same comparison for a third water (CO GW II; TOC: 1.5 mg/L) without any co-solute addition, a greater capacity reduction is observed: 52% for the 15 minute EBCT as shown in Figure 3.6. The 7.5 minute EBCT had the same capacity reduction. Table 3.3 summarizes the capacity comparisons between organic-free and columns containing two different GWs with different concentrations of DOM. DOM competition is believed to be responsible for reducing GAC capacity. Although cVOC concentrations are slightly less in the DOM-containing columns, the DOM component of the background matrix outcompetes the 1,2 DCA for sorption sites and capacity reductions result.

Table 3.2 Experimental set up to compare GAC capacity for 1,2 DCA in natural waters and deionized water. EBCTs: 7.5 min and 15 min.

1,2 DCA concentration (µg/L)	TCE concentration added after 1,2 DCA breakthrough (µg/L)	Bed Volumes Co-solute was added (K)	Background Matrix	TOC	Experimental or Model
53.2	0.4	26.8	CO GW I	0.3	Experimental
	0.7	31.1			
	1.6	35.3			
4.3	0.6	24.8	CO GW I	0.3	Experimental
	1.0	28.9			
	3.0	33.7			
5.0	0.4	35.6	DI	0.1	Experimental
	0.6	40.0			
	1.6	44.9			
5.0	0.4	35.6	DI	0.1	Model
	0.6	40.0			
	1.6	44.9			

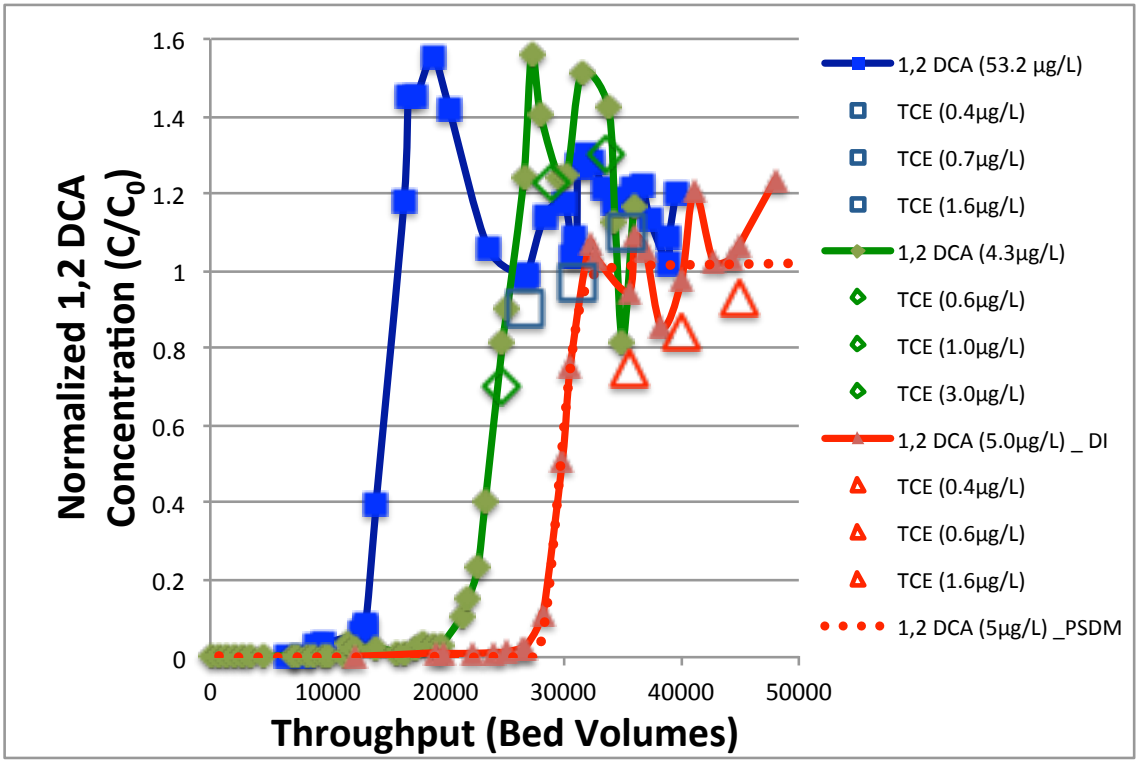

Figure 3.5 Experimental 1,2 DCA breakthrough in CO GW I (TOC: 0.3 mg/L) and in DI water. EBCT: 15min; Dotted line: PSDM prediction for 1,2 DCA breakthrough in organic-free water; open symbols: bed volumes where TCE was added. TCE concentrations were increased with each addition (i.e. for 53.2 µg/L column: 0.4 µg/L TCE increased to 0.7 µg/L TCE, etc.).

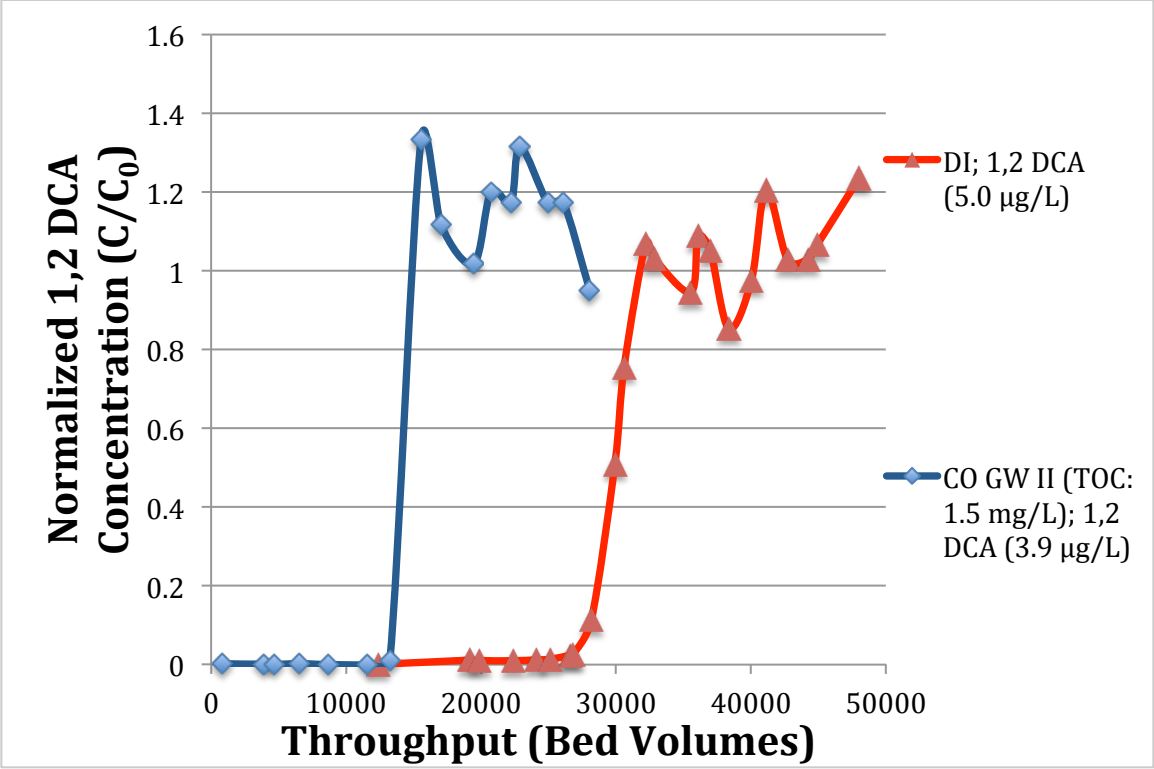

Figure 3.6 Experimental 1,2 DCA breakthrough in CO GW II (TOC: 1.5 mg/L) and in DI water. EBCT: 15min.

Table 3.3. Capacity differences: DOM containing waters vs organic-free water. Capacities are reported in Throughput (bed volumes) to 10% and 50% breakthrough and are denoted as BV10 and BV50.

1,2 DCA C_o (µg/L)	Background Matrix	TOC (mg/L)	EBCT (min)	BV10	BV50	Capacity Reduction_BV10 vs DI (%)	Capacity Reduction_BV50 vs DI (%)
5.0	DI	0.1	15	28000	30000	-	-
4.3	CO GW I	0.3	15	21317	24000	24%	20%
3.9	CO GW II	1.5	15	13500	14500	52%	52%
5.0	DI	0.1	7.5	30300	33300	-	-
4.3	CO GW I	0.3	7.5	20643	23000	32%	31%
3.9	CO GW II	1.5	7.5	14500	16200	52%	51%

More displacement is seen immediately after breakthrough in the columns with a background matrix containing DOM compared to the DI column. This same phenomenon was observed in the columns with a 7.5 minute EBCT. This is indicative of displacement

competition caused by DOM and supported by the fact that a second co-solute has not yet been added to the influent. Columns with background matrices of DI had between 0% and 3% displacement, while DOM-containing columns exhibited between 6% - 22% displacement. A summary of results for the DI and DOM-containing columns is presented in Table 3.4.

Table 3.4 Displacement observed experimentally as a function of DOM: DI background matrix vs. GW background matrix (TOC: 0.3 mg/L).

1,2 DCA C_o (µg/L)	Background Matrix	EBCT (min)	q - 1,2 DCA solid-phase concentration at BT (µg/g GAC)	q - 1,2 DCA solid-phase concentration after initial (DOM) displacement (µg/g GAC)	bed volume difference (1,2 DCA BT to start of TCE addition) (K)	reduction in q (%)
5.0	DI	15	353	353	5	0%
5.0	DI	7.5	373	360	33	3%
53.2	CO GW I	15	1754	1514	10	14%
53.2	CO GW I	7.5	1898	1486	28	22%
4.3	CO GW I	7.5	163	154	27	6%

Displacement competition from both DOM and co-solutes is observed in these RSSCT results. Effluent concentrations of 1,2 DCA after the addition of TCE increase to concentrations greater than the influent. Table 3.5 shows the percent reduction in q for five experimental runs at two different EBCTs. Good agreement is seen between the columns with different EBCTs. The RSSCTs' results in DI had less displacement than that from the columns containing DOM. Essentially columns containing DOM have two components causing displacement (co-solute and DOM) while the DI columns have one (co-solute). The addition of the DOM is responsible for the greater displacement. Finally, the column containing DOM with an initial 1,2 DCA concentration of 4.3 µg/L had the largest displacement (57%). Several reasons may explain this behavior. As stated above, the presence of DOM increases the displacement competition.

Additionally, the TCE concentrations added to this column were about twice that added to the other columns. In total, 57 µg of TCE were added to this DOM column while only 17 µg of TCE were added to the DI column.

Table 3.5 Displacement observed experimentally as a function of DOM and co-solute: DI background matrix vs. GW background matrix (TOC: 0.3 mg/L)

1,2 DCA C_o (µg/L)	TCE C_o (addition after BT) (µg/L)	Background Matrix	EBCT (min)	q - 1,2 DCA solid-phase concentration *before* TCE addition (µg/g GAC)	q - 1,2 DCA solid-phase concentration *after* TCE addition (µg/g GAC)	bed volume difference (TCE addition to column termination) (K)	reduction in q (%)
5.0	0.4/0.6/1.6	DI	15	353	343	13	3%
5.0	0.4/0.6/1.6	DI	7.5	360	341	29	5%
53.2	0.4/0.7/1.6	CO GW I	15	1514	1270	13	16%
53.2	0.4/0.7/1.6	CO GW I	7.5	1486	1269	32	15%
4.3	0.6/1.0/3.0	CO GW I	7.5	154	66	23	57%

After determining that displacement competition was occurring, the degree of co-solute competitive interaction was investigated. Specifically co-solute competition based upon the adsorptive tendencies was evaluated. cVOCs were grouped according to their Freundlich adsorption coefficients into weak, moderate, and strongly adsorbing compounds as shown in Table 3.6. During this portion of the research, compounds were added simultaneously to the GAC columns. Results from a bisolute column containing 1,2 DCA and TCE (a weak and strong compound) can be seen in Figure 3.7. Results from a bisolute column containing 1,2 DCA and 1,1 DCA (two weak compounds) can be seen in Figure 3.8. Both the model and the experimental data show the effect of a strongly adsorbing compound on a weakly adsorbing compound to be rather small. Additionally, the model and the experimental data show the effect of a weakly adsorbing compound on another weakly adsorbing compound to be more pronounced. Table 3.7

compares how strong and weak co-solutes affect breakthrough. Two experimental columns (weak-strong and weak-weak adsorbing cVOCs) and the corresponding model runs at two different EBCTs (7.5 min and 15 min) for 10% and 50% breakthrough capacities are expressed in the table. Considering both experimental and model results, Table 3.8 is a summary table showing compounds with similar adsorptivities affected breakthrough at least 4 times more than compounds with dissimilar adsorptivities.

Table 3.6 Classifying cVOCs as strong, moderate, or weak adsorbers based on Fruendlich K values

cVOC	Freundlich K $(\mu g/g)/(L/\mu g)^{1/n}$	Freundlich 1/n	Adsorption Classification
1,1 Dichloroethane	64.6	0.706	weak
1,2 Dichloroethane	129	0.533	weak
Carbon Tetrachloride	387	0.594	moderate
Trichloroethylene	1180	0.484	strong

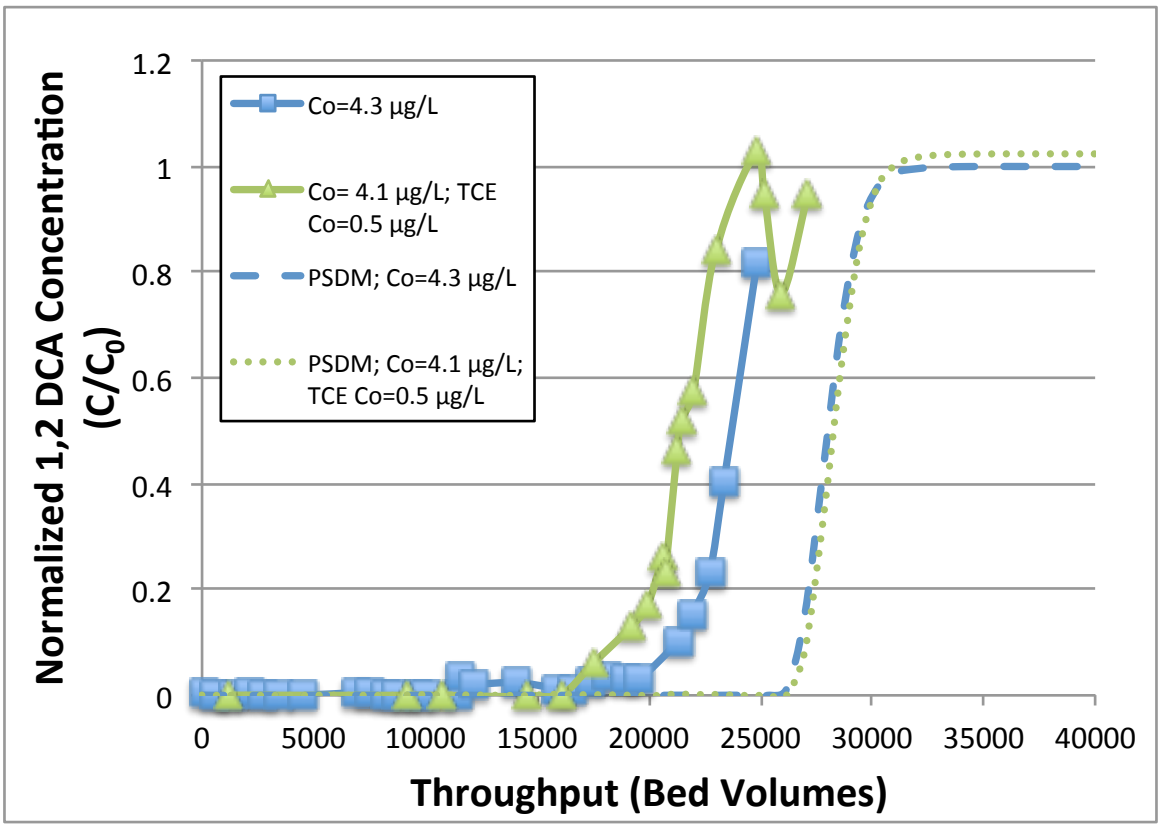

Figure 3.7 Co-Solute Competitive Effects: A Strong adsorber affecting a Weak Adsorber; EBCT: 15 min; CO GW I (TOC: 0.3 mg/L). Concentrations in legend are for 1,2 DCA unless explicitly stated at TCE.

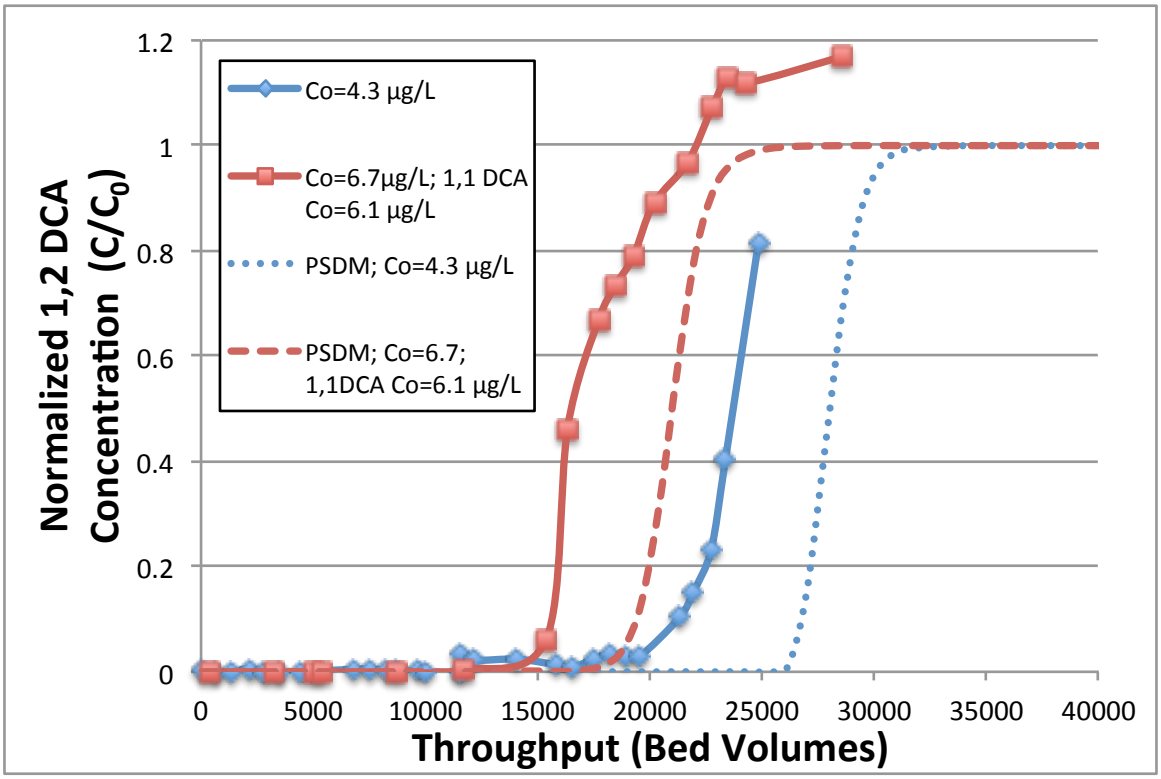

Figure 3.8 Co-Solute Competitive Effects: A Weak adsorber affecting a Weak Adsorber; EBCT: 15 min; CO GW I (TOC: 0.3 mg/L). Concentrations in legend are for 1,2 DCA unless explicitly stated at 1,1 DCA.

Table 3.7 Experimental Observations and PSDM Predictions of Co-solute Competition as a function of Co-solute Adsorptive Strength; All experimental columns with CO GW I (TOC: 0.3 mg/L); All model columns with organic-free water. Each column at 2 EBCTs (7.5 min and 15 min): Single Solute, Strong and Weak Bi-Solute, and Weak and Weak Bi-Solute Column

Experimental

Single Solute 1,2 DCA; 7.5 min		w/ Strong Co-solute (TCE) - 7.5 min				w/ Weak Co-solute (1,1 DCA) - 7.5 min			
BV10	BV50	BV10	% earlier BT	BV50	% earlier BT	BV10	% earlier BT	BV50	% earlier BT
20643	23000	22000	-6.6%	23000	0.0%	16000	22.5%	20000	13.0%
		average % earlier breakthrough			-3.3%	average % earlier breakthrough			17.8%
Single Solute 1,2 DCA; 15 min		w/ Strong Co-solute (TCE) - 15 min				w/ Weak Co-solute (1,1 DCA) - 15 min			
BV10	BV50	BV10	% earlier BT	BV50	% earlier BT	BV10	% earlier BT	BV50	% earlier BT
21317	24000	18000	15.6%	21300	11.3%	15500	27.3%	17000	29.2%
		average % earlier breakthrough			13.4%	average % earlier breakthrough			28.2%
		overall average % earlier breakthrough (7.5 min and 15 min; BV10 and BV50)			5.1%	overall average % earlier breakthrough (7.5 min and 15 min; BV10 and BV50)			23.0%

Model

Single Solute 1,2 DCA; 7.5 min		w/ Strong Co-solute (TCE) - 7.5 min				w/ Weak Co-solute (1,1 DCA) - 7.5 min			
BV10	BV50	BV10	% earlier BT	BV50	% earlier BT	BV10	% earlier BT	BV50	% earlier BT
25300	27800	25500	-0.8%	28000	-0.7%	17800	29.6%	20800	25.2%
		average % earlier breakthrough			-0.8%	average % earlier breakthrough			27.4%
Single Solute 1,2 DCA; 15 min		w/ Strong Co-solute (TCE) - 15 min				w/ Weak Co-solute (1,1 DCA) - 15 min			
BV10	BV50	BV10	% earlier BT	BV50	% earlier BT	BV10	% earlier BT	BV50	% earlier BT
26700	28000	27100	-1.5%	28300	-1.1%	19400	30.7%	21000	25.0%
		average % earlier breakthrough			-1.3%	average % earlier breakthrough			27.9%
		overall average % earlier breakthrough (7.5 min and 15 min; BV10 and BV50)			-1.0%	overall average % earlier breakthrough (7.5 min and 15 min; BV10 and BV50)			27.6%

Table 3.8 Summary Table of Competition as a Function of Co-Solute Adsorptive Strength

Interaction Type	Average % Earlier Breakthrough (both 7.5 min and 15 min; both BV10 and BV50)
experimental; weak - strong	5.1%
model; weak - strong	-1.0%
experimental; weak - weak	23.0%
model; weak - weak	27.6%

With good agreement between the model predictions and the experimental data, co-solute effects based on adsorptive tendency was further explored with the AdDesignS model. Figure 3.9 shows the breakthrough predictions produced by the model when creating a tri-solute column comprised of a strong, a moderate, and a weak adsorbing compound. A comparison of tri-solute and single solute bed volumes to 10% breakthrough is shown in Table 3.9. Overall the model predicts a small difference in capacity with the tri-solute column having about 12% less capacity than the single solute column. Based on these results a tri-solute column was run experimentally with rather small competitive effects expected.

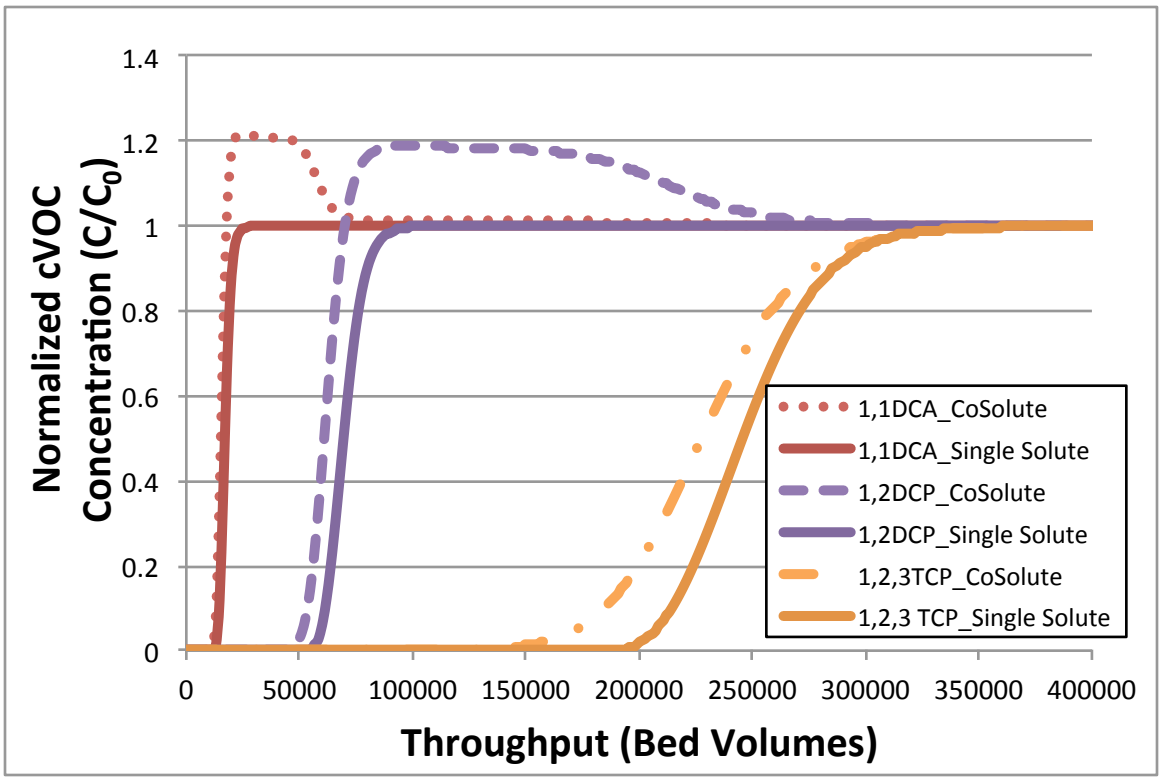

Figure 3.9 PSDM Predictions comparing Single Solute Columns vs Tri-Solute Column with Co-Solutes having dissimilar adsorptivities (one strong, one moderate, and one weak solute)

Table 3.9 Predicted PSDM Capacity reductions in Tri-Solute Column vs. Single Solute Column

cVOC and condition	Freundlich K $(\mu g/g)/(L/\mu g)^{1/n}$	Freundlich 1/n	Adsorption Classification	BV10 Bed Volumes	% Earlier BT with Tri-solute
1,1 DCA single-solute	64.6	0.706	weak	14.7	11%
Tri-solute				13.1	
1,2 DCP single solute	313	0.597	moderate	60.6	11%
Tri-solute				53.7	
1,2,3 TCP single solute	1080	0.613	strong	215	13%
Tri-solute				186	

The single solute 1,2 DCA breakthrough curve at an influent concentration of 4.3 µg/L and the 1,2 DCA breakthrough curve in a tri-solute column with an influent concentration of 4.5

µg/L are shown in Figure 3.10. The influent concentrations for the other co-solutes, carbon tetrachloride and TCE, were 1.8 µg/L and 1.4 µg/L, respectively. The model again predicts about 12% less capacity for this tri-solute column compared to the single solute column. The experimental data shows the same capacity for both the tri-solute and single solute columns. No difference in capacity between the single and tri-solute columns was observed in the 15 min EBCT column either (data not shown).

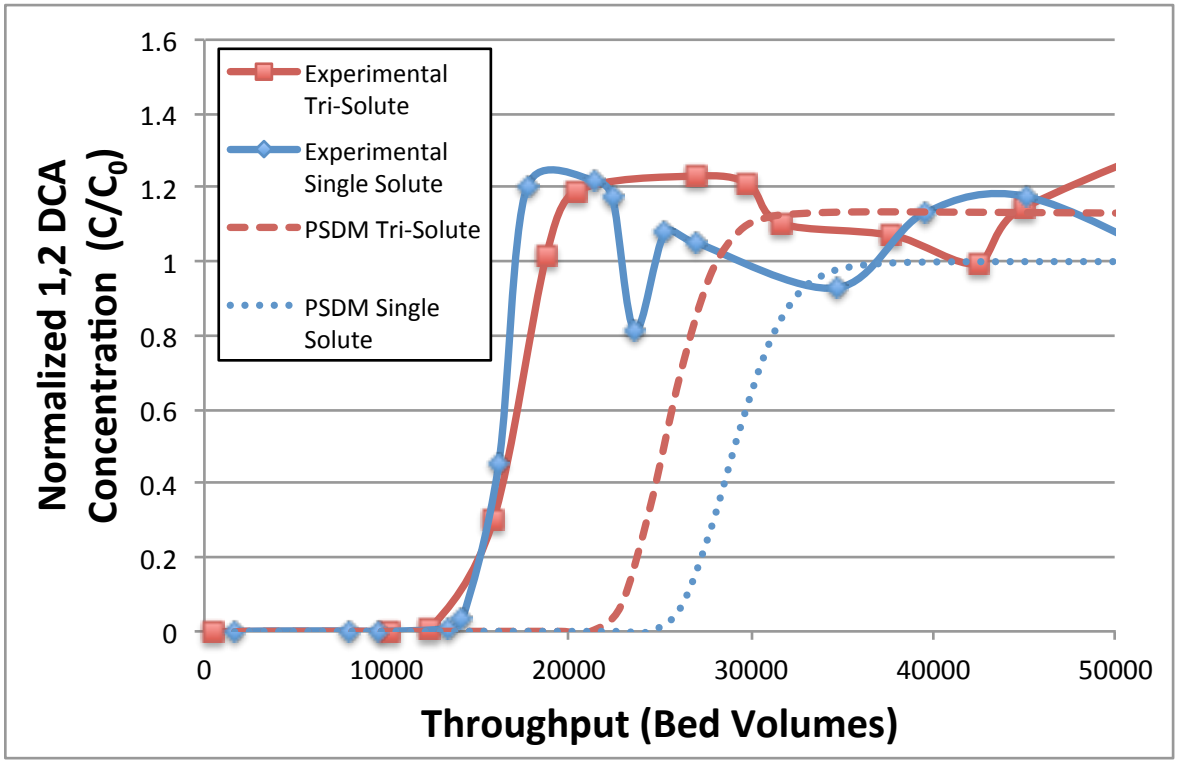

Figure 3.10 Experimental Observations and PSDM predictions of 1,2 DCA Single Solute (C_0 = 4.5 µg/L) breakthrough vs 1,2 DCA (C_0 = 4.3 µg/L) breakthrough in a Tri-Solute column with Co-Solutes of dissimilar adsorptivities (moderate adsorber: CT C_0 = 1.8 µg/L; strong adsorber: TCE C_0 = 1.4 µg/L). EBCT: 7.5 minutes. Experimental Water: CO GW II (TOC: 1.5 mg/L); Model predictions based on organic-free water.

Numerous studies have shown that DOM has deleterious effects on GAC's capacity to remove target organics (Corwin, 2012; Hand et al., 1989; Jarvie et al., 2005; Kennedy, 2013; Sontheimer et al., 1988; Speth, 1991; Summers et al., 1989). This can be observed in all of the

breakthrough curve comparisons between the model and experimental data that have been presented in this chapter. Compared to experimental data, the model's predicted GAC capacity is always over-predicted because the model predictions are based on organic-free water. Although DOM in groundwater tends to be lower in concentration and have more recalcitrant properties than it's surface water counterpart (Thurman, 1985), the DOM in the matrix of the waters used this study are still adversely affecting target organic adsorption. Although co-solute competition was expected to be low (~12%), little to no capacity reductions were seen in the experimental results. This may also be explained by DOM interactions. Although not dominating the system to such an extent that normalized breakthrough is occurring independent of the influent concentration, it may be possible that the DOM competition dampens the co-solute competition predicted by the model. The cVOC concentrations range from 0.1% to 0.3% of the DOM concentration. This disparity in concentration produces an environment where DOM competition is overwhelming cVOC competition and little to no capacity differences are observed.

Results of the tri-solute solute column are shown in Figure 3.11. The model overpredicts the capacity of the GAC for both 1,2 DCA and CT. As previously stated, this behavior is expected because of the lack of DOM competition in the model calculations. The TCE did not breakthrough at the time of RSSCT termination (92 K bed volumes). Once again, the model doesn't predict the magnitude of displacement initially seen at 1,2 DCA breakthrough. As carbon tetrachloride breaks through, the model's cumulative displacement increases at a rate greater than the experimental observations but is still kinetically retarded. As seen in Table 3.10, a 77% reduction in 1,2 DCA solid-phase reduction is seen experimentally. This occurs at 71 K bed volumes after the initial 1,2 DCA breakthrough is complete. The model predicts nearly the

same reduction in solid-phase concentration (82%) but requires 10x more bed volumes before this equilibration is reached. If the model predictions are stopped at the same 71 K bed volumes after 1,2 DCA breakthrough, a 31% reduction in q is predicted. Initially, at the completion of 1,2 DCA breakthrough, the solid phase concentrations are within 15% of one another. The experimental solid-phase concentration is lower than the model's prediction because of the presence of DOM in the experimental column. Stated otherwise, the displacement competition is and should always be greater than the model prediction because model conditions are absent of DOM. Little to no capacity reductions seen in the model and experimental observations provides the opportunity to incorporate target organics of different adsorbtivities into a single RSSCT and obtain approximations of single solute breakthrough curves for each target organic. As in the case of this experimental design, combining three co-solutes into one RSSCT reduces resource requirements by one third (e.g. 1/3 the water required, 1/3 the samples collected, only one RSSCT set-up, etc.).

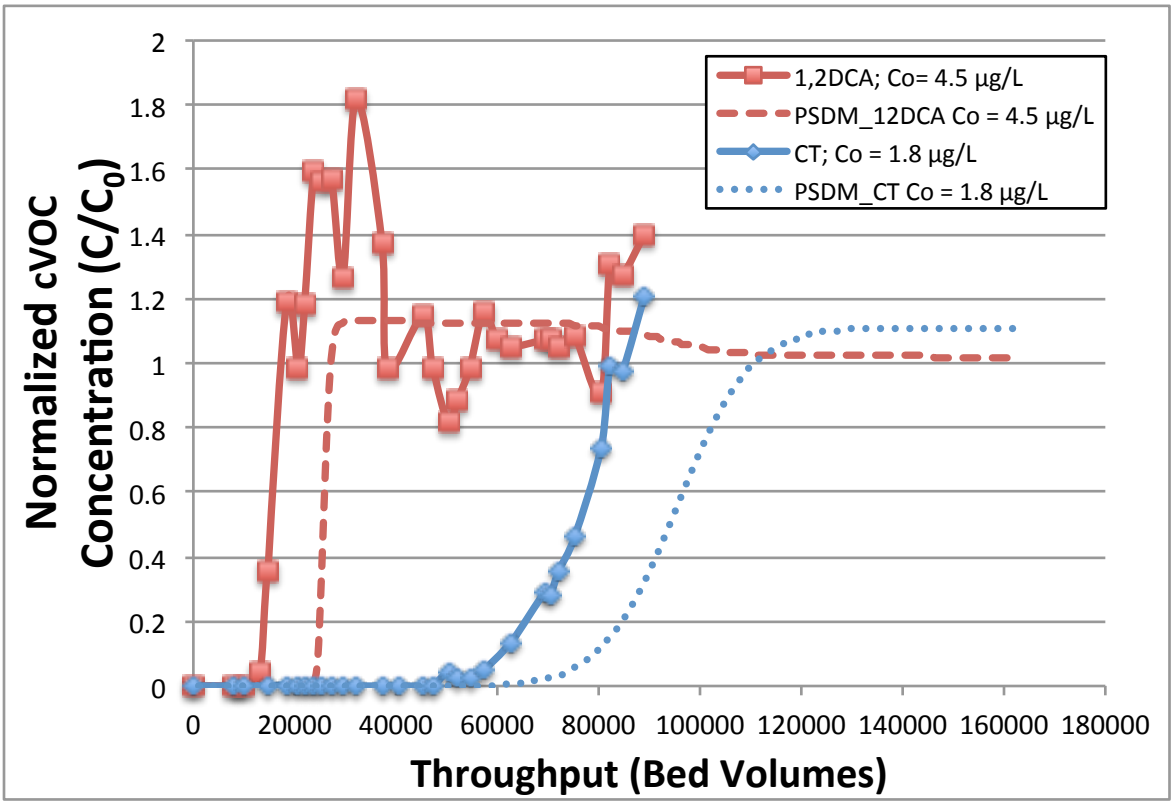

Figure 3.11 Experimental Observation vs. PSDM Prediction: TriSolute Column with Co-Solutes of dissimilar adsorptivities; 1,2 DCA C_0 = 4.5 µg/L; CT C_0 = 1.8 µg/L; TCE C_0 = 1.4 µg/L; CO GW II (TOC: 1.5 mg/L). EBCT: 15 min; TCE did not breakthrough the experimental column in 92K bed volumes

Table 3.10 Experimental observation vs PSDM predictions: Displacement in Tri-Solute Column with Co-Solutes of dissimilar adsorptivites

Condition	1,2 DCA C_o (µg/L)	CT C_o; TCE C_o (µg/L)	Background Matrix	EBCT (min)	q - 1,2 DCA solid-phase concentration *at 1,2 DCA BT* (µg/g_{GAC})	q - 1,2 DCA solid-phase concentration *after* displacement (µg/g_{GAC})	bed volume difference (1,2 DCA BT to column termination) (K)	reduction in q (%)
Experimental	4.5	1.8; 1.4	CO GW II	15	150	35	71	77%
Model	4.5	1.8; 1.4	DI	15	266	47	713	82%
Model	4.5	1.8; 1.4	DI	15	266	182	71	31%

3.6 Conclusions

Competition with cVOCs in groundwaters at and below the µg/L level has not been studied before. Possible forthcoming regulation from the U.S. EPA makes this effort both pertinent and timely. Three types of competition were evaluated in this chapter. DOM competition was investigated comparing the capacity of GAC for a single cVOC solute with and without DOM in the background matrix of the water. In the low TOC end member water (CO GW I; TOC: 0.3 mg/L), GAC capacity was reduced by 31% and 20% for the 7.5 minute and 15 minute EBCT columns, as compared with bed volumes to 50% breakthrough in organic-free water. Greater capacity reductions were seen in a third, higher TOC water (CO GW II; TOC: 1/5mg/L). Co-solute competition was also observed but to a lesser extent. Grouping co-solutes by their Freundlich adsorption coefficients, co-solutes with similar adsorptivities were found to affect capacity 4-5x more than co-solutes with dissimilar adsorptivities. Displacement competition caused by DOM was observed. Immediately after breakthrough, columns with background matrices of DI had between 0% and 4% displacement, while DOM-containing columns exhibited greater displacement (6% - 17%). Displacement competition, caused by both DOM and co-solutes, was also observed throughout this effort. Co-solute competition occurred when a 3-5% reduction in the solid-phase concentration of 1,2 DCA was observed in organic-free water after addition of TCE. Due to DOM competition, this displacement increased to 15–57% after addition of TCE in columns containing natural water.

Since DOM is not considered in the PSDM, the model was limited to single solute predictions and co-solute interactions. Overall, the PSDM predicts the solid-phase concentration of a target organic before co-solute addition well (within ~8% of experimental results). The

model was useful in elucidating the effects of weak, moderate, and strong co-solutes on capacity. Kinetically the model had difficulty predicting displacement as a function of throughput.

Chapter 4 Effect of DOM on 1,2 Dichloroethane Adsorption in Groundwaters

4.1 Abstract

The impact of groundwater dissolved organic matter (DOM), empty bed contact time (EBCT) and influent concentration in the µg and sub-µg/L level on the adsorption of 1,2 dichloroethane (1,2 DCA) was investigated in this chapter. Different EBCTs had little effect on GAC capacity for 1,2 DCA in the four groundwaters studied, thereby indicating that DOM pre-loading was not a function of bed depth. The breakthrough behavior of carbon tetrachloride (CT) was also not impacted by EBCT when expressed on a throughput basis. DOM competition was observed by a 32% reduction in 1,2 DCA adsorption capacity when comparing an organic-free background matrix against a groundwater background matrix containing 0.3 mg/L TOC. Correlations were developed to predict 10% breakthrough of 1,2 DCA and were applied to 22 breakthrough curves from four different groundwaters with 1,2 DCA concentrations spanning 2.5 orders of magnitude. Various DOM characteristics as measured by fluorescence, UV spectroscopy, and size exclusion chromatography were considered. The best predictors of throughput to 10% breakthrough of 1,2 DCA were Peak C / UV_{340} * 1,2 DCA concentration (R^2 = 0.82, n = 22) and Peak C / UV excitation * 1,2 DCA concentration (R^2 = 0.82, n = 22). Using only UV_{254} absorbance and 1,2 DCA concentration, another predictive regression was created. Although this regression has a slightly lower R^2 value (R^2 = 0.74, n = 22), values can be obtained without the cost and expertise required with fluorescence analytics.

4.2 Introduction

Many factors can influence the adsorption process. Factors include differences in the

target organic concentration and type (polarity, molecular size, K_{OW}), the type and properties of the adsorbent (pore size distribution, surface charge, polarity), and the concentration and character of DOM (concentration, molecular size distribution, charge, polarity) in the background matrix (Matsui et al., 2002b). Many studies have shown reduced GAC capacity for target organics in natural waters due to the presence of DOM (Corwin, 2012; Hand et al., 1989; Jarvie et al., 2005; Kennedy, 2013; Sontheimer et al., 1988; Summers et al., 1989). These efforts however, mainly focused on surface waters or involved target compound concentrations that were significantly higher than the low µg/L range. The heterogeneous nature of DOM continues to make prediction of GAC capacity reduction elusive.

The overall objective of this study is to understand the impact of DOM on 1,2 DCA adsorption at low contaminant concentrations. Six waters (four GWs, one surface water, and lab grade deionized water) with TOC concentrations ranging from 0.1 mg/L to 1.5 mg/L and a range of DOM characteristics were used. The influence of EBCT, 7.5 minutes or 15 minutes, was investigated with 27 adsorption column experiments with influent 1,2 DCA concentrations (C_0) ranging from 0.1 mg/L to 53 µg/L. All 27 columns contained 1,2 DCA with one column containing the co-solutes carbon tetrachloride and trichloroethylene (TCE) in addition to 1,2 DCA. The impact of groundwater DOM concentration was investigated with influent TOC concentrations ranging from 0.1 mg/L for the organic-free water to 1.5 mg/L for one groundwater and the surface water. GAC capacity as a function of the character of DOM was also examined using high performance size exclusion chromatography (HPSEC), ultraviolet spectroscopy (UV-Spec) and fluorescence analysis. Correlations were identified and regressions created to predict 10% breakthrough for 1,2 DCA in RSSCT columns.

4.3 Background

4.3.1 Effect of Empty Bed Contact Time

In the presence of DOM, adsorption capacity for target organics can increase, decrease, or be unaffected when the empty bed contact time of an adsorber is increased. Initially, both DOM and target organics compete for adsorption sites; this phenomenon is called "co-loading". Longer EBCTs can improve GAC efficiency (as measured by carbon use rate or specific throughput) when co-loading conditions are dominant (Hand et al., 1989; Kennedy, 2013). Improved GAC performance occurs as the ratio of the target organic mass transfer zone to the bed length decreases as EBCT increases (Hand et al., 1989). Concurrently, as DOM and target organics travel through an adsorber, DOM develops a longer mass transfer zone because of its wide range of molecular weights and heterogeneous nature. A portion of the DOM travels ahead of the target organic, adsorbs to GAC sites, and reduces the carbon's capacity for target organic; this phenomenon is called "pre-loading". When pre-loading conditions are dominant, longer EBCTs can result in decreased target organic adsorption capacity (Corwin, 2010; Zimmer, 1988). The transition between the two phenomena occurs when two different EBCTs have the same capacity for target organics. Several research efforts have demonstrated the continuum from co-loading through transition to pre-loading conditions (Chowdhury et al., 2013; Corwin and Summers, 2012; Summers et al., 2013). The influence of EBCT was investigated with 27 RSSCT experiments using four different groundwaters (TOCs from 0.3 mg/L to 1.5 mg/L), and deionized water. EBCTs were either 7.5 minutes or 15 minutes and influent 1,2 DCA concentrations ranged from 0.1 µg/L to 53 µg/L. All 27 columns contained 1,2 dichloroethane (1,2 DCA) with one column containing the co-solutes carbon tetrachloride (CT) and trichloroethylene (TCE) in addition to 1,2 DCA.

4.3.2 Effect of influent target compound concentration

In the presence of DOM, removal of target organics normalized to their influent concentration has been shown to be independent of the initial concentration. Using Ideal Adsorption Solution Theory (IAST) and the Pore and Surface Diffusion Model equations, the theoretical basis for this behavior has been explained (Knappe et al., 1998; Matsui et al., 2002b; 2003). Experimentally, this behavior has been demonstrated with both powdered activated carbon (PAC) batch experiments (Gillogly et al., 1998; Graham et al., 2000; Knappe et al., 1998; Matsui et al., 2003; Westerhoff et al., 2005) and with GAC flow-though experiments (Corwin and Summers, 2012; Matsui et al., 2002b; Summers et al., 2013). Rossner used GAC in batch experiments to show this phenomenon (Rossner et al., 2009). These efforts used both groundwaters and surface waters but to our knowledge, no experimental design has looked at the combination of GAC and GW and flow-through columns. Additionally, the efforts cited above investigated pesticides and herbicides, taste and odor compounds, and pharmaceuticals and personal care products; work with 1,2 DCAs and normalized adsorption independent of influent concentration has yet to be reported.

4.3.3 Effect of GAC properties

The pore structure of GAC varies based upon the precursor material and the activation conditions. Different GACs possess different distributions of pore sizes. Pore sizes can be classified as micropores ($d_p < 2$ nm), mesopores (2 nm $< d_p <$ 50 nm), and macropores ($d_p >$ 50 nm) (AWWA, 2011a; Zhang et al., 2007). Coconut based carbons generally have a larger proportion of micropores, bituminous coal carbons tend to have a desirable bimodal distribution of large and small pores, while wood-based carbons have larger pore sizes (Zhang et al., 2007).

4.3.4 Effect of influent background DOM

DOM has been shown to adversely affect adsorption of target organics (Sontheimer et al., 1988). DOM can reduce GAC capacity via pre-loading, and/or direct competition for sorption sites, and/or a pore blockage mechanism that prohibits target organics from reaching sorption sites (Carter and Weber, 1994; Corwin, 2010; Kilduff et al., 1998) Another mechanism proposed involves higher MW DOM agglomerating on the exterior of the GAC particle and reducing the external film mass transfer rate (Schideman et al., 2006). Increasing DOM concentrations have been shown to reduce GAC capacity for taste and odor compounds in surface waters (Summers et al., 2013). The effect DOM has on 1,2 DCA adsorption in groundwaters is investigated in this effort with TOC concentrations ranging from 0.3 mg/L to 1.5 mg/L.

A quantitative estimate of DOM does not provide an accurate assessment of the competitive-portion of the heterogeneous DOM. DOM composition varies both spatially and temporally (Hudson et al., 2007). DOM will also compete differently with different target organics because of the variance in target organic characteristics (Matsui et al., 2002b). This creates a competitive fraction of DOM that is different in time and space and a function of the different target organics and therefore, cannot be quantified by a simple TOC concentration. Heterogeneous DOM, being comprised humic substances, non-humic substances, wastewater effluent organic mater, and synthetic organic compounds covers a range of molecular sizes (Kennedy, 2013). In addition to concentration, the size of the DOM affects target organic adsorption. A large DOM surrogate (polystyrene sulfonate; MW: 1800 Da) affected atrazine adsorption by pore blockage while a small DOM surrogate (para-dichlorobenzene; MW: 147 Da) reduced capacity by direct competition (Li et al., 2003b). Another study found humic substances with low MWs were preferentially adsorbed over larger MW DOM components because of size

exclusion (Summers and Roberts, 1988). Due to size exclusion, some portion of DOM is prevented from reaching smaller micropore adsorption sites that may be available to target organics.

DOM containing aromatic moieties and/or conjugated double bonds absorb light in the UV wavelength range (AWWA, 2011a). To compare UV absorbance for different waters, the absorbance can be normalized by the TOC value to produce the specific ultraviolet absorbance, or SUVA. SUVA values are indicative of the humic content of a water; values above 3 L/mg-m are indicative of a high humic acid fraction while values below 2 L/mg-m signal a low humic acid fraction (AWWA, 2011a). UV absorption can also be used as a surrogate for the TOC content of a water (AWWA, 2011a; Kennedy, 2013).

Fluorescence has been used to characterize DOM (Baker and Genty, 1999; Baker et al., 2008; Coble, 1996; Fellman et al., 2010; Hudson et al., 2007; Nguyen et al., 2005). Using the optical properties of DOM, fluorescence can distinguish between different types and sources of DOM in natural waters (Coble et al., 1990). Fluorescent characterization involves subjecting an aqueous sample containing DOM to a variety of energies via photons of known wavelength and measuring how much energy is absorbed and how much energy is re-emitted as fluorescent light. Energies are applied across a range of wavelengths and emissions measured over a similar range. The excitation energies and the emission energies (both wavelength and intensity) are specific to a particular molecule and, when a sample's total excitation and emission profile (referred to as an excitation-emission matrix, or EEM) is examined, inferences can be drawn about the characteristics of the molecules in the DOM matrix. Interpreting the data contained in an EEM can be done by a variety of methods. Intensity of fluorescence contained in regions of the EEM has been correlated to DOM properties. Figure 4.1 was taken from Korak and shows regions of

interest called A, B, C, and T and the fluorescent index (FI) metric (Korak et al., 2014). Regions A and C have been correlated to humic-like character, while regions B and T have been associated with the amino acids tyrosine and tryptophan (Cammack et al., 2004; Coble, 1996; Hudson et al., 2008; Mayer et al., 1999). The FI is a ratio of emission intensities at two wavelengths (470 nm and 520 nm) obtained from an excitation wavelength of 370 nm and has been used to differentiate between terrestrial and microbial sources of organic matter (Cory et al., 2010; McKnight et al., 2001). Another ratio used to characterize DOM is the humification index (HIX). The HIX compares fluorescent intensities across two emission ranges (435 nm - 480 nm : 300 nm – 345 nm). Increasing conjugation, resonance, and substituted aromatic structure in DOM result in a red-shifted emission (emission at longer wavelengths), resulting in a higher HIX and indicative of greater humic characteristics (Kalbitz et al., 1999). Having a better idea of the DOM characteristics can provide support for functional assay observations. Baker found relationships using peak C emission intensity, the ratio between peak T and peak C, and the ratio between peak C and UV absorbance at 340 nm to predict functional assay results (e.g. benzo[a]pyrene binding, alumina adsorption, hydrophilicity, and buffering capacity) (Baker et al., 2008). Hudson found correlation between the tryptophan-like peak T and BOD_5 (Hudson et al., 2008).

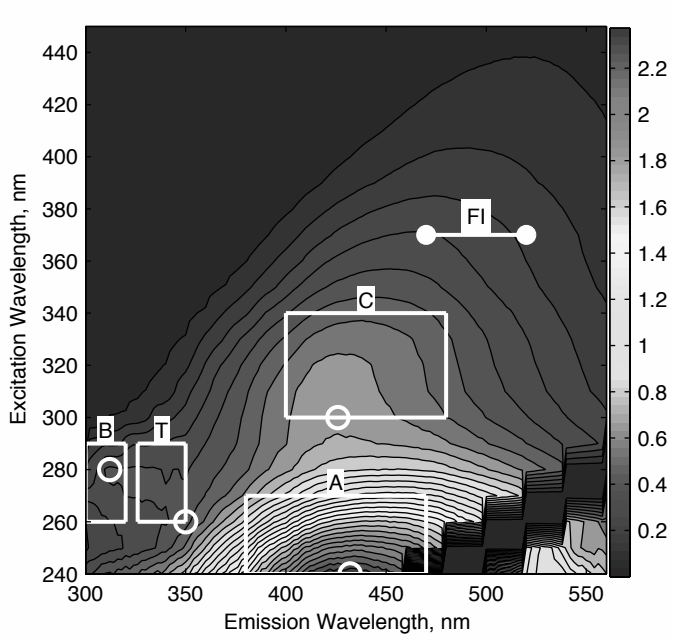

Figure 4.1 Example of Excitation Emission Matrix showing four peak regions of interest (A, B, C, T) and the two points used to determine the I_{470}/I_{520} Fluorescence Index (FI). Open circles indicate the location of the peak intensity in each region. Secondary Y-axis is in Raman units and is indicative of fluorescent intensity. Figure taken from Korak's dissertation (Korak, 2014)

4.4 Materials and Methods

4.4.1 Materials

4.4.1.1 Source Water.

Groundwater was collected from two different sources in Colorado and a source in Ohio. A surface water was collected from a rural mountain community, Big Elk Meadows (BEM) in Larimer County, CO.

The first Colorado groundwater source, designated CO GW I, was collected from a privately-owned 170 foot well in 4-mile canyon outside of Boulder, CO. The second Colorado GW source, designated CO GW II, was from another site in Boulder County and extracted from two 600' deep wells in the Laramie-Fox Hills aquifer. The Ohio water source was from the Greater Cincinnati Water Works Bolton Water Treatment Plant, Well #6. All groundwaters were

natural waters directly out of the ground with no augmentation to the background matrix with the exception of dilCO II, which is a diluted version of CO GW II. CO GW II was also run through a 25 mm ID column of GAC with an EBCT of 8.1 min to remove DOM for use as a dilution water. The processed water was mixed with CO GW II to create dilCO II at a desired TOC of 0.8 mg/L. dilCO II was processed in this manner to reduce the TOC of CO GW II but maintain the same inorganic matrix. BEM water was collected from Mirror Lake, a low alkalinity source with high TOC (~10-16 mg/L; depending upon season). The BEM water was processed through a 25 μm cartridge filter (DGD-7525-20, Pentek Inc., Uppers Saddle River, NJ) before entering into a low-pressure RO membrane (FILMTEC LE-4040, Dow Chemical Co., Midland, MI). The RO system was run in batch mode; permeate was discharged to a laboratory sink and retentate was recirulated back to the membrane. This was continued until the feed water had a conductivity of approximately 600 μS, which equated to a TOC of approximately 75 mg/L. Aluminum sulfate was then used to coagulate the concentrate; this reduced the TOC to approximately 50 mg/L. This stock water was diluted with DI water to obtain BEM water at the desired TOC concentration of 1.5 mg/L. Deionized water was obtained from a Barnstead Nanopure water purification unit by Thermo Fisher Scientific Inc. Additional details of the water sources and pre-treatment are discussed in Chapter 2. Water quality parameters are provided in Table 2.1.

4.4.1.2 Adsorbates.

Carcinogenic volatile organic compounds were obtained from Sigma Aldrich of St Louis, MO. All cVOCs were *analytical standard* grade and in neat form. The majority of the effort focused on 1,2 DCA, however a multi-solute column was also operated. The cVOCs for the multi-solute column were selected to represent a range of applicable adsorbtivities: one weakly

adsorbing compound (1,2 dichloroethane), one moderately adsorbing (carbon tetrachloride) and one strongly adsorbing compound (trichloroethylene). Table 2.4 details properties of the compounds (excluding 1,1 DCA) researched in this chapter.

4.4.1.3 Adsorbents

Norit GAC 400 granular activated carbon from CabotNorit was used for this effort. Norit GAC 400 is bituminous-based GAC and is representative of a range of bituminous-based GACs. The log-mean diameter of the as-received GAC was 0.92 mm (12 x 40 US Standard Sieve). The density of the GAC was determined to be 470 kg/m^3. Pore size distribution for Norit GAC 400 are given in Table 2.2.

4.4.2 Methods

4.4.2.1 Rapid small-scale column test (RSSCT) set-up

The specific design and set-up of the RSSCT-PD was done in accordance with the EPA Manual for Bench- and Pilot-Scale Treatment Studies (EPA, 1996); for the sake of brevity a summary overview is provided here. Using a mortal and pestle, GAC was ground to a sieve size of 100 x 200 (US Standard Sieve Size) equating to a log-mean diameter of 0.11 mm. Fines were decanted using DI water. The GAC was placed under vacuum for 24 hours; visible air bubbles were no longer seen when agitating the GAC beaker. Using a Pasteur pipette, GAC was transferred to a 4.76 mm ID Teflon column with glass wool inserted into the base to provide support for the GAC media. The ratio of Teflon column size to GAC diameter provided an aspect ratio of 44 and thereby eliminated the concern of wall effects (i.e. short-circuiting of water around the media). Two columns were run in series: the first contained 0.76 g of GAC and the second contained 1.52 g of GAC. Operated at a flow rate of 2.0 mL/min produced equivalent

full-scale EBCTs of 7.5 min and 15 min, respectively. Influent and effluent samples were collected every 1 to 2 days.

4.4.2.2 Sample preparation and analysis

All samples were collected headspace free in 40 mL glass VOC vials. VOC vials were washed were washed with Alconox detergent powder, triple rinsed in tap water followed by triple rinse in deionized water. Vials were muffled at 451C for 3 hours and stored in aluminum foil until use. Samples were preserved to a pH <2 and all attempts were made to complete analysis within 30 days of collection, although some samples exceeded this holding time.

4.4.2.3 GC/MS

The EPA's Office of Research and Development in Cincinnati, OH performed sample analyses for cVOCs. The Water Supply and Water Resources Division, National Risk Management Research Laboratory used a split-less head space injection method (modified EPA method 524.3) on an Agilent 7890A gas chromatography unit paired with a 5975C mass spectrometer. QA, QC and calibration recommendations from EPA method 524.3 were followed. Method Reporting Limits were less than 37 ppt for all cVOCs discussed within this chapter.

4.4.2.4 Size Exclusion Chromatography

SEC was accomplished using an Agilent 1220 High-Performance Liquid Chromatography instrument with a Protein Pack column (PT WAT 084-601; Waters Corporation). An Agilent diode array was used to measure UV_{254} absorbance. MWs (both weight-averaged and number-averaged) were determined inputting the sample elution time into the standard curve regression equation. Additional information on sample preparation, mobile phase, injection volumes, and calibration curve details are provided in Chapter 2.

4.4.2.5 Total Organic Carbon / Ultraviolet Absorbance / Ferrous and Total Iron / pH / Conductivity / Alkalinity

All measurements of these parameters were conducted in accordance with the applicable method from the U.S. E.P.A or Standard Methods from the American Public Health. Further details are provided in Chapter 2 of this work.

4.4.2.6 Fluorescence

Fluorescence analysis was conducted using a Horbia spectrofluorometer (Fluoromax-4, John Yvon Horiba Corporation). Lamp scans and cuvette checks were performed prior to analysis. Excitation wavelengths were from 240 nm to 450 nm in 10 nm increments with a 5 nm slit width. Emission wavelengths were integrated over 0.25 seconds and measured from 300 nm to 560 nm in 2 nm increments with a 5 nm slit width. Fluorescence intensities were measured in the (signal to reference) ratio mode. Instrument specific signal and reference detector correction factors were applied. Inner filtering effects were accounted for using sample UV absorbance data. Raman normalization (excitation: 350 nm; emission: 365 nm – 450 nm) accounted for Raman scattering by subtracting fluorescence observed in DI water blanks. First and second order Rayleigh scattering was removed through masking.

4.5 Results and Discussion

A summary of the 1,2 DCA breakthrough behavior can be seen in Table 4.1. Included is one run with CT. Multiple RSSCT experiments (n = 22; 11 sets of 2 EBCTs) were conducted with EBCTs of 7.5 minutes and 15 minutes.

Table 4.1 Summary of 1,2 DCA Breakthrough Behavior. 11 RSSCT experiments, each at 2 EBCTs (7.5 min and 15 min); 4 GWs, 1 surface water, and 1 DI water column. Bed volumes (BV) to 10% and 50% breakthrough are used to determine capacity differences at each EBCT. Horizontal lines indicated different source water or, in the case of CO II, a multi-solute column. All data is for 1,2 DCA with the exception of the last entry which reflects CT breakthrough data.

Water	TOC (mg/L)	1,2 DCA C_0 (µg/L)	BV10 (7.5 min)	BV10 (15 min)	BV50 (7.5 min)	BV50 (15 min)	BV10 diff (%)	BV50 diff (%)
CO I	0.3	53.2	13700	13300	15000	14400	3.0%	4.2%
CO I	0.3	4.3	20643	21317	23000	24000	-3.2%	-4.2%
CO I	0.3	0.4	24800	23300	25200	-	6.4%	
CO I	0.3	0.1	24500	26400	29700	29500	-7.2%	0.7%
CO II	1.5	49.0	8000	-	11300	-		
CO II	1.5	3.9	14500	13500	16200	14100	7.4%	14.9%
CO II	1.5	0.4	16000	18400	21900	21400	-13.0%	2.3%
CO II	1.5	4.2 (& CT: 1.8; TCE: 1.4)	13900	13500	16800	15300	3.0%	9.8%
BEM	1.5	4.6	16500	-	17700	-		
BEM	1.5	0.5	20200	-	22100	-		
dilCO II	0.8	4.8	16900	-	20000	-		
dilCO II	0.8	0.5	16600	-	27500	-		
OH	1.0	5.6	18400	22500	25500	23500	-18.2%	8.5%
OH	1.0	0.5	21400	17300	28000	19500	23.7%	43.6%
DI	0.1	5.0	30300	28200	33300	30000	7.4%	11.0%
DI	0.1	0.2	17400	17500	19800	23300	-0.6%	-15.0%
CO II	1.5	**CT: 1.8** (& 1,2DCA: 4.2; TCE: 1.4)	52500	61700	75400	75900	-14.9%	-0.7%

Figure 4.2 shows EBCT results from four columns in CO GW I at 1,2 DCA concentrations of 4.3 µg/L and 53.2 µg/L. At both concentrations the difference in 10% and 50% breakthrough was less than 5%. These differences can be explained with experimental error that occurred over an approximate 4-week experimental run time.

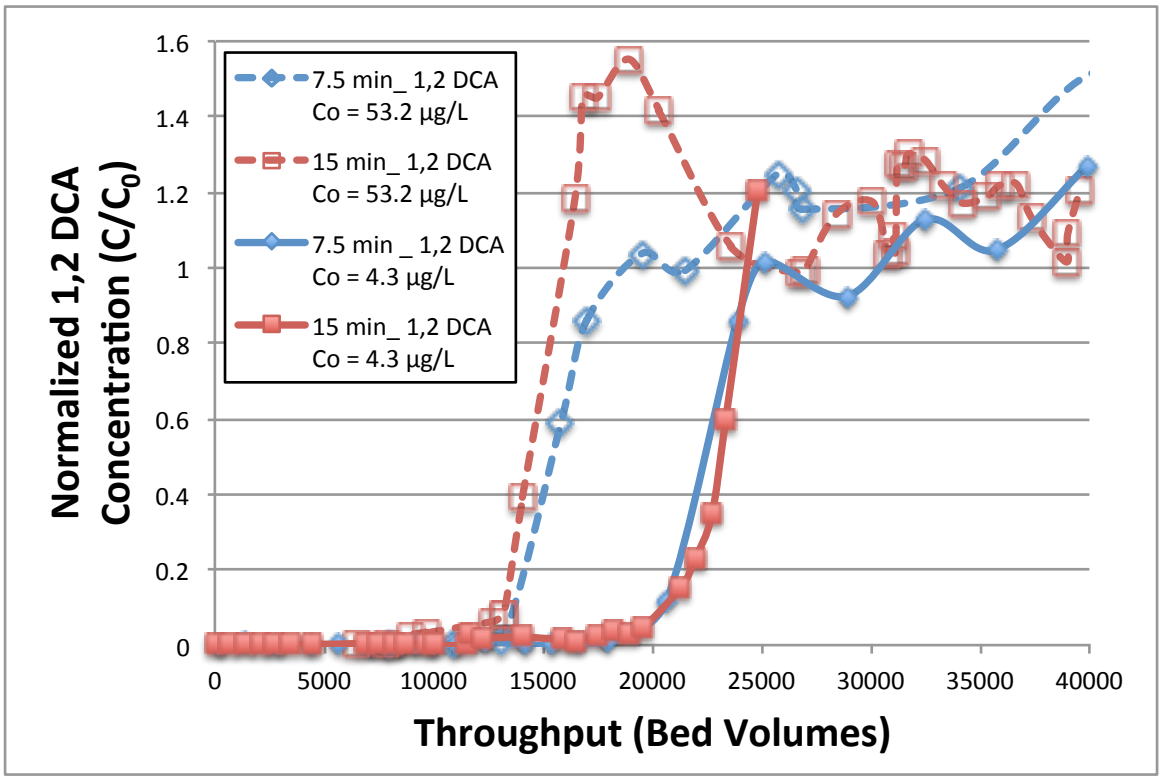

Figure 4.2 Effect of EBCT on 1,2 DCA Breakthrough at 2 different concentrations. Single Solute Columns; CO GW I (TOC: 0.3 mg/L); EBCTs: 7.5 min and 15 min.

Figure 4.3 shows results from the multi-solute column conducted in CO GW II (1,2 DCA C_0 = 4.2 µg/L; CT C_0 = 1.8 µg/L; TCE C_0 = 1.4 µg/L). Little difference, <10% in 1,2 DCA capacity, was found between the different EBCTs at both 10% and 50% breakthrough. The CT capacities were slightly larger but still modest; 15% and 1% differences at 10% and 50% breakthrough.

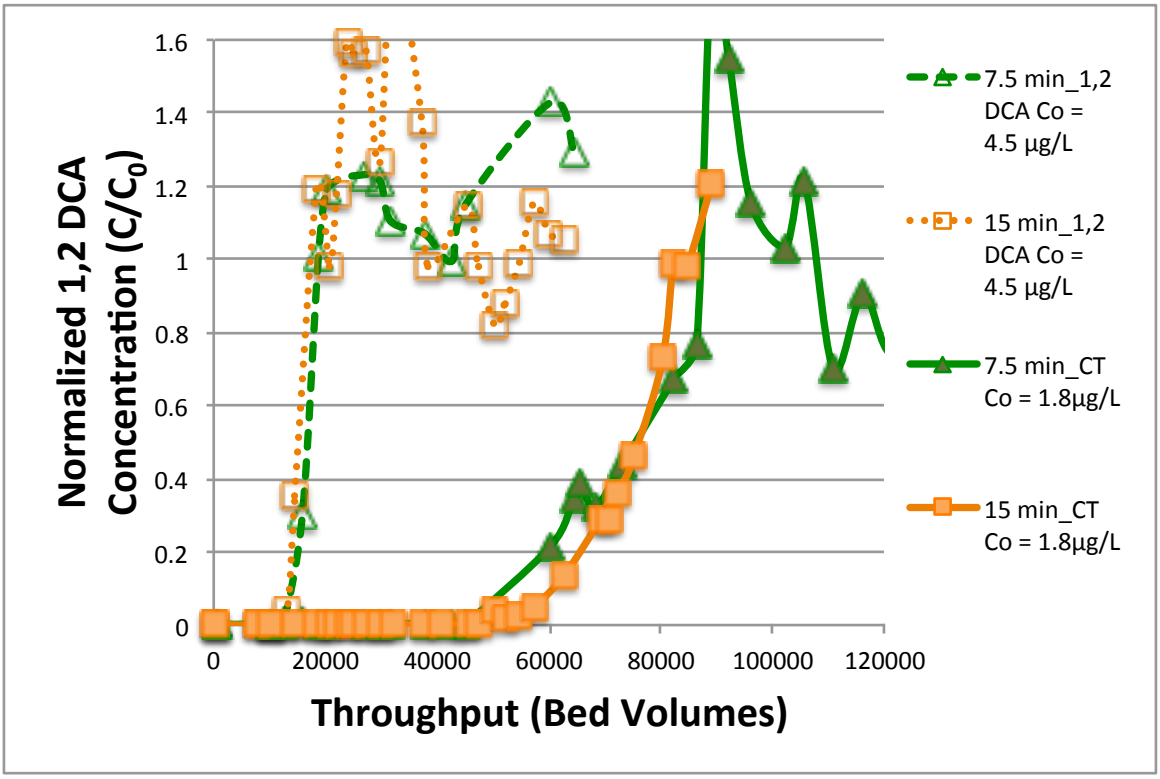

Figure 4.3 Effect of EBCT on 1,2 DCA and CT Breakthrough. Tri-Solute Column; CO GW II (TOC: 1.5 mg/L); EBCTs: 7.5 min and 15 min.

The difference in capacity measured at 10% breakthrough and 50% breakthrough of the initial concentration for the two EBCTs are reported in Table 4.1 for all experiments. Modest differences in capacity are seen but neither EBCT consistently demonstrates different throughput. 17 of 21 experiments showed capacity differences of 15% or less between the two EBCTs at breakthrough. Overall the difference between 7.5 minute and 15 minute EBCTs for 10% breakthrough was 3.0% with a standard deviation of 13%. These numbers are heavily influenced by the larger variability seen with the OH data. The four OH groundwater experiments showed capacity differences ranging between –18.2% and 43.6% for the two EBCTs but a large number of bed volumes passed during breakthrough without an effluent sample being collected and bed volume values at 10% and 50% breakthrough had to be estimated. If the OH data is removed the mean difference and standard deviation is 0.6% and 8%, respectively. All experiments (i.e. 13 of

13) conducted in the two Colorado groundwaters had capacity differences of less than 15%. The low concentration DI column (1,2 DCA C_0 = 0.2 μg/L) had results that were complicated by experimental and analytical variability in this concentration range approaching the analytical detection limit. Additional experimentation with nine other cVOCs was conducted elsewhere using OH GW using the same methodology and EBCTs. The bed volumes to 10% breakthrough reveals that the different capacities between EBCTs was the largest with 1,2 DCA (the data included in Table 4.1), but on average, the capacity difference for all 10 cVOCs was < 1% with a standard deviation of 11% between the two EBCTs.

The lack of consistent differences in capacity between the two EBCTs may be explained by characteristics of the adsorbate. Small, nonpolar target organics have been shown to more effectively displace preloaded DOM than their larger polar counterparts (Matsui et al., 2002a). 1,2 DCA is both non-polar and small in size (99 Da). The recalcitrant DOM character and lower DOM quantity in the groundwater background matrix is also believed to be responsible for the absence of capacity reduction with EBCT, as discussed in the background.

Greater displacement of 1,2 DCA is observed directly after breakthrough in the columns with 15 minute EBCTs, compared to that at 7.5 minutes. In the RSSCT experiments at 15 minute EBCT that were operated beyond complete breakthrough, five or eight curves had greater displacement in the 15 minute column with the three remaining columns having equal displacement to that at 7.5 minute EBCT. When including the OH data, seven columns had greater displacement while one column exhibited greater displacement in the 7.5 minute column and four columns had equal displacement. Merk had similar results but with much higher target organic concentrations, mg/L (Merk et al., 1981). The behavior may be explained by a competing fraction of DOM that is co-loading and competing with the target organic. As this

fraction migrates through a bed with a greater mass of GAC (i.e. bed with a longer EBCT), more displacement of the target organic is observed in the effluent.

The lack of reduced capacity with increasing EBCT is indicative that DOM fouling is not increasing with depth; however, DOM is reducing GAC capacity for target organics. This can be seen in Table 4.1 and the results for the RSSCT conducted in DI water. The DI column had almost 50% more capacity for 1,2 DCA on a bed volume basis than the lowest TOC groundwater (CO GW I; TOC: 0.3 mg/L). The experimental breakthrough curves for four groundwaters (TOC range: 0.3 mg/L – 1.5 mg/L) and 1 surface water (TOC adjusted to 1.5 mg/L) are shown in Figure 4.4 with the influent 1,2 DCA in the narrow range of 5.6 to 3.9 µg/L. The RSSCT conducted in DI is also shown on this figure. As TOC values increase, the GAC capacity for 1,2 DCA is reduced. The OH and dilCO II waters do not follow this trend. Although the OH GW had a higher TOC than the dilCO II (1.0 vs. 0.8 mg/L, respectively), size exclusion chromatography revealed that dilCO II contained a smaller sized DOM and therefore could compete better against the target organic. This is discussed further in the SEC section below.

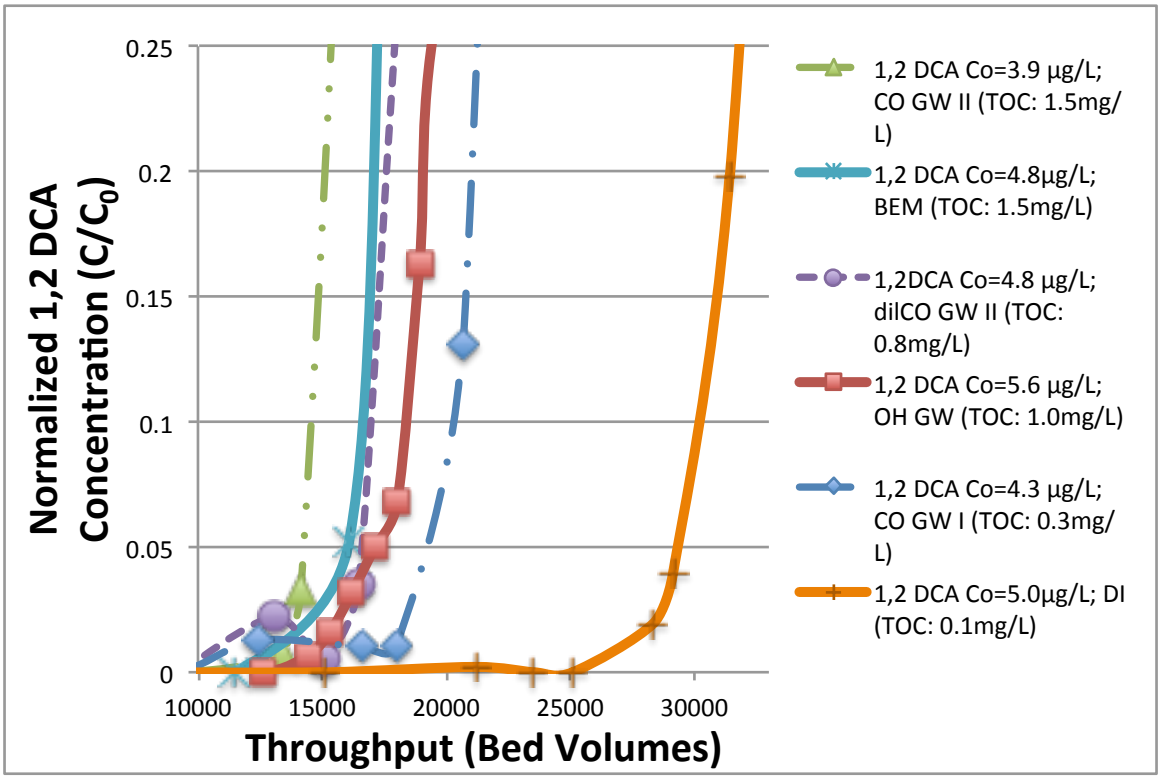

Figure 4.4 1,2 DCA Throughput as a function of Water Source; 4 GWs, 1 surface water and 1 DI water column; EBCT: 7.5 minutes.

Applying a regression line (solid line in Figure 4.5; n = 9; power function) to the 10% breakthrough data from RSSCT experiments with 1,2 DCA influent concentrations of approximately 5 µg/L, an R^2 value of 0.85 is obtained. The coefficient of determination was similar (R^2 = 0.84; n = 9) when correlating the bed volumes to 50% breakthrough as a function of TOC. When applying a regression (dashed line in Figure 4.5) to the 10% breakthrough data from RSSCT columns with 1,2 DCA influent concentrations of approximately 0.5 µg/L a lower R^2 value of 0.61 is obtained. Fewer data points available for this regression (n = 6) may explain the lower correlation. The 0.5 µg/L correlation does predict greater capacity than the model with at an influent concentration of 5 µg/L, making the output plausible. The predictive power of the regression is heavily influenced by the target organic concentration and correlation significantly drops off when all concentrations of 1,2 DCA are included. Summers saw similar results with a

power regression (R^2 = 0.82 and 0.84 for breakthrough to 10% and 50%; n = 16 and 13, respectively) for MIB adsorption at two different EBCTs; however influent MIB concentrations were kept constant (Summers et al., 2013).

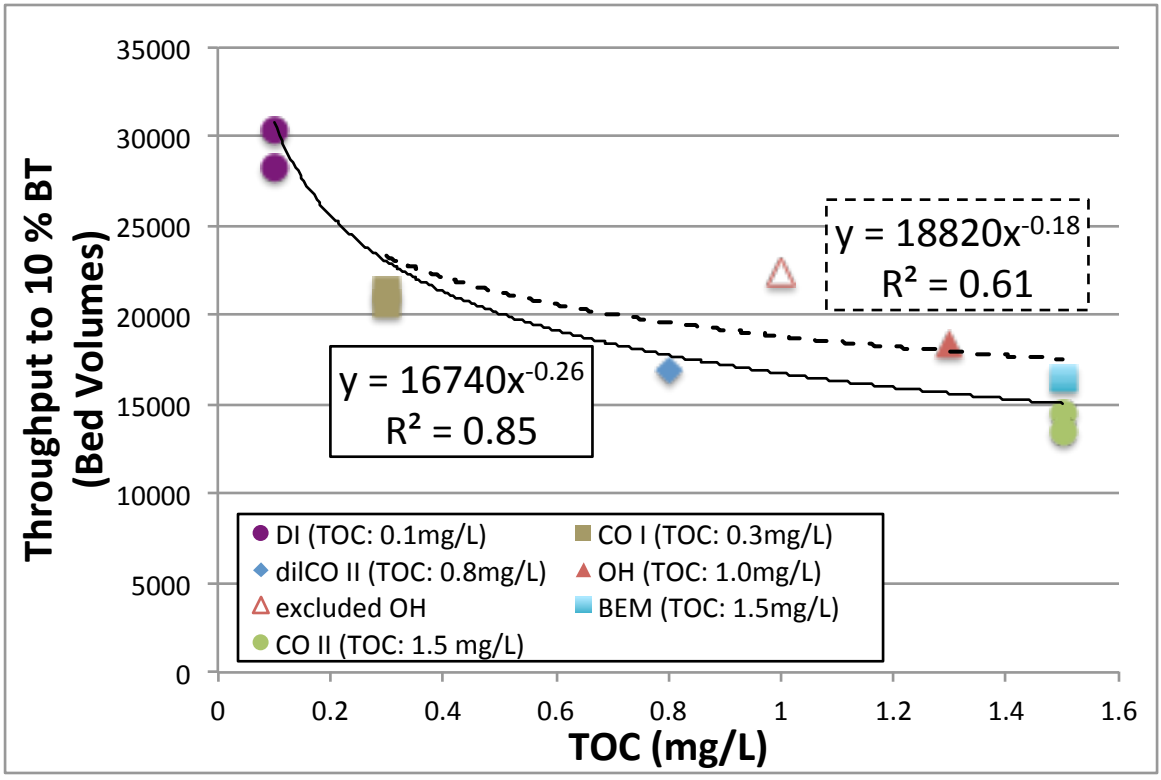

Figure 4.5 1,2 DCA Throughput as a function of TOC Concentration; Throughput measured to 10% breakthrough; 4 GWs, 1 surface water and 1 DI water column; EBCT: 7.5 min and 15 min; solid regression line and solid boxed regression equation represent all waters and all data points (excluding 1 EBCT: 15 min, OH GW data point) with average 1,2 DCA C_0 = 4.7 µg/L (range: 3.9 – 5.6 µg/L) (n = 9); dashed regression line and dashed boxed equation regression equation represent all waters and all data points with average 1,2 DCA C_0 = 0.5 µg/L (range: 0.40 – 0.51 µg/L) (n = 6).

To determine the effect of influent 1,2 DCA concentration on GAC capacity, multiple RSSCT experiments were run varying the influent concentrations between 0.1 µg/L and 53.2 µg/L. Breakthrough with the effluent concentration normalized to the influent concentration, was not found to be independent of influent concentration as it has been in other studies (Corwin and Summers, 2012; Rossner et al., 2009; Summers et al., 2013; Westerhoff et al., 2005). As can

be seen in Figure 4.6 for the low TOC end member of the GWs tested, CO GW I (TOC: 0.3 mg/L), the 1,2 DCA breaks through at distinctly different throughput values for influent concentrations spanning 2.5 orders of magnitude. The same behavior was observed for three other RSSCT columns using the high TOC end member (CO GW II; TOC: 1.5 mg/L) with influent 1,2 DCA concentrations ranging from 0.4 µg/L to 49.0 µg/L. Additional experimentation was not conducted at influent concentrations lower than 0.1 µg/L. Concentrations lower than this are well below the current maximum contaminant level of 5 µg/L and the MCL being considered, 0.5 µg/L, and thus are less of a concern for drinking water plant operators.

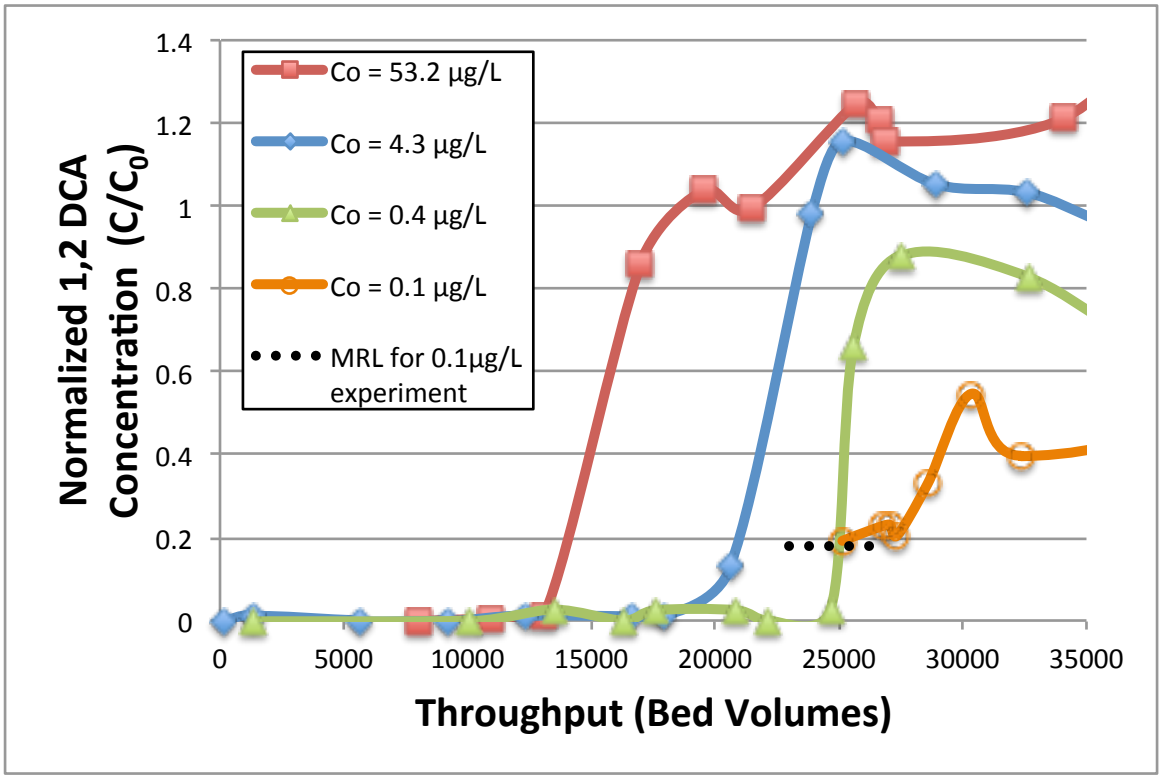

Figure 4.6 1,2 DCA Capacity as a function of C_0. CO GW I (TOC: 0.3 mg/L) EBCT: 7.5 min. Black dotted line represents the analytical method reporting limit for the RSSCT experiment conducted at an intial 1,2 DCA concentration of 0.1 µg/L.

The lack of influent concentration independence, or stated otherwise, the dependence of

breakthrough on influent concentration is expressed in Figure 4.7. Regressions using bed volumes to 10% breakthrough for CO GW I (dashed) and CO GW II (solid) are shown on the figure. The coefficients of determination are quite high (R^2 = 0.91 and 0.90, respectively) but these regressions only consider data from their respective water sources. When different water sources are considered, R^2 values drop dramatically (R^2 = 0.27). The reason for the lack on influent concentration independence is again believed to involve the background matrix of GW DOM. In addition to lower median concentrations of DOM in GWs (TOC: 0.8 mg/L vs surface water median: 3.7 mg/L), fractionation of organic carbon has shown GW to be significantly more hydrophilic than surface water (Krasner et al., 1995; Thurman, 1985). The longer residence times of DOM in GW results in the hydrophobic portion sorbing onto aquifer solids and/or degrading into simple organic acids by bacteria in the aquifer (Thurman, 1985). The independence of influent concentration occurs when the solid phase concentration of target organic is very small compared to the solid phase concentration of DOM (Matsui et al., 2002b). Since the concentration of the DOM in groundwater is both lower and less likely to adsorb to the GAC, the solid phase concentration may not be great enough to cause the independence of influent concentration effect to occur.

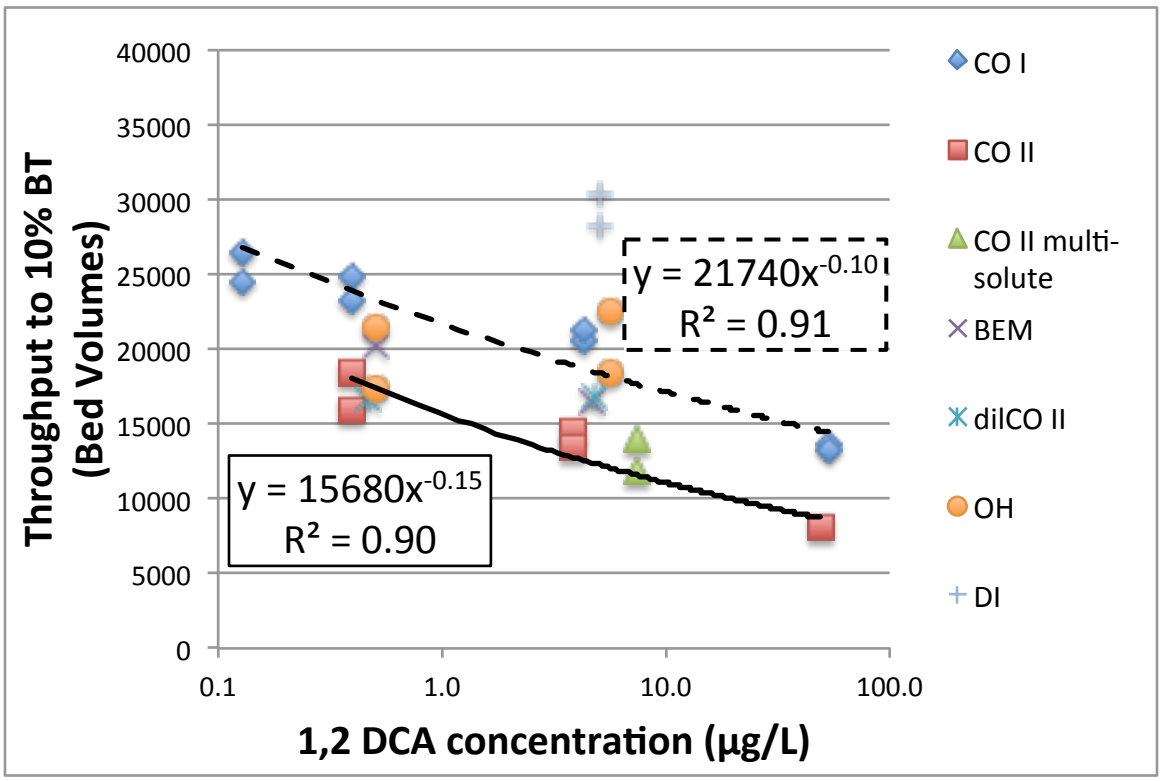

Figure 4.7 Throughput to 10% Breakthrough as a function of influent 1,2 DCA concentration. EBCT: 7.5 and 15 min. Solid line regression considers all CO GW II experiments (n = 6); dashed line regression considers all CO GW I experiments (n = 8).

Although the *quantity* of both the target organic and the DOM were shown to affect adsorption, the *character* of the DOM also affects GAC capacity and kinetics. High performance size exclusion chromatography (SEC), UV spectroscopy and fluorescence analysis were conducted in the four groundwaters to explore how different DOM characteristics affect adsorption.

SEC with UV detection was used to determine the MW distribution of the various background matrices in the four groundwaters used in this study. Results of the SEC are in Table 4.2; figures of the MW distribution (normalized to TOC and non-normalized) are included in the appendix. Results for the different waters were somewhat inconclusive, as the SEC results did not have the fidelity to distinguish significant differences in the MWs of the DOM.

Although SEC-UV has often been used to determine MW distributions of DOM, Her found this analysis to be lacking because UV absorbance at 254 nm only detects a particular group of chromophores and consequently other chromophores go unaccounted (Her et al., 2002). One observation; however, can be drawn. dilCO II MW_w is about 30% smaller than OH GW and although the OH GW had a higher TOC (1.0 mg/L vs. dilCO II: 0.8 mg/L), higher influent concentration of 1,2 DCA (5.6 µg/L vs. dilCO II: 4.8 µg/L), and a similar SUVA value (1.55 L/mg-m vs. dilCO II: 1.53 L/mg-m), the dilCO II breakthrough occurred first. Comparing breakthrough to 10% and 50%, the dilCO II column had 8% and 22% less capacity than the OH GW, respectively. These results are in agreement with other work that has shown target organic adsorption is more adversely affected by smaller DOM MWs (Kennedy, 2013; Matsui et al., 2002a).

Table 4.2 Size Exclusion Chromatography Results for 4 GWs

Water	TOC (mg/L)	MW_w (Da)	d (polydispersity)
dilCO II	0.8	511	1.5
OH GW	1.0	732	2.1
CO GW II	1.5	837	2.1
CO GW I	0.3	972	4.1

Various fluorescence metrics were investigated to determine their utility in predicting 1,2 DCA breakthrough. High correlation values ($R^2 \sim 0.95$) can be obtained when using one 1,2 DCA concentration and fluorescent properties such as peak A and C intensities, however, R^2 values drop significantly ($R^2 \sim 0.43$) when concentrations across the 2.5 orders of magnitude used in this study are included. Fluorescent properties such as those proposed by Kalbitz and Baker (e.g. HIX, peak T to peak C ratio, peak C to UV_{340} ratio, etc) produced similar low R^2 values when all 1,2 DCA concentrations were considered. Quantifying fluorescent properties by

applied a DOM mass term (e.g. multiplying or dividing by TOC concentration or using UV_{254} absorbance as a TOC surrogate), also resulted in low R^2 values when applied across the 1,2 DCA concentration range. Fluorescent properties were also adjusted by applying a TOC mass term *and* a 1,2 DCA mass term. The use of UV_{254} absorbance as a surrogate to TOC concentration term has previously been demonstrated (Kennedy, 2013) and was used in certain cases during this study to represent TOC mass. Figure 4.8 shows the results of 22 RSSCT experiments and compares bed volumes to 10% breakthrough as a function of the FI * TOC concentration * 1,2 DCA concentration. Accounting for the entire range of 1,2 DCA concentrations in this study (0.1 µg/L to 53.2 µg/L) the regression has an R^2 value of 0.79. The regression equation is presented as equation 4.1.

$$Throughput_{BV\ 10\%}^{PD-RSSCT} = 19400 * (FI * TOC * 1{,}2\ DCA\ C_0)^{-0.12} \qquad (eqn.\ 4.1)$$

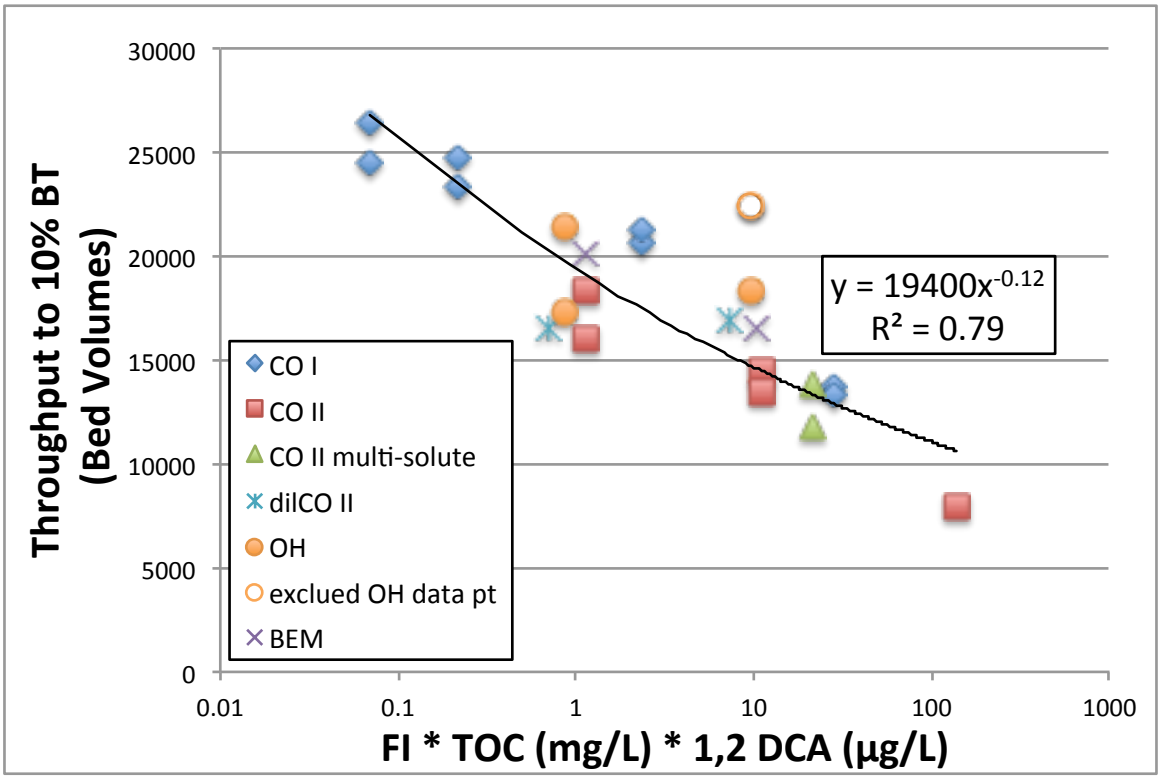

Figure 4.8 1,2 DCA Throughput as a function of FI * TOC * 1,2 DCA; n = 22; Throughput measured to 10% breakthrough; 4 GWs, 1 surface water; single solute columns except where noted multi-solute; EBCT: 7.5 min and 15 min; regression represents all waters and all data points (excluding 1 EBCT: 15 min, OH GW data point) with 1,2 DCA C_0 ranging from 0.1 µg/L – 53.2 µg/L.

Similar R^2 values were obtained when applying TOC (or UV absorbance) and 1,2 DCA mass terms to the HIX (R^2 = 0.79), and Peak C (R^2 = 0.79). The best predictors included a 1,2 DCA mass term, a UV absorbance term and surrogate terms for fluorescence quantum yield: 1,2 DCA concentration*Peak C/UV_{340} (R^2 = 0.82; n = 22) and 1,2 DCA concentration*Peak C/UV max absorbance (R^2 = 0.82; n = 22). The UV absorbance data is provided in the appendix. Table 4.3 summarizes eight regressions correlating various fluorescent properties to predict bed volumes to 10% 1,2 DCA breakthrough.

Table 4.3 Summary Table of Regressions created to Predict RSSCT BV_{10} from DOM Characteristics. *N = 19 for the OH excluded column; ** Regression 1 considers 1,2 DCA concentrations ~5 µg/L; all other regressions consider 1,2 DCA C_0 range = 0.1 µg/L – 53.2 µg/L

Regression ID	Descriptor	n	function	y	x	a	b	R^2	R^2* (OH excluded)
1**	Peak A	10	y = ax+b	RSSCT BV_{10}	PeakA	-9090	21400	0.95	-
2	Peak A	22			PeakA	-8650	21570	0.43	-
3	microbial - terrestrial	22	$y = ax^{-b}$	RSSCT BV_{10}	FI*TOC*1,2DCA	19400	0.12	0.79	0.83
4	humic				HIX*TOC*1,2DCA	19910	0.10	0.79	0.84
5	aromaticity				PeakC/TOC*1,2DCA	14130	0.12	0.79	0.84
6	size				PeakC/UV_{340}*1,2 DCA	26260	0.12	0.82	0.87
7	labile - recalcitrant				PeakT/PeakC*TOC*1,2DCA	18400	0.11	0.54	0.56
8	aromaticity				SUVA*TOC*1,2DCA	18970	0.12	0.74	0.78

As discussed earlier, experiments for the OH GW were conducted elsewhere and not under direct observation at CU-Boulder. Additionally, effluent samples were not collected in timely manner during breakthrough for some of the OH data requiring estimates to be made about breakthrough. For these reasons, the OH data points were removed from the regression. Figure 4.9 shows bed volumes to 10% breakthrough as a function of 1,2 DCA concentration*PeakC/ UV_{340} (R^2 = 0.87; n = 19). Equation 4.2 is regression based on these characteristics.

$$Throughput_{BV\ 10\%}^{PD-RSSCT} = 26250 * \left(\frac{Peak\ C}{UV_{340}} * 1{,}2\ DCA\ C_0\right)^{-0.12} \qquad (eqn.\ 4.2)$$

The other fluorescent metrics in Table 4.3 showed similar increases in R^2 when the OH data was excluded.

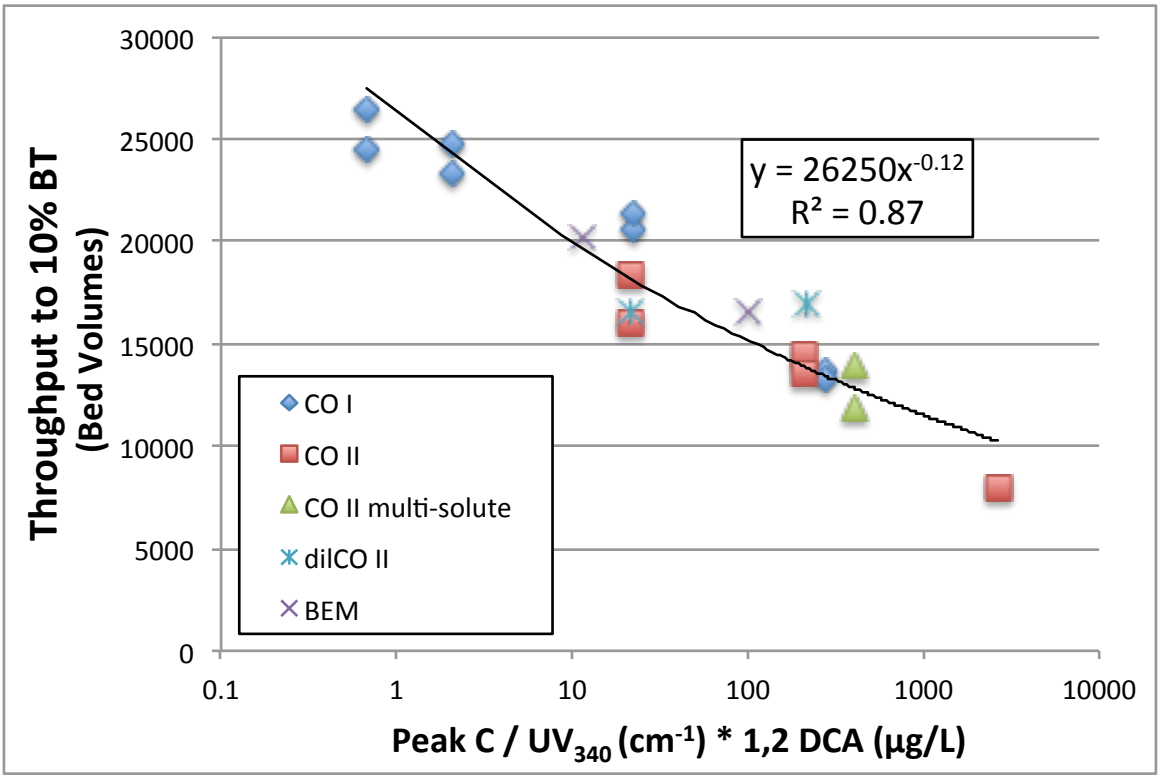

Figure 4.9 1,2 DCA Throughput as a function of Peak C / UV_{340} * 1,2 DCA; n = 22; Throughput measured to 10% breakthrough; 3 GWs, 1 surface water; single solute columns except where noted multi-solute; EBCT: 7.5 min and 15 min; regression represents all water and all data points shown; 1,2 DCA C_0 range from 0.1 µg/L – 53.2 µg/L.

The use of fluorescence is relatively easy and quick, *if* the capability exists at a site. For cases where fluorescence capability is not available, the use the specific ultraviolet absorbance was investigated. This value is the TOC-normalized absorbance at 254 nm and is easy to obtain with a spectrophotometer. The bed volumes to 10% breakthrough as a function of the SUVA * TOC concentration * 1,2 DCA concentration can be seen in Figure 4.10. Relatively high coefficients of determination were found when using a power function regression (R^2 = 0.74; n = 22). When the OH data is excluded a slightly higher R^2 value is achieved (data not shown; R^2 = 0.78; n = 19). Multiplying the SUVA value and the TOC concentration together eliminates the TOC mass term, which eliminates the need for TOC analytical capabilities. Therefore, UV absorbance and 1,2 DCA concentration are the only analytical capabilities required to predict 1,2

DCA breakthrough using this regression which is represented as equation 4.3.

$$Throughput_{BV\ 10\%}^{PD-RSSCT} = 18970 * (UV_{254} * 1{,}2\ DCA\ C_0)^{-0.12} \qquad (eqn.\ 4.3)$$

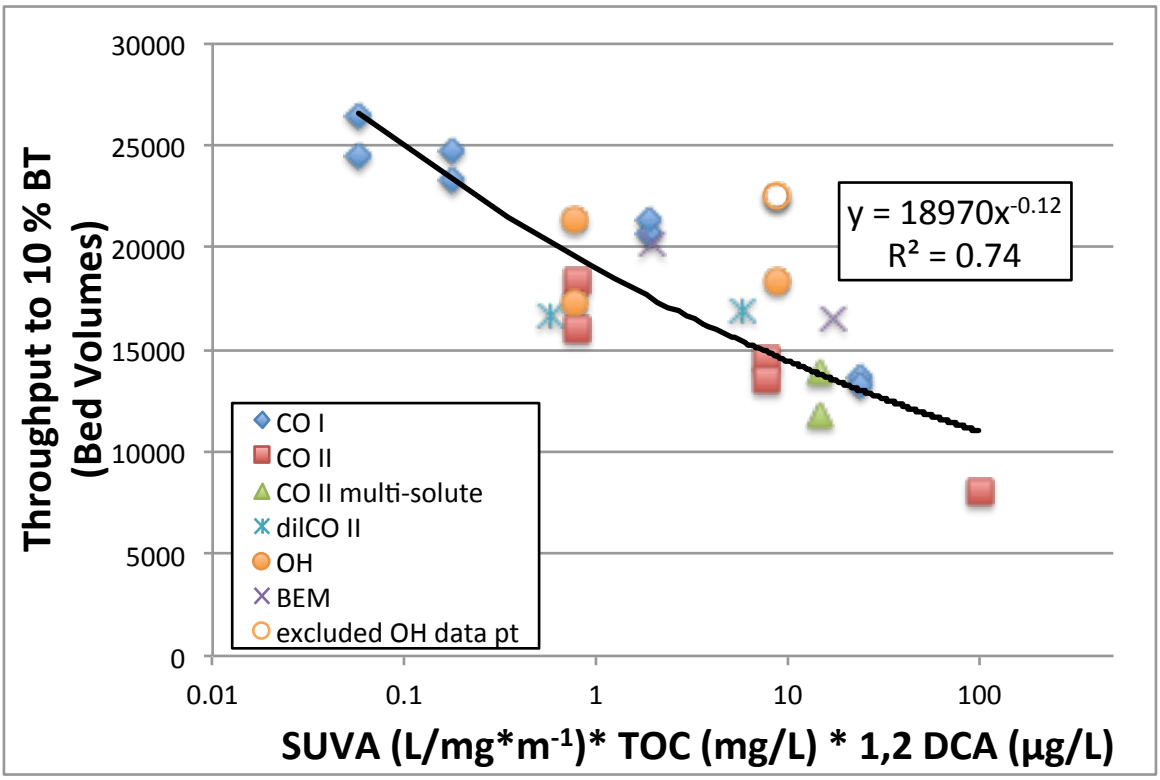

Figure 4.10 1,2 DCA Throughput as a function of UV_{254} * 1,2 DCA; n = 22; Throughput measured to 10% breakthrough; 4 GWs, 1 surface water; single solute columns except where noted multi-solute; EBCT: 7.5 min and 15 min; regression represents all water and all data points shown (excluding OH GW data point; EBCT: 15 min) (open circle symbol); 1,2 DCA C_0 range from 0.1 µg/L – 53.2 µg/L.

4.6 Conclusions

Understanding how DOM affects the efficacy of 1,2 DCA removal by GAC in groundwaters is crucial to water treatment operations. This effort investigated DOM effects on four GWs and one surface water. Longer EBCTs did not significantly reduce the GAC capacity for 1,2 DCA and therefore increased GAC fouling with depth is not occurring. DOM does however reduce the overall GAC capacity for 1,2 DCA as demonstrated by a throughput reduction of between 20% and 32% when comparing organic-free water to the lowest TOC end

member GW (CO GW I; TOC: 0.3 mg/L). This capacity reduction is indicative of DOM co-loading and direct site competition occurring in the GAC column. Spanning 2.5 orders of magnitude, this effort did not find normalized breakthrough to be independent of influent concentration, unlike other efforts (Corwin and Summers, 2012; Matsui et al., 2002b; Summers et al., 2013). In addition to concentration, characteristics of the DOM were investigated with HPSEC, UV absorbance, and fluorescence. Regressions were created to predict bed volumes to 10% 1,2 DCA breakthrough. A regression involving peak C fluorescent intensity, UV_{340} absorbance, and 1,2 DCA concentration was the best predictor of breakthrough. Other regressions incorporated 1,2 DCA and DOM mass terms with the HIX, FI, peak C intensity produced similar results. A simpler regression eliminating the fluorescence term and using only UV_{254} absorbance and 1,2 DCA concentration was also created with satisfactory results.

Chapter 5 Scale-Up of RSSCT Results to Predict Full-Scale Adsorber Performance

5.1 Abstract

The use of bench-scale GAC columns with a smaller media and column size to predict full-scale adsorber capacity offer several advantages; shorter time to results, smaller volume of water, reduced analytical sample load, and greater experimental control are just a few of the benefits. However, if the veracity of the bench-scale results is uncertain, the effort is less useful. The overall objective of this study is to increase the confidence in bench-scale proportional diffusivity - rapid small scale column tests (PD-RSSCT) results by applying current, and developing new, scale-up methods to accurately predict full-scale adsorber performance. Two PD-RSSCT columns using different GAC particle diameters (log mean: 0.11 mm and 0.49 mm) were operated at EBCTs of 7.5 minutes and 15 minutes to treat water containing 5 µg/L or less of 1,2 DCA, CT and TCE. Both columns used a groundwater background matrix with a TOC of 1.5 mg/L.

No difference in the DOM solid-phase concentration was observed between columns using two different sized GAC particles, however significantly greater capacity for 1,2 cVOCs was observed in the columns containing the smaller GAC. The overprediction of throughput to 50% breakthrough ranged from 42% to 140% and was not as great as observed in other experiments involving a majority of surface waters (300% +/- 120%; n = 101) (Kennedy, 2013). Groundwater DOM is more hydrophilic and will not contribute to GAC pore blockage as much as its surface water counterpart and therefore will affect GAC particles of different sizes to a lesser extent. Nearly 97% of the adsorbed 1,2 DCA was displaced by the more strongly adsorbing CT. Significant differences were observed in the solid-phase concentration of cVOC

on the two GAC particle sizes. For 1,2 DCA, the 0.11 mm column had approximately 50% more loading than the 0.49 mm column for both EBCTs of 7.5 and 15 minutes. For CT, the difference was more pronounced: 2.7 more loading occurring on the column containing the smaller GAC. A fouling index (FI) was applied to address RSSCT over-prediction (Corwin and Summers, 2010). Visual fouling factors, existing regression equations, and two new models determining Y as a function of C_0/TOC_0 were used. Existing regression equations predicted the two Y values for CT exceptionally well (within 5% and 10%), but, failed to adequately correct the two 1,2 DCA columns (overcorrects by 30%). A model developed with this effort performed well - all four Y values were within the 95% CI for the model simulation.

5.2 Introduction and Background

Evaluating GAC performance can be done with multiple methodologies. Full-scale and pilot-scale operations provide a direct measure of GAC performance but can be resource intensive in regards to time, sampling and volume of water required. Often modifications to process variables cannot be easily made without significant effort (e.g. change of empty bed contact time). Other times, unintended changes may be beyond the operators' control and constant conditions may not be able to be maintained over the column run time (e.g. change to influent concentration).

Batch systems and isotherm work can provide capacity comparisons between different adsorbents but drawbacks exist. Batch systems and flow-though columns differ in the adsorbate-adsorbent interaction. In a flow-through column, the mass transfer zone (MTZ) for the adsorbate is often shorter than the DOM's MTZ. When the adsorbate reaches deeper into the carbon bed, the carbon is already loaded with DOM. This can result in pre-loading of the carbon and resulting in both reduced GAC capacity and kinetics (i.e. carbon fouling). This is the not case

with batch isotherm work when both the adsorbate and the DOM are introduced at the same time and each component 'sees' fresh carbon simultaneously. Batch isotherm work and flow-through columns also have different driving forces for the adsorption process. In the flow-through column, the concentration gradient in the bulk flow is very small and gradually increases as the MTZ travels through. The opposite is the case for batch systems where the strongest concentration gradient is first encountered and gradually decreases as the fixed quantity of adsorbate in the batch is removed. Conducting batch isotherms with carbon preloaded with DOM has been done but doesn't resolve the issue entirely because the flow-through columns are dynamic and non-steady state; preloading carbon with DOM only provides one incremental point in the mass-transfer continuum. Once calibrated, model predictions can result in significant time savings and be a valuable design tool, however, kinetic and isotherm work with the natural water of interest is often required first (Sontheimer et al., 1988).

The rapid small-scale column test (RSSCT) is another methodology used to predict GAC capacity for contaminants of concern. The RSSCT offers three primary advantages over alternative experimental methods: (1) an RSSCT may be conducted in a fraction of the time that is required to conduct pilot studies; (2) unlike predictive mathematical models, extensive isotherm or kinetic studies are not required to obtain a full-scale performance prediction; and, (3) a small volume of water is required to conduct the test (Crittenden et al., 1987). Overall, it has been estimated that less than 10% of the time and water is required for RSSCT experiments to produce comparable full-scale column data (Berrigan, 2004). In addition, the RSSCT also provides greater experimental control. Variables such as the EBCT, carbon type, and parallel or series adsorber configuration can be adjusted with predicted full-scale performance in a fraction of the time. The value of these advantages is negated though if accurate scale-up cannot be

accomplished. Previous work has explored the utility of the RSSCT to accurately project full-scale column performance but results have varied. Additionally, the previous scale-up work was either done with contaminants other than cVOCs or at concentrations higher than the sub-µg/L range (Corwin and Summers, 2010; Crittenden et al., 1989; Kennedy, 2013; Knappe et al., 1997; Speth and Miltner, 1989; Summers et al., 1989).

Maintaining similitude between the small-scale and full-scale dimensionless numbers responsible for mass transfer, Crittenden demonstrated that the RSSCT could predict full-scale adsorber performance (Crittenden et al., 1987; 1986a). The mass transfer mechanisms considered in the design of the RSSCT come from equations in the dispersed flow pore and surface diffusion model and include advective flow, axial dispersion and diffusion, liquid-phase mass transfer resistance, local adsorption equilibrium, and surface and pore diffusion (Speth and Miltner, 1989). Two key assumptions must also be made to equate the RSSCT capacity with a full-scale adsorber: the properties (adsorbent capacity, porosity, and surface area) of the small- and large-GAC particles are identical and all adsorbates have equal access to all adsorption sites (Corwin and Summers, 2010). Generally, one of two RSSCT designs is used to simulate full-scale adsorbers. One is the constant diffusivity (CD) design and the other is the proportional diffusivity (PD) design. These designs differ in the scaling of the intraparticle diffusion of the target organic. The CD design assumes a constant diffusivity occurring within GAC particles of different sizes. The PD design uses a diffusivity value that is linearly proportional to GAC particle sizes in the full-scale and RSSCT. More discussion on the design of the RSSCT is included in chapter two of this document.

Selecting the design of the RSSCT depends upon the objective of the study. Past research has shown the CD-design to accurately predict contaminant breakthrough in organic-

free water and the early portion of contaminant breakthrough in natural waters (Crittenden et al., 1991; Knappe et al., 1997; Summers et al., 1989). The PD-design has been shown to accurately predict the DOM breakthrough profile in natural waters (Crittenden et al., 1991; Cummings and Summers, 1994). As DOM is the primary source of competition with trace organic contaminants for adsorption sites, and treatment in natural waters is emphasized in this effort, the PD-RSSCT was chosen as the design type for this effort.

Although the RSSCT will theoretically produce identical results to full-scale adsorber performance, previous research efforts involving natural waters have not shown this to be the case. Historically, the RSSCTs over-predict full-scale GAC capacity (Corwin and Summers, 2010; Crittenden et al., 1989; Fotta, 2012; Kennedy, 2013; Summers et al., 1989). A variety of causes have been cited as responsible for the over-prediction. The effects of DOM in the background matrix are greater on a larger GAC particle, resulting in increased small-scale capacity (Corwin and Summers, 2010). Pore blockage is the proposed explanation for this where more surface area is blocked behind the pore of a large GAC particle than behind the pore of a small GAC particle (Corwin and Summers, 2010). Direct competition between DOM and the target organic for a limited number of adsorption sites is another major contributor to reduced GAC capacity (Sontheimer et al., 1988). Specifically, the molecular weight and the concentration differences of the DOM and the target organic have been shown to reduce target organic capacity (Kennedy, 2013; Kilduff et al., 1998; Li et al., 2003a; Matsui et al., 2003). DOM has also been suggested to increase the boundary layer around a GAC particle and thereby reduce the external film mass transfer rate (Schideman et al., 2006). Another explanation for improper scaling between the RSSCT and full-scale adsorbers may be due to a surface complexation reaction occurring between DOM and the GAC surface (Summers et al., 1989).

Increased concentrations of oxygen in the process water can promote this surface complexation and results have shown a reduced capacity for target organics (Cerminara et al., 1995; Vidic et al., 1992). Surface complexation reactions are not accounted for in RSSCT scaling equations.

Attempts have been made to scale-up RSSCT results to accurately predict full-scale adsorber performance. Using both GWs and surface waters, Jarvie developed an empirical equation based on the target organic chemical class to produce a reduced Freundlich K as a function of DOM exposure time that is input into the PSDM to predict full-scale adsorber performance (Jarvie et al., 2005). Again based on empirical evidence, Kennedy developed a regression using 73 pairs of bench- and full-scale breakthrough curves to predict full-sized adsorber performance (Kennedy, 2013). Earlier, using breakthrough data from six micropollutants, Corwin and Summers developed a correction factor called the fouling index (FI). The FI is based on the scaling factor between two adsorbers using different sized media and is raised to some power.

The objective of this study was to increase the confidence in the PD-RSSCT for use with cVOCs in groundwater. The approach was to apply current, and develop new, scale-up methods to accurately predict full-scale adsorber performance. Two PD-RSSCT columns using different GAC particle diameters (log mean: 0.11 mm and 0.49 mm) were operated at EBCTs of 7.5 minutes and 15 minutes to treat GW with a TOC of 1.5 mg/L and containing 5 µg/L or less of 1,2 DCA, CT and TCE. The FI approach, as explained further in the materials and method section, was used in three ways in this chapter: visually, and with two different correlations involving the log D molecular property of a compound, RSSCT capacity, and a ratio of influent concentrations of the target organic and DOM.

5.3 Materials and Methods

5.3.1 Materials

5.3.1.1 Water

A Colorado groundwater, designated CO GW II, was used for the scale-up portion of this research. CO GW II is extracted from two 600' deep wells that reach into the Laramie-Fox Hills aquifer in the eastern portion of Boulder County, CO. Properties and pre-treatment details for CO GW II are provided in Chapter 2 and Table 2.1.

5.3.1.2 Adsorbates

Carcinogenic volatile organic compounds were obtained from Sigma Aldrich of St Louis, MO. All cVOCs were *analytical standard* grade and in neat form. The three cVOCs used in this effort represented a range of applicable adsorbtivities; one weakly adsorbing (1,2 dichloroethane), one moderately adsorbing (carbon tetrachloride) and one strongly adsorbing (trichloroethylene) cVOC were used in each tri-solute RSSCT. Table 2.4 provides additional details about these three solutes.

5.3.1.3 Adsorbents

Norit GAC 400 granular activated carbon from CabotNorit was used for this effort. Norit GAC 400 is virgin bituminous-based GAC and is representative of a range of bituminous-based GACs. The log-mean diameter of the as-received GAC was 0.92 mm (12 x 40 US Standard Sieve). The bed density of the GAC was determined to be 470 kg/m3. Pore size distribution for Norit GAC 400 are given in Table 2.2.

5.3.2 Methods

5.3.2.1 RSSCT set-up

The proportional diffusivity design was chosen for the RSSCT in this effort because it has been shown to accurately predict DOM breakthrough (Crittenden et al., 1991; Cummings and Summers, 1994). The specific design and set-up of the PD-RSSCT was done in accordance with the EPA Manual for Bench- and Pilot-Scale Treatment Studies (EPA, 1996). The reader is referred to Chapter 2 for more information regarding the methods used to design and construct the RSSCTs used in this chapter.

5.3.2.2 Sample preparation and analysis

All samples were collected headspace free in 40 mL glass VOC vials. VOC vials were washed were washed with Alconox detergent powder, triple rinsed in tap water followed by triple rinse in deionized water. Vials were muffled at 451C for 3 hours and stored in aluminum foil until use. Samples were preserved to a pH < 2 and all attempts were made to complete analysis within 30 days of collection, although some samples exceeded this holding time.

5.3.2.3 Analytics

The EPA's Office of Research and Development in Cincinnati, OH performed sample analyses for cVOCs. The Water Supply and Water Resources Division, National Risk Management Research Laboratory used a split-less headspace injection method (modified EPA method 524.3) on an Agilent 7890A gas chromatography unit paired with a 5975C mass spectrometer. QA, QC and calibration recommendations from EPA method 524.3 were followed. An 8-point calibration curve was used and a blank or check sample was run every ten samples. Method Reporting Limits were less than 37 ppt for all cVOCs discussed within this chapter.

5.3.2.4 Scaling Equations

The FI concept was used in this effort to scale up RSSCT results. The FI corrects the throughput of a column using a smaller GAC particle to predict the capacity of a second, larger GAC particle size column. The throughput of a full-scale adsorber can be predicted with equation 5.1.

$$Throughput_{\text{full-scale}} = \frac{Throughput_{\text{RSSCT}}}{\text{FI}} \qquad (eqn.\,5.1)$$

where throughput is measured in number of bed volumes passed until the treatment objective is exceeded, and FI is the scaling factor (SF) raised to a fouling factor, Y. The scaling factor is the ratio of GAC particle diameters in the larger and smaller columns. The FI is represented by equation 5.2.

$$\text{FI} = \text{SF}^{\text{Y}} = \left[\frac{\text{diameter}_{\text{GAC(full-scale)}}}{\text{diameter}_{\text{GAC(RSSCT)}}}\right]^{\text{Y}} \qquad (eqn.\,5.2)$$

The FI can be determined visually by adjusting the Y value until the RSSCT throughput matches the full-scale adsorber. This approach requires two RSSCTs using different sized GAC particles to obtain the Y factor. The visual approach to determine Y was used in this effort.

Attempts using the target organic's octonol-water partition coefficient have been made to predict the fouling factor without conducting multiple RSSCTs (Fotta, 2012). Expanding upon this and using the parameters of the target organic's pH dependent octanol-water partition coefficient (log D), the ratio of the target organic concentration to the TOC concentration, and the RSSCT throughput to 10% breakthrough, Kennedy developed a regression equation to predict Y values (Kennedy, 2013). Results from 73 RSSCT breakthrough curves were used in the development of the equation 5.3.

$$Y = [2.59 + 3.94 * \frac{C_0^{MP}}{TOC_0} - 7.87 * BV_{10\%}^{PD-RSSCT} - 0.402 * logD +$$

$$4.2 * 10^{-4} * \left(\frac{C_0^{MP} * BV_{10\%}^{PD-RSSCT}}{TOC_0}\right) + 2.86 * 10^{-6} * BV_{10\%}^{PD-RSSCT} * logD]^{-1.47} \quad (eqn. 5.3)$$

MP stands for the micropollutant, or target organic. Predictions using this regression are compared to visual FI approximations and the regressions created during this effort as discussed below.

5.4 Results and Discussion

Figure 5.1 shows the TOC breakthrough curves for PD-RSSCTs using two different GAC particle diameters (0.11 mm and 0.49 mm) at two different EBCTs (7.5 min and 15 min). The curves for the groundwater columns are very similar from 10% to 70% breakthrough. By integrating the area above the breakthrough curves and accounting for throughput and mass of carbon in each RSSCT, the solid phase concentration (q) of the DOM can be determined. Table 5.1 shows q at 50% and 70% of TOC breakthrough, q_50 and q_70, respectively. The q_70 values are essentially the same between the 0.11 mm/7.5 min small column and the larger 0.49/15 min column and while the q_50 values have a slightly greater difference, the overall trend of TOC breakthrough is predicted well with the PD-RSSCT design used in this study. An empirical model was used to generate the DOM breakthrough for a third particle size and EBCT (0.92 mm; 10 min) (Zachman and Summers, 2010). The model was developed using results from 221 RSSCTs; 84% of which were surface water sources. Groundwater DOM is more recalcitrant than it's surface water counterpart and therefore the earlier breakthrough of GW DOM is expected.

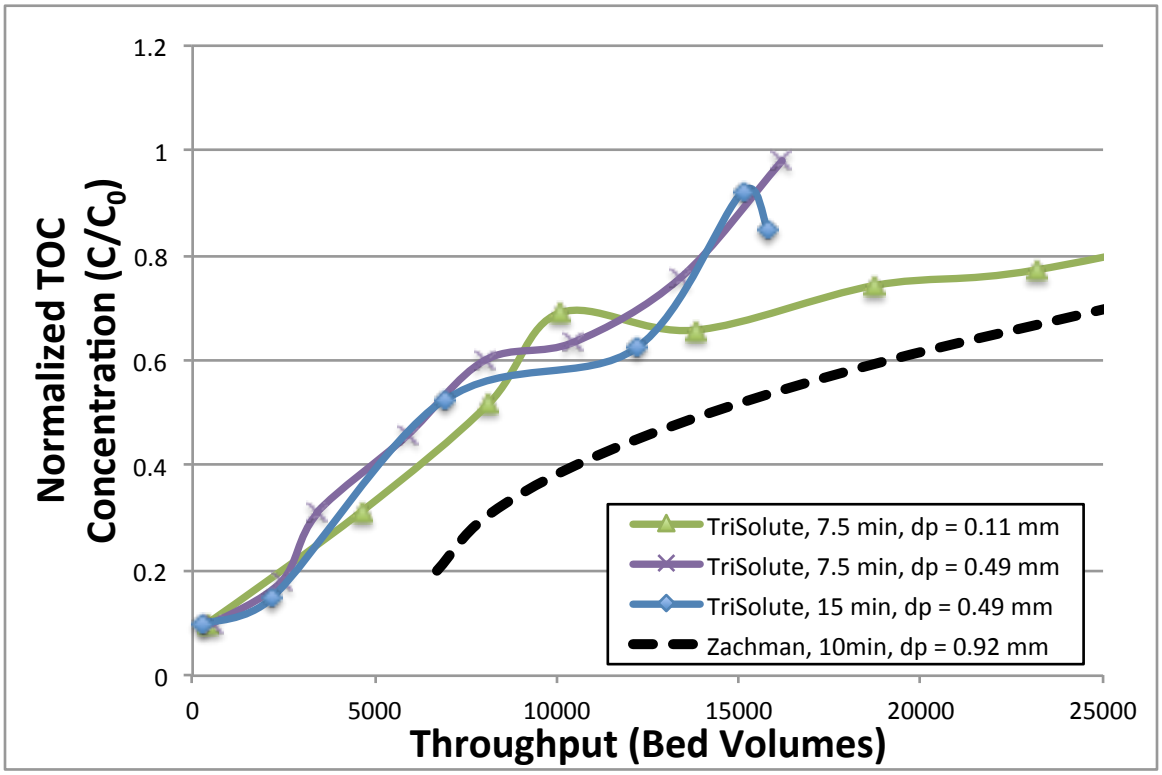

Figure 5.1 TOC Breakthrough as a function of GAC particle size. CO GW II (TOC: 1.5 mg/L); dashed line represents output from Zachman model; inset table showing solid phase concentration of DOM at different particle sizes.

Table 5.1 Solid-phase concentration of DOM as a function of GAC particle size.

d_{GAC} (mm)	EBCT (min)	q_50 (mg_{TOC}/g_{GAC})	q_70 (mg_{TOC}/g_{GAC})
0.11	7.5	20.1	23.7
0.49	7.5	14.6	21.0
0.49	15	15.3	23.6

Breakthrough curves for 1,2 DCA and carbon tetrachloride (CT) are shown in Figure 5.2. For both compounds, the column using the smaller carbon (d_{GAC}: 0.11 mm) exhibited significantly more capacity than the column using the larger GAC (d_{GAC}: 0.49 mm). Measuring the throughput at 10% and 50% breakthrough of 1,2 DCA, the 0.11 mm column had 59% and 42% more capacity, respectively, than the 0.49 mm column. The CT capacity differences were

more pronounced: the small column had a factor of 1.4 more capacity at both the 10% and 50% breakthrough points when compared to the column containing larger GAC particles. Four breakthrough curves at different EBCTs demonstrated the same behavior.

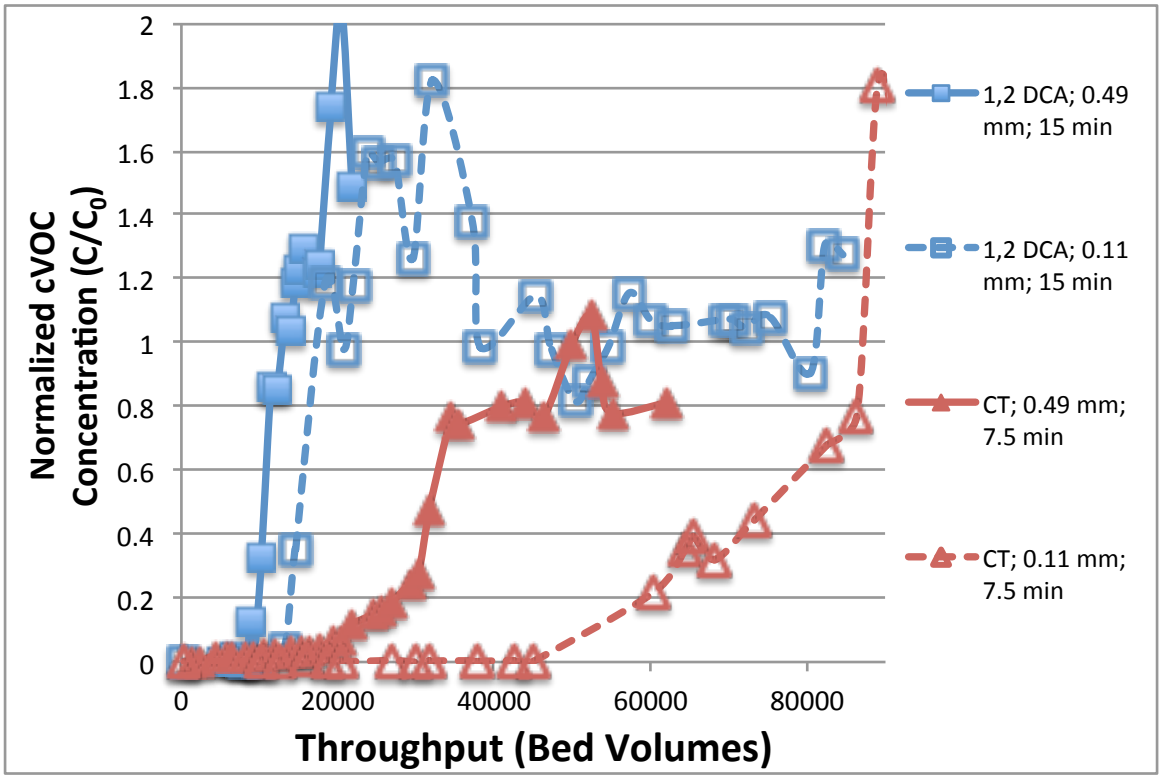

Figure 5.2 Capacity for cVOC as a function of GAC particle size. CO GW II (TOC: 1.5 mg/L) EBCT: 1,2 DCA = 15 min; CT = 7.5 min

This behavior is not unexpected. Corwin suggested that DOM via a "pore blockage" mechanism is responsible for the capacity differences (Corwin and Summers, 2010). When DOM blocks the pore of a GAC particle the adsorption sites behind the pore are prevented from participating in further adsorption. A larger GAC particle will have more surface area blocked behind a pore than a smaller GAC particle (Corwin and Summers, 2010). Using a comparison of 101 RSSCT and full-scale results, Kennedy found the PD-RSSCT over predicted capacity by a factor 3.0 +/- 1.2 (Kennedy, 2013). The scaling factor used in this study, 4.5, was near the lower bound spanned by Kennedy's analysis (4.3 – 13.6). Using a greater scaling factor would likely

produce greater capacity differences but groundwater DOM is likely another factor responsible for the lower over-prediction. In addition to lower median TOC concentrations of DOM in GWs (0.8 mg/L vs surface water median: 3.7 mg/L), fractionation of organic carbon has shown GW to be significantly more hydrophilic than surface water (Krasner et al., 1995; Thurman, 1985). The longer residence times of DOM in GW results in the hydrophobic portion sorbing onto aquifer solids and/or degrading into simple organic acids by bacteria in the aquifer (Thurman, 1985). The DOM remaining in solution is less labile and contributes to pore blockage to a lesser extent.

The mass of cVOC applied versus the mass adsorbed is presented in Figure 5.3 and Figure 5.4 for an EBCT of 7.5 minutes. Similar behavior was observed with the 15 min EBCT columns. As no TCE breakthrough occurred during the experimental run time, the applied and adsorbed TCE plots were removed from Figure 5.4 to improve clarity. By integrating the area above the breakthrough curve, the solid-phase concentration, q, was obtained. Table 5.2 compares q between the 0.11 mm and the 0.49 mm particle size RSSCTs. q values were calculated at complete breakthrough for the chemical of interest. Significant differences exist between the columns with the smaller column exhibiting more capacity. For 1,2 DCA, the 0.11 mm column had approximately 50% more loading than the 0.49 mm column for both EBCTs of 7.5 and 15 minutes. For CT, the difference is more pronounced: 2.7 more loading occurring on the column containing the smaller GAC. This observation violates a key assumption made during the initial design and scaling of the RSSCT; namely that GAC of different particle sizes maintain the same properties of density, surface area, porosity, and adsorption capacity. The significant decrease in q is synonymous with unequal adsorption capacity and without correction factors, the PD-RSSCT results cannot be expected to scale up accurately.

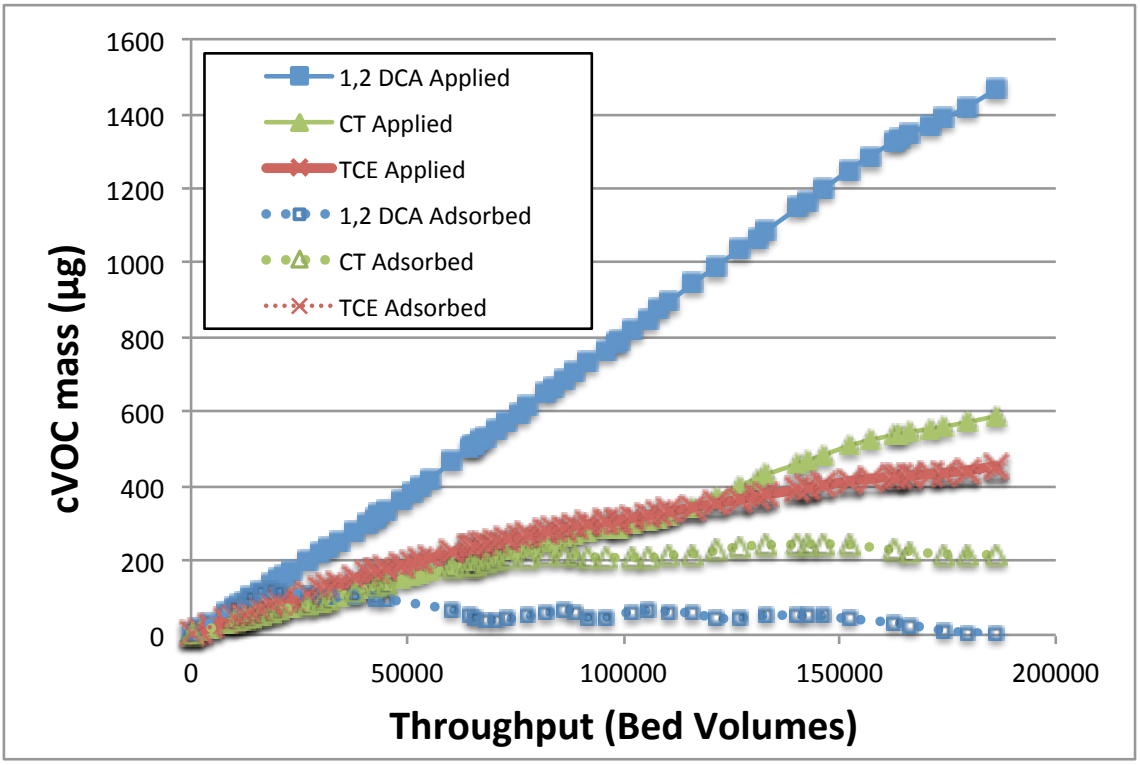

Figure 5.3 cVOC Mass Applied vs. Mass Adsorbed at d_{GAC} = 0.11 mm; CO GW II (TOC: 1.5 mg/L); EBCT: 7.5 min

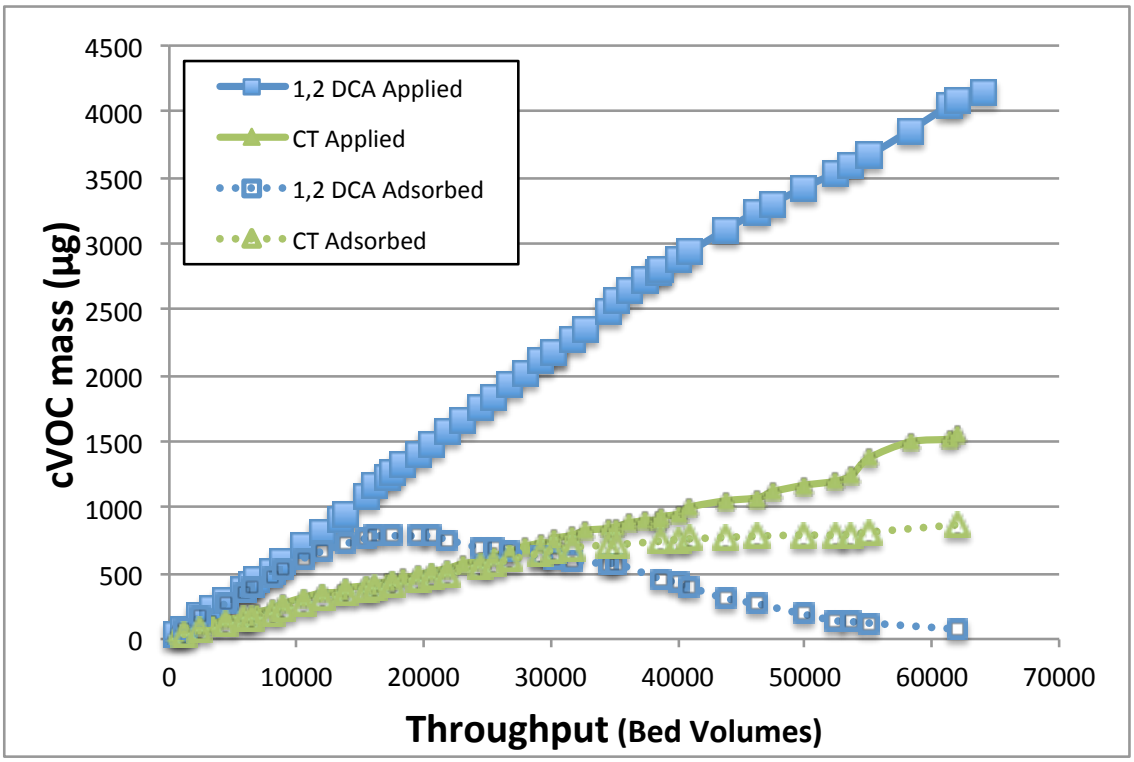

Figure 5.4 cVOC Mass Applied vs. Mass Adsorbed at d_{GAC} = 0.49 mm; CO GW II (TOC: 1.5 mg/L); EBCT: 7.5 min

Table 5.2 Solid-Phase concentration of cVOC as a function of GAC Particle Size; CO GW II (TOC: 1.5 mg/L).

Compound	d_{GAC} (mm)	EBCT (min)	q at 100% breakthrough ($\mu g_{cVOC}/g_{GAC}$)
1,2 DCA	0.11	7.5	159
1,2 DCA	0.49	7.5	105
1,2 DCA	0.11	15	150
1,2 DCA	0.49	15	103
CT	0.11	7.5	286
CT	0.49	7.5	106
CT	0.11	15	303
CT	0.49	15	-

Plotting mass applied versus mass adsorbed also allows displacement to be observed. In both Figure 5.3 and Figure 5.4, the breakthrough of the moderately adsorbing CT can be related to the displacement of the weaker 1,2 DCA compound. At termination, almost the entire adsorbed mass of 1,2 DCA in the 0.11 mm / 7.5 min column had had been displaced. The q value decreased from a maximum of 159 µg/g at complete 1,2 DCA breakthrough to 5 µg/g after CT had completely broken through. Similar results are expected for the 15 minute column if it had operated for a longer period of time. Such displacement can have significant implications to water plant operations. Effluent concentrations in excess of the influent concentrations can result in increased carbon costs or, if unchecked, non-potable product water and/or regulatory compliance issues.

While the agreement in TOC solid phase loading confirms the PD-RSSCT as an accurate predictor of TOC breakthrough, the disparity between target organic solid phase concentrations highlights the need of a capacity correction factor for columns using smaller GAC particle sizes. Figure 5.5 and Figure 5.6 show the same breakthrough data seen in Figure 5.2 with breakthrough curves adjusted with Corwin's Fouling Index also shown. Two methods were used to determine

the fouling factors to apply to the data: visual and Kennedy's regression. Visually adjusting the capacity involved selecting a Y value and applying the correction as discussed in the introduction section above. The Y values were increased or decreased as needed until the column capacities matched one another at 50% breakthrough. Once Y is determined for one set of RSSCTs it can be applied to columns with the same background matrix but with different scaling factors (i.e. a full-scale adsorber). Although this methodology is rather easy to accomplish, it does require two RSSCTs for each water. Kennedy's regression requires only one RSSCT and uses the target organic's pH-dependent log K_{ow} (log D), the ratio of target organic concentration to TOC concentration, and the RSSCT bed volumes to 10% breakthrough. Using equation 5.3, Y is found and the FI is determined and applied to the scaling factor to correct overcapacities seen in the RSSCT. Figure 5.5 shows the breakthrough curves for CT. Kennedy's regression predicted a Y value of 0.56, nearly identical to the visual Y value of 0.57. Using Y = 0.56 to correct the breakthrough data resulted in the corrected smaller column breaking through 10% earlier than the larger column. In Figure 5.6, the visual Y methodology produced a fouling factor of 0.24 and corrected the 1,2 DCA capacity differences between the 0.11 mm and the 0.49 mm column. Kennedy's regression over-predicted the degree of correction required; applying the Y value of 0.37 resulted in the smaller column breaking through 30% earlier than the larger column. When considering the 95% confidence intervals about Kennedy's predicted Y values, the range did not contain the Y value obtained visually for the either the 7.5 minute or the 15 minute 1,2 DCA curves. Conversely, both the predicted Y values for the CT curves were close to the visually determined Y and resulted in only 10% and 5% overcorrection for the column using the 0.11 mm GAC particle.

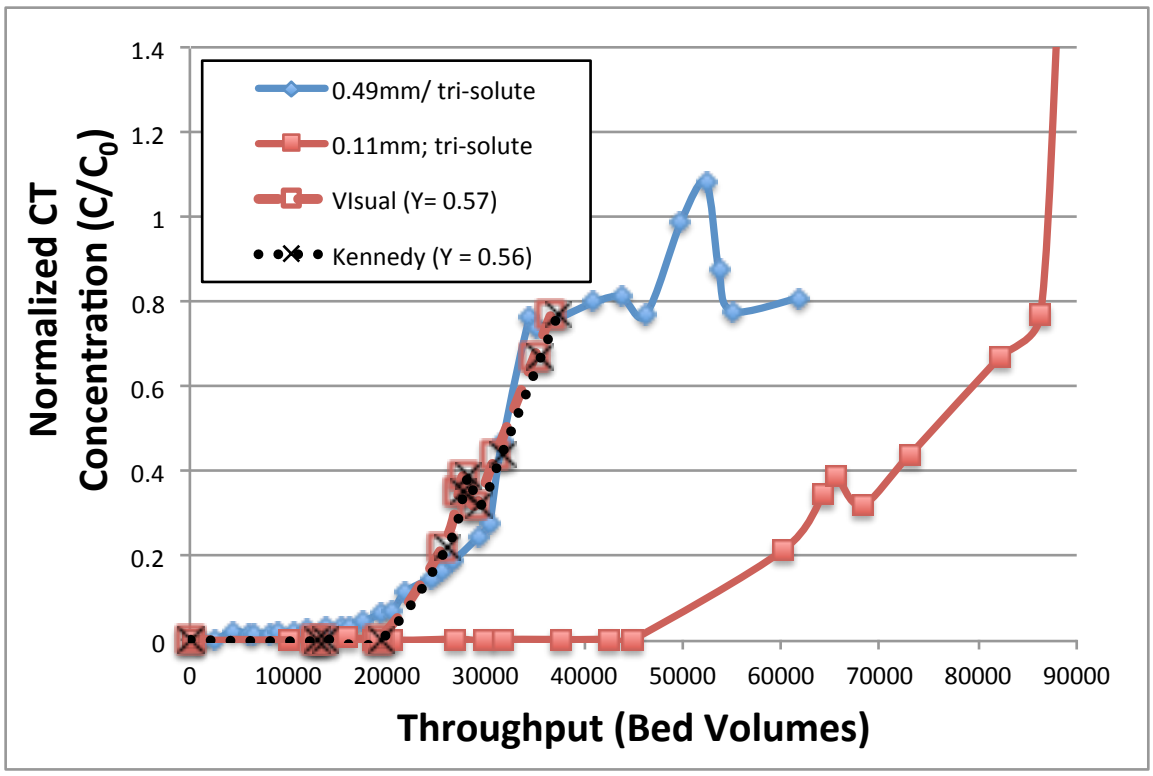

Figure 5.5 Scale-Up of RSCCT predicting CT breakthrough using fouling index. FI applied both visually (open symbols) and with Kennedy's regression (dotted line) (Kennedy, 2013). EBCT: 7.5 min; CO GW II (TOC: 1.5 mg/L)

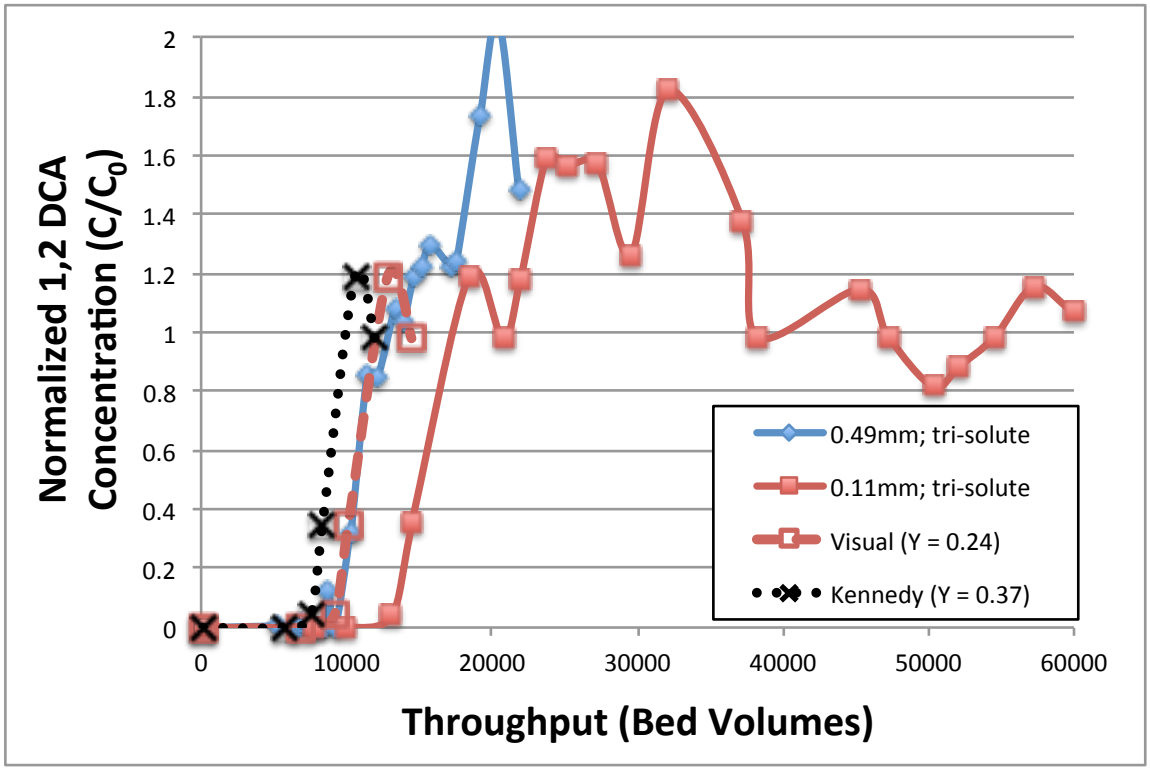

Figure 5.6 Scale-Up of RSCCT predicting 1,2 DCA breakthrough using FI. FI applied both visually (open symbols) and with Kennedy's regression (dotted line) (Kennedy, 2013). EBCT: 15 min; CO GW II (TOC: 1.5 mg/L)

The fouling factor values determined for the cVOC data in Figure 5.5 and Figure 5.6 were lower than those reported by Corwin (Y = 0.6 to 0.8; n = 6). The CT Y values were within the average range reported by Kennedy (Y_{avg} = 0.48 +/- 0.14, n = 23) but the 1,2 DCA Y values were lower. A lower Y value results in less correction to RSSCT capacity predictions. As discussed above, a more hydrophilic GW DOM is not expected to reduce GAC capacity as much as an equal concentration of surface water DOM. The majority of waters investigated by Corwin and Kennedy were surface waters and therefore a smaller Y value is expected for the groundwater used in this study.

The properties of the adsorbate may also contribute to the lower Y values. Smaller adsorbates are not affected by pore size exclusion to the same extent as larger compounds. The average MW of the compounds used in the Corwin and Kennedy research efforts were 256

Daltons (Da) and 283 Da, respectively. The MWs of 1,2 DCA and CT are 99 Da and 154 Da, respectively. It is plausible that these smaller compounds can better compete with DOM resulting in smaller overall GAC capacity reduction. The fouling factors determined in this effort followed the trends observed with Kennedy's assessment: increasing Y with increasing bed volumes to 10% breakthrough and with increasing log K_{ow}. Corwin suggested a relationship between Y and the ratio of the influent target organic concentration to the influent TOC concentration, C_0/TOC_0 (Corwin, 2010). Corwin's data, this effort, and other research accomplished since Corwin completed his effort were combined into one dataset and the C_0/TOC_0 correlation was investigated further. A regression was created to predict the fouling factor, Y. Using the 95% confidence intervals for the predicted fouling factor, 4 breakthrough curves involving 2 different EBCTs and 2 different cVOCs in a groundwater matrix were accurately captured. A subset of the data was used to create a similar regression that involved previous work on cVOCs and the PD-RSSCT. Figure 5.7 shows the two correlations to predict Y based on C_0/TOC_0. The solid line represents the regression using all points listed in the legend and is shown as equation 5.4.

$$Y = 0.17 * \left(\frac{C_0}{TOC_0}\right)^{-0.12} \qquad (R^2 = 0.78;\ n = 40) \qquad (eqn. 5.4)$$

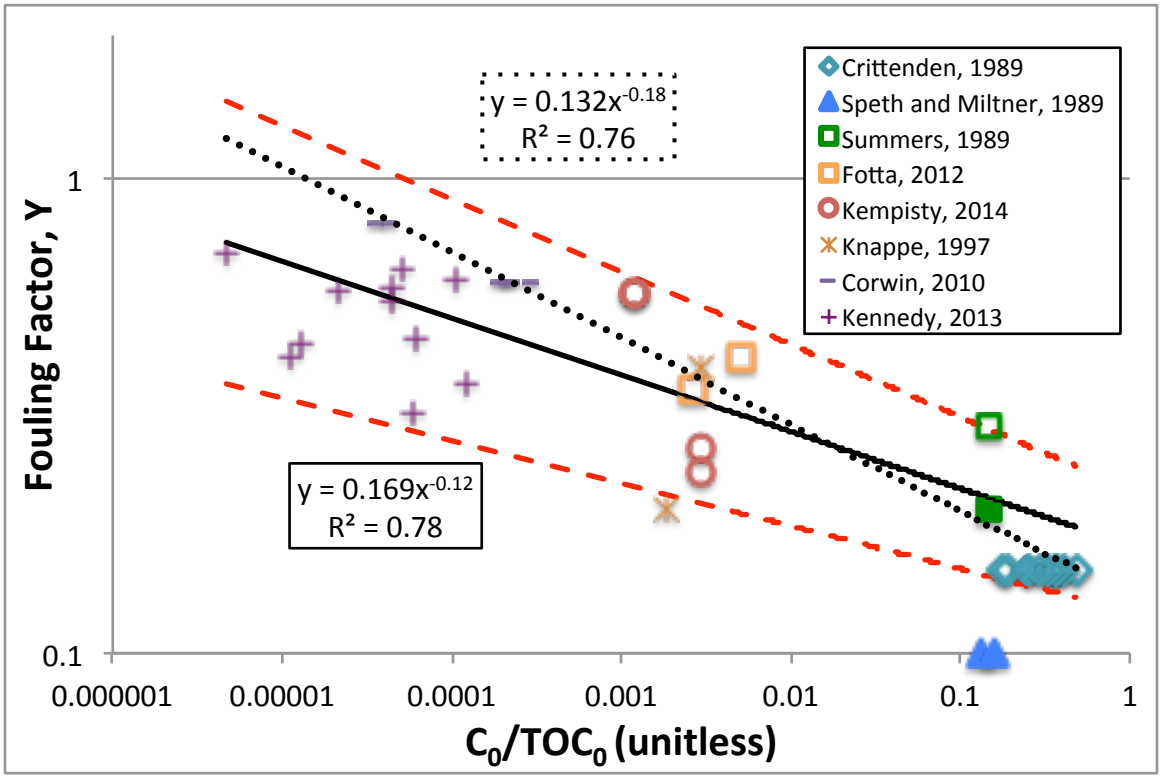

Figure 5.7 Fouling factor, Y, as a function of C_0/TOC_0. Solid regression line and equation (with 95% confidence intervals (dashed lines) generated using all data points on the graph (n = 40); dotted regression line and equation generated using only volatile compounds using the PD-RSSCT design (n = 12); data pts for volatile/PD regression are shown as open symbols and include ½ of the Crittenden points; EBCT range: 4.8 min – 15 min; TOC range: 0.4 mg/L – 5.3 mg/L.

The dashed line in Figure 5.7 considers only volatile compounds that used a RSSCT with a proportional diffusivity design. The data points representing the volatile/PD-RSSCT combination are represented by open symbols. The regression is shown as equation 5.5.

$$Y = 0.13 * \left(\frac{C_0}{TOC_0}\right)^{-0.18} \qquad (R^2 = 0.76;\ n = 12) \qquad (eqn.\ 5.5)$$

While the R^2 value for the volatile/PD-RSSCT regression is quite high, the limited number of data points, 12, used to create it results in an unreasonably large 95% confidence interval (predicted breakthrough to 50% occurring between ~1300 and 13000 bed volumes). Further research providing additional volatile/PD-RSSCT data points is warranted to determine

the veracity of this model. Figure 5.8 and Figure 5.9 apply the regression that used all data points available and Kennedy's regression to determine Y values and correct the 0.11 mm RSSCT capacity for both 1,2 DCA and CT. As the regression developed in this effort contains the data being forecast, the model output is referred to as a "simulation" to differentiate it from a true "prediction" that Kennedy's regression produces. Figure 5.8 shows the 0.49 mm column breakthrough is captured within the simulation's CI while the confidence interval about Kennedy's prediction overcorrects by 30% as discussed earlier. Figure 5.9 shows that although the Y value from the simulation does not correct the CT over-prediction enough, the correct capacity is still captured in the 95 % CI of simulated Y values. Kennedy's prediction for the CT correction is superior and predicts the bed volumes to 50% breakthrough within 10%.

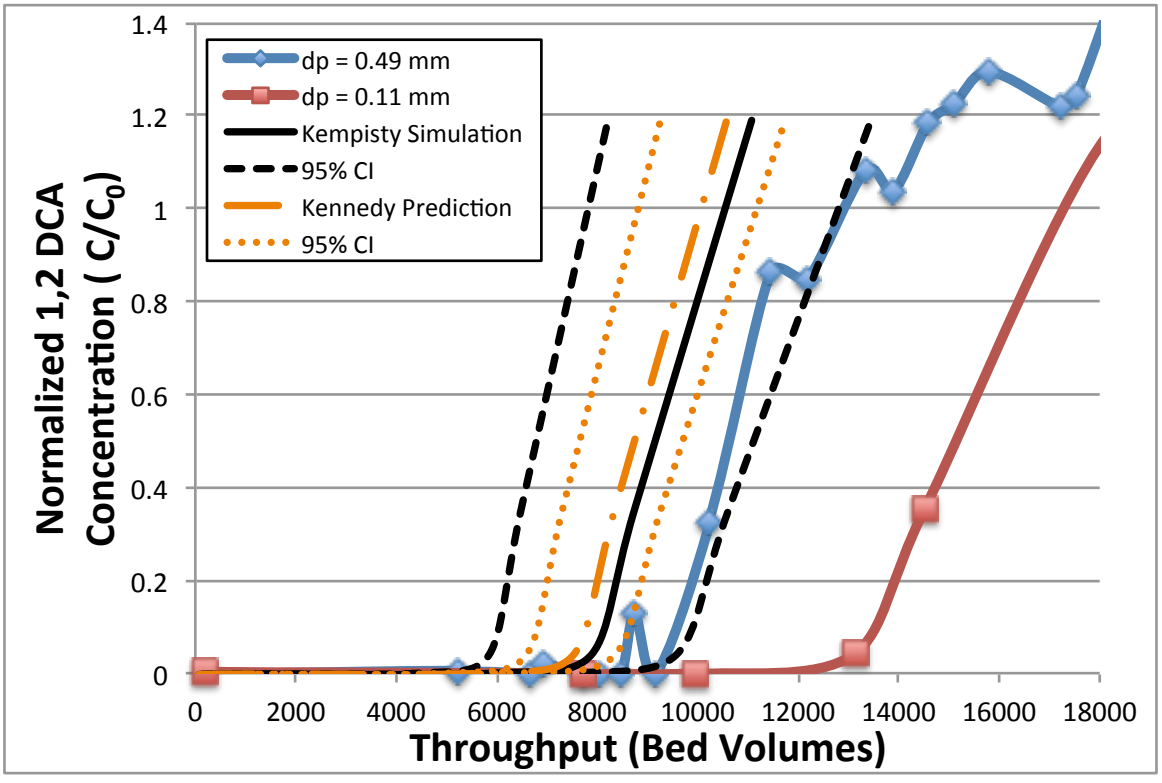

Figure 5.8 Application of predicted and simulated Y values from the Kennedy and Kempisty regressions to scale-up RSSCT results for 1,2 DCA breakthrough. Dotted lines represent 95% CI around the Kennedy regression; dashed lines represent 95% CI around the Kempisty regression; CO GW II (TOC: 1.5 mg/L), EBCT: 15 min.

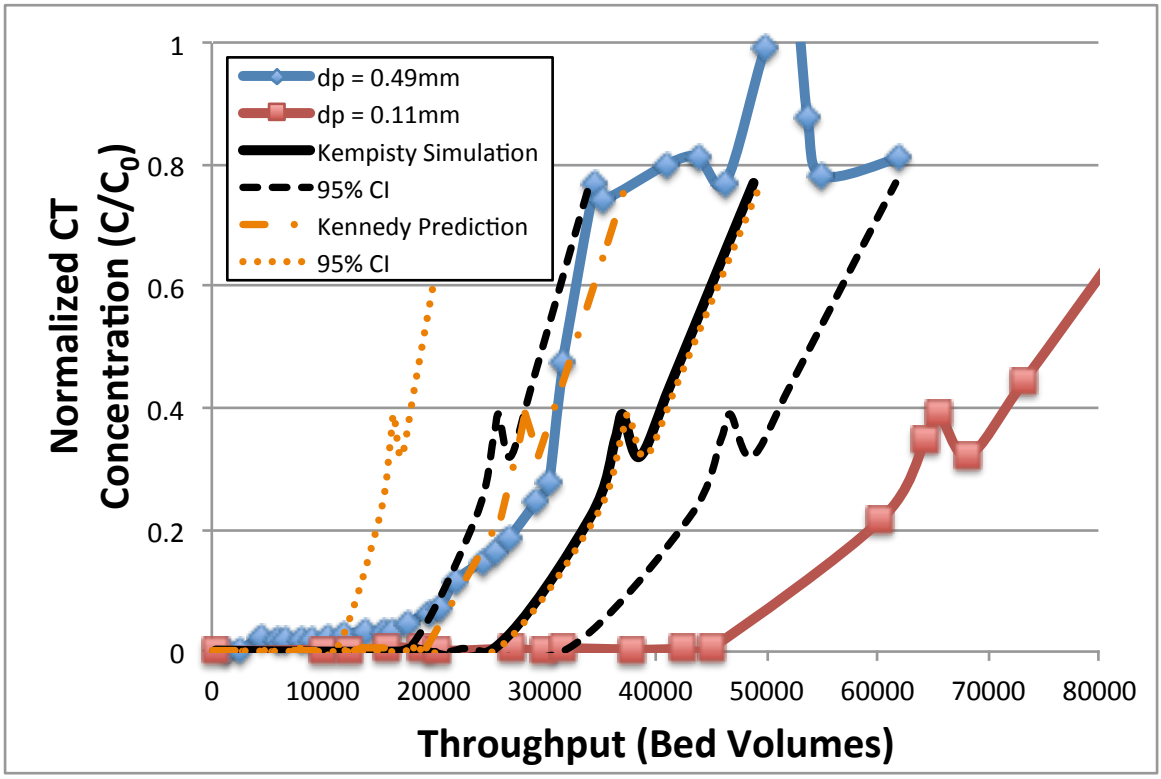

Figure 5.9 Application of predicted and simulated Y values from Kennedy and Kempisty regressions to scale-up RSSCT results for CT breakthrough. Dotted lines represent 95% CI around Kennedy regression; dashed lines represent 95% CI around Kempisty regression; CO GW II (TOC: 1.5 mg/L), EBCT: 7.5 min.

5.5 Conclusions

As expected the PD-RSSCT accurately predicted DOM breakthrough at a larger particle size. No difference in the solid-phase TOC concentration was observed between columns using two different sized GAC particles. As found with other work, the column using the smaller GAC particle size had significantly more capacity for cVOC than the column using the larger GAC particle. The over-prediction of throughput to 50% breakthrough ranged from 42% to 140% and was not as great as observed in other experiments (300% +/- 120%; n = 101) (Kennedy, 2013). About 90% of the 101 data points Kennedy analyzed involved surface waters. Groundwater DOM used in this research is believed to be responsible for this observation; GW is more hydrophilic and will contribute to pore blockage to a lesser extent and therefore affect

GAC particles of different sizes to a lesser extent. Nearly the entire mass of adsorbed 1,2 DCA was displaced by the more strongly adsorbing CT. The 1,2 DCA solid phase concentration of 159 µg/g was reduced by 97% to 5 µg/g at the time of column termination. Similar displacement was seen in a second column with a different EBCT. Significant differences were observed in the solid-phase cVOC concentration on the two GAC particle sizes. For 1,2 DCA, the small GAC had approximately 50% more loading compared to the larger GAC for both EBCTs of 7.5 and 15 minutes. For CT, the difference was more pronounced: 2.7 times more loading occurring on the column containing the smaller GAC. This violates the initial assumption of RSSCT design that states adsorption capacity of GAC particles of difference size are equal. If the RSSCT is to accurately predict capacity of a larger GAC particle, a scale-up correction factor needs to be applied. Corwin's concept of a fouling index was applied to address RSSCT over-prediction (Corwin and Summers, 2010). Visual fouling factors, predictions from a fouling factor regression developed by Kennedy (Kennedy, 2013), and two new models determining Y as a power function of C0/TOC0 were used to correct overcapacities observed in this effort. Determining Y visually requires breakthrough data from two columns each using different sizes of GAC. Benefit can still be realized with this method, as accomplishing two RSSCTs is likely easier to accomplish than operating a pilot adsorber. Kennedy's regression predicted the two Y values for CT exceptionally well (within 5% and 10%), but, even using the 95% CI values, failed to adequately correct the two 1,2 DCA columns (overcorrects by 30%). The model developed with this effort performed well - all four Y values were within the 95% CI for the model simulation. Adding more data points to the power regression would tighten the confidence intervals and improve credence in the output.

Chapter 6 Removal of PFAAs from Groundwater using GAC

6.1 Abstract

Due to their ubiquitous presence in the environment and prolific use in industry, perfluoroalkyl acids (PFAAs) are a class of compounds receiving increased attention. Conventional water treatment technologies have not shown the ability to substantially remove PFAAs (Appleman et al., 2014). Using data from both full- and bench-scale granular activated carbon (GAC) adsorbers, this chapter investigated the use of GAC as a viable treatment technology. Scale-up of bench-scale results to predict full-scale adsorber performance was attempted with the fouling index and three different correlations. Due to greater hydrophobicity with increasing chain length, GAC had a greater capacity for the longer chained PFAAs. Possibly due to hard/soft acid/base theory, specific interactions, or larger size, the sulfonate-containing compounds broke through later than their carboxylic-containing counterparts. At different empty bed contact times (EBCTs), neither the RSSCT nor the full-scale adsorber showed significantly different capacity for a PFAA. This is indicative that fouling of the GAC by groundwater DOM is not occurring with depth. The RSSCT over-predicted full-scale capacity of PFAAs by a factor of 1.7 (about 70%). Generally, the RSSCT over-predicts by a factor of 3.0+/-1.2 (Kennedy, 2013). The groundwater's lower TOC quantity and more recalcitrant character are believed to be the reason for the lack of fouling with longer EBCTs and the smaller capacity over-prediction. Consistently, the two regression correlations over-corrected RSSCT capacities and thereby under-predicted capacity seen in the full-scale adsorber. Variable full-scale influent concentrations, and unequal influent concentrations between the RSSCT and the full-scale adsorber, are believed to be responsible for some of the scale-up

difficulty. Carbon use rates (CURs) were calculated for a total of 20 RSSCT and full-scale breakthrough curves and were in the range of 4 mg/L to 54 mg/L. The four carbon-chained PFBA is the only compound where GAC treatment is in the transition range between practical and unfeasible; all other compounds were under accepted carbon use thresholds for feasibility, 24 mg/L, and GAC treatment should be considered practical.

6.2 Introduction

Recent advances in analytical techniques have led to a large number of trace organic contaminants or micropollutants (MPs) being detected in drinking water sources as well as finished drinking waters worldwide (Barnes et al., 2008; Benotti et al., 2009; Focazio et al., 2008; Jones-Lepp et al., 2012; Kim et al., 2007; Kolpin, 2002; Loos et al., 2009; Prieto-Rodriguez et al., 2012). One class of chemicals that is receiving increased attention is the perfluorinated compounds (PFCs). PFCs, specifically perfluoroalkyl acids (PFAAs), have a carbon backbone surrounded by fluorine atoms and a terminal carboxylic or sulfonic acid group; are environmentally stable and water soluble; and are ubiquitous in the environment. PFAAs have been widely used in industrial and commercial applications such as the textile manufacture, fire-fighting foam production, non-stick cooking materials, cardboard coatings on food packaging and in stain repellant applications. A number of studies have identified PFAA concentrations in the natural environment at the ng/L level (Bao et al., 2012; Cai et al., 2012; Flores et al., 2013; Plumlee et al., 2008; Sun et al., 2011). These natural environments include surface waters, groundwaters, and waste-water effluents. Small, but nonetheless, statistically significant adverse health effects have been linked with exposure to PFAAs including association with total cholesterol, glucose metabolism, body mass index, thyroid function, infertility, uric acid, lowered immune response to vaccinations, and attention deficit/hyperactivity disorder

(Grandjean et al., 2012; Saikat et al., 2013). The human dose-response curve for several of these effects is steepest at the lower exposure levels and seemingly without threshold (Post et al., 2012). Due to PFAAs resistance to degradation in the environment, its relatively high water solubility, and wide-spread detection in waters around the world, determining adequate treatment technologies is timely and prudent.

Conventional water treatment technologies, including coagulation, flocculation, sedimentation, filtration, biofiltration, oxidation (chlorine, ozone or advanced oxidation processes), UV irradiation and low pressure membranes, have not shown the ability to substantially remove PFAAs (Appleman et al., 2014; Rahman et al., 2014). Early evidence exists that activated carbon, high pressure membranes and ion exchange may have greater success at effective removal of PFAAs from water sources (Rahman et al., 2014) This paper evaluates the merit of using granular activated carbon (GAC) as a viable treatment technology for the removal of PFAAs. To accomplish this, bench scale experiments using natural groundwater impacted with eight PFAA compounds were conducted at empty bed contact times (EBCTs) of 7.5 minutes and 13 minutes. Results were compared to full-scale adsorber data from the same source water and that was operated for a period of 4.8 years (Appleman et al., 2014). Differences between the EBCTs of 13 and 26 minutes for the full-scale adsorber were investigated.

6.3 Background

Predicting full-scale GAC adsorber performance can be difficult. Large volumes of water and time are required to determine operational performance of a full-scale adsorber and process variables such as EBCT, GAC type and influent concentrations are difficult to control or change to determine optimal operating parameters. Modeling efforts can be valuable providing

preliminary design criteria but often require pilot-scale validation. Batch experiments can also provide insight into GAC's ability to effectively remove target organics, but often times only apply to the specific water being treated. Batch experiments also differ in the adsorbate-adsorbent interaction when compared to flow-through adsorbers. In a flow-through column, the mass transfer zone (MTZ) for the target organic is often shorter than the MTZ of dissolved natural organic matter (DOM) contained in the background matrix of the water being treated. When the target organic reaches deeper into the adsorber bed, the GAC has already interacted with and adsorbed a portion of the DOM that previously traveled through the bed. This results in both reduced GAC capacity (i.e., carbon fouling) for the target organic. This is the not case with batch isotherm work when both the target organic and the DOM are introduced at the same time with each of these components 'seeing' fresh carbon simultaneously. This creates a different driving force for the adsorption process. In the flow-through column, the concentration gradient in the bulk flow is very small and gradually increases as the MTZ travels through. The opposite is the case for batch systems where the strongest concentration gradient is initially encountered and gradually decreases as the fixed quantity of adsorbate is removed. Conducting isotherms with carbon preloaded with DOM has been done but doesn't resolve the issue entirely because the mass transfer processes in flow-through columns are dynamic and non-steady state; preloading carbon with DOM only provides one incremental point in the mass-transfer continuum.

Bench-scale experiments and the use of the rapid small scale column test (RSSCT) avoid the issues discussed above. RSSCTs use relationships from the diffused flow pore and surface diffusion model and the principles of similitude to replicate adsorption phenomena but do so in a fraction of the time required by pilot-scale columns (Berrigan, 2004; Crittenden et al., 1987).

Using GAC of a smaller diameter and maintaining similitude between the dimensionless parameters responsible for the mass transfer of the target organic in the full-scale and small-scale columns creates a column (i.e., RSSCT) that behaves as a full sized column (Crittenden et al., 1986a; Grandjean et al., 2012; Saikat et al., 2013). Overall, it has been estimated that less than 10% of the time and water is required for RSSCT experiments to produce comparable full-scale column data (Berrigan, 2004).

Theoretically, the RSSCT will produce identical results to full-scale adsorber performance; however, past performance has not shown this to be the case for specific organic compounds. Historically, the RSSCTs over-predict full-scale GAC capacity (Corwin and Summers, 2010; Crittenden et al., 1991; Summers et al., 1989). This over-prediction can be attributed to the effects of DOM in the background matrix, which are not addressed in the RSSCT scaling equations. Reduced GAC capacity for target organics is termed 'fouling'. The "pore blockage" explanation for this states that there is more surface area blocked behind the pore of a large GAC particle than behind the pore of a small GAC particle (Corwin and Summers, 2010). Competition for a limited number of adsorption sites between a large concentration of DOM and a trace concentration of target organic is another mechanism responsible for reduced target organic removal (Corwin and Summers, 2010; Sontheimer et al., 1988). Another explanation for improper scaling between the RSSCT and full-scale adsorbers has been proposed due to due to a surface complexation reaction occurring between DOM and the GAC surface (Summers et al., 1989). This surface complexation is not considered in RSSCT scaling equations.

Attempts have been made to scale-up RSSCT results to accurately predict full-scale adsorber performance. Corwin and Summers developed a correction factor, called the fouling

index (FI), based upon the ratio of sizes of GAC in the full-scale adsorber and the RSSCT raised to some power (Corwin and Summers, 2010). The FI concept was furthered using the target organic's octonol-water partition coefficient to project scale-up (Fotta, 2012). A combination of the target organic's pH dependent octonol-water partition coefficient, the ratio of the target organic concentration to the TOC concentration and the RSSCT throughput to 10% breakthrough, were also investigated as for their ability to provide accurate FIs (Kennedy, 2013). Additional relationships, independent of the FI concept, have also been explored to predict full-scale capacity from RSSCT performance with mixed results (Kennedy, 2013). None of these efforts however have been attempted for experiments treating PFAAs.

6.4 Materials and Methods

6.4.1 Materials

6.4.1.1 Water

Groundwater was collected from the City of Oakdale, MN municipality in eastern Minnesota. Water is drawn from the Jordan aquifer using eight wells that are between 501-588 feet in depth. Properties for the water are in Table 6.1. Once received water was filtered through a 5 µm polypropylene cartridge filter (Culligan Sediment Cartridges; Model P5-145358) and placed into a HDPE storage drum until needed for experimental use. The influent concentrations of PFAA to the full-scale adsorber are reported in Table 6.2. Influent concentrations to the RSSCT experimental set-up are provided in Table 6.3.

Table 6.1 Water quality of PFAA impacted GW.

Water	Source	pH	TOC (mg/L)	UVA_{254} (cm^{-1})	SUVA (L/mg-m)
Oakdale MN	GW	7.0	0.7	0.011	1.53

Table 6.2 Average Influent Concentrations of PFAA compounds to Full-Scale adsorber that was operated from 4.8 years from 11/2006 to 6/2011 (Appleman, 2014)

Compound	Avg C_0 (ng/L)
PFBA	1448
PFPeA	40.5
PFHxA	154.2
PFOA	555.8
PFBS	2.7
PFHxS	67.7
PFOS	845.2

6.4.2 Methods

6.4.2.1 Full-scale GAC adsorber

The full-scale GAC adsorber used Calgon Carbon Filtrasorb 600 GAC (F-600). F-600 is a reagglomerated virgin bituminous-based GAC. Screen size for the GAC was 12 x 40 size (U.S. Standard Sieve Size) equating to a log-mean diameter of 0.92 mm. Characteristics of F-600 GAC are in Table 2.3. Adsorber vessels were 12' tall by 10' in diameter and operated in series (lead-lag configuration) at a flow rate of 380-400 gallons per minute. GAC depth inside the vessel was 8.9' and the EBCT was 13 minutes. The adsorbers were operated for a period of 4.8 years and were sampled monthly from Oct 2006 to June 2011 (Appleman et al., 2014).

6.4.2.2 RSSCT set-up

The specific design and set-up of the RSSCT-PD was done in accordance with the EPA Manual for Bench- and Pilot-Scale Treatment Studies (EPA, 1996); for the sake of brevity a summary overview is provided here. RSSCTs used the same F-600 GAC as the full-scale adsorber. Using a mortal and pestle, GAC was ground down to a sieve size of 100 x 200 (US Standard Sieve Size) equating to a log-mean diameter of 0.11 mm. Fines were decanted using

DI water. The GAC was placed under vacuum for 24 hours or until no visible air bubbles could be seen when agitating the GAC beaker. Using a Pasteur pipette, GAC was transferred to a 4.76 mm ID Teflon column with glass wool inserted into the base to provide support for the GAC media. The ratio of Teflon column size to GAC diameter equates to an aspect ratio of 44 and thereby eliminates the concern of wall effects (i.e. short-circuiting of water around the media). Two columns were run in series: the first contained 0.66 g of GAC and the second contained 0.48 g of GAC. Operated at a flow rate of 1.2 mL/min produced equivalent full-scale EBCTs of 7.5 min and 13 min, respectively. Influent and effluent samples were collected every 3 to 4 days.

6.4.2.3 Analytics

All samples for the RSSCTs were collected in 20mL plastic scintillation vials. Samples were prepared and analyzed by isotope dilution using direct injection with liquid chromatography (LC)/tandem mass spectrometry (MS/MS) on an ABSciex 3200, a method detailed in a previous study (Guelfo and Higgins, 2013). Limits of quantification (LOQs) were 20 ng/L for all of the PFCAs, and 10 ng/L for all of the PFSAs. RSSCT samples were processed in two separate batches on different dates. QA/QC requirements were met on both runs, however, both influent and effluent samples in the second batch of processed samples were higher than the first batch. Sample and standard preparation issues are believed to be the cause for the discrepancy. Since both influent and effluent samples increased in relation to each other, effluent samples were normalized to the respective batch they were analyzed in. No obvious break in the data is observed between batch 1 and batch 2 samples when presented in this manner. Influent PFAA concentrations from both batch 1 and batch 2 are included in Table 6.3 below.

6.4.2.4 Quality assurance and quality control

For the LC/MS/MS runs, a double blank was placed in between sets of six samples. For

all batches analyzed in this study, at least three blanks containing only the stable isotope surrogate standards were analyzed to evaluate possible sample carryover. To ensure the Teflon tubing was not sorbing or leaching PFAAs into the water, two influent samples were collected during multiple sampling events. One influent sample was collected immediately before contact with the GAC media and the second influent sample was collected at the influent water reservoir. Water collected at the influent water reservoir traveled through approximately 6 linear feet of Teflon tubing before coming in contact with the GAC media. No statistical difference was seen between the 15 sets of two influent samples, thereby eliminating the question of PFAA contributions or omissions from the Teflon tubing.

6.4.2.5 Data Analysis

A metric to evaluate GAC efficiency is the carbon use rate (CUR). The CUR is expressed in terms of mass of GAC required to treat a volume of water to a desired treatment objective. It is often provided in terms of mg GAC required to treat a L of water or pounds of GAC required to treat 1000 gallons of water. Lower CURs are indicative of more efficient use of GAC and are preferred. The apparent capacity term, K*, was used to determine the carbon use rate in this effort. K* was developed by Corwin and Summers and is similar to the Freundlich isotherm K term, but involves water with a background matrix containing DOM and represents flow-through column conditions (Corwin and Summers, 2011). As shown below, if K* can be accurately assessed, the carbon use rate can easily be found and the feasibility of using GAC as a treatment technique can be quantified.

Combining empirical and theoretical concepts, K* can be developed from the Freundlich isotherm equation represented in equation 6.1.

$$q = \frac{x}{M_{GAC}} = K_F \times C^{1/n} \qquad (eqn.\ 6.1)$$

where q is the solid phase concentration of the contaminant (mass of adsorbate per mass adsorbent), x is the mass micropollutant absorbed to the carbon; M_{GAC} is the mass of carbon; C is the equilibrium concentration of the micropollutant; and K_F and 1/n are Fruendlich coefficients representing the absorbent's capacity for the micropollutant and the heterogeneity of site energies available for sorption, respectively. Performing a mass balance around the aqueous phase and assuming no losses to the atmosphere, x can be expressed as equation 6.2.

$$x = \left(C_0 - C_{eff}\right)\ Q \times t \qquad (eqn.\ 6.2)$$

where Q is flow and t is time. Additionally, an ideal adsorber operating under plug flow conditions has a C_{eff} of 0 until breakthrough occurs. When micropollutant concentrations are low compared with the background dissolved DOM concentration, research has shown 1/n behaves as if it is 1 (Graham et al., 2000; Knappe et al., 1998). Equation 6.3 assumes that the volume of water treated at 50% breakthrough in a flow-through column is equal to the volume treated at breakthrough in an ideal reactor. Sontheimer showed this assumption is valid as long as the breakthrough curve is nearly symmetrical (Sontheimer et al., 1988).

$$BV_{50} \times Vol_{bed} = Q \times t \qquad (eqn.\ 6.3)$$

Incorporating equations 6.2 and 6.3 and the assumptions above into equation 6.1 produces equation 6.4. K_F has been replaced with K* to represent the new apparent capacity term.

$$K^* = \frac{BV_{50} \times Vol_{bed}}{M_{GAC}} \qquad (eqn.\ 6.4)$$

K* can also be represented as the volume of water treated at 50% breakthrough divided by the mass of GAC which is the inverse of the carbon use rate as shown in equation 6.5.

$$K^* = \frac{Volume\ of\ Water\ Treated}{M_{GAC}} = \frac{1}{(CUR)} \qquad (eqn.\ 6.5)$$

6.5 Results and Discussion

Results of the RSSCT are shown in Figure 6.1. For accuracy, only data points above the analytical detection limit are displayed. The breakthrough order from the column follows two distinct patterns: 1) longer chained PFAAs have a greater affinity for GAC and breakthrough later than their shorter chained counterparts and 2) sorption of PFAAs containing a sulfonate moiety is greater than counterpart PFAAs containing a carboxylic functional group. This behavior is expected. One study found the adsorption potential to increase with increasing chain length (Zhou et al., 2013). With the addition of each C-F_2, the PFAA compound increases in hydrophobicity and consequently, adsorption potential. One study found that partition coefficients increase for each additional C-F_2 bond by a factor of 0.50 - 0.60 log units (Higgins and Luthy, 2006). In the same study, the partition coefficient for sulfonate containing PFAAs (PFSAs) was determined to be 0.23 log units higher than equivalent carbon chain length carboxylic-containing PFAAs (PFCAs) (Higgins and Luthy, 2006). Increased partition coefficient factors of 0.52 – 0.75 per additional C-F_2 bond and 0.71 – 0.76 for PFSAs compared to PFCAs has been reported elsewhere (Ahrens et al., 2010). The mechanistic reason for the difference in sorption potential between PFSAs and PFCAs has yet to be determined. If only non-selective electrostatic interactions were solely responsible for sorption, such large capacity differences would not be seen. It has been suggested that the larger size of the sulfonate group and/or the existence of specific electrostatic interactions occurring with each moiety may be responsible for increasing the hydrophobicity and sorption strength of PFSAs (Higgins and Luthy, 2006). The specific interactions may be explained using Pearson's concept of hard and soft acids and bases (HSAB), with the hard base sulfonate group being more readily adsorbed

than the soft base carboxylic moiety (Xiao et al., 2013). To explore this further, an analysis of the adsorbent should be accomplished to investigate HSAB characteristics of the GAC (Alfarra et al., 2004). The specific interactions may also be due the greater potential for electron-donor interactions due to the larger number of pi bonds in the sulfonate moiety compared with the carboxylic moiety.

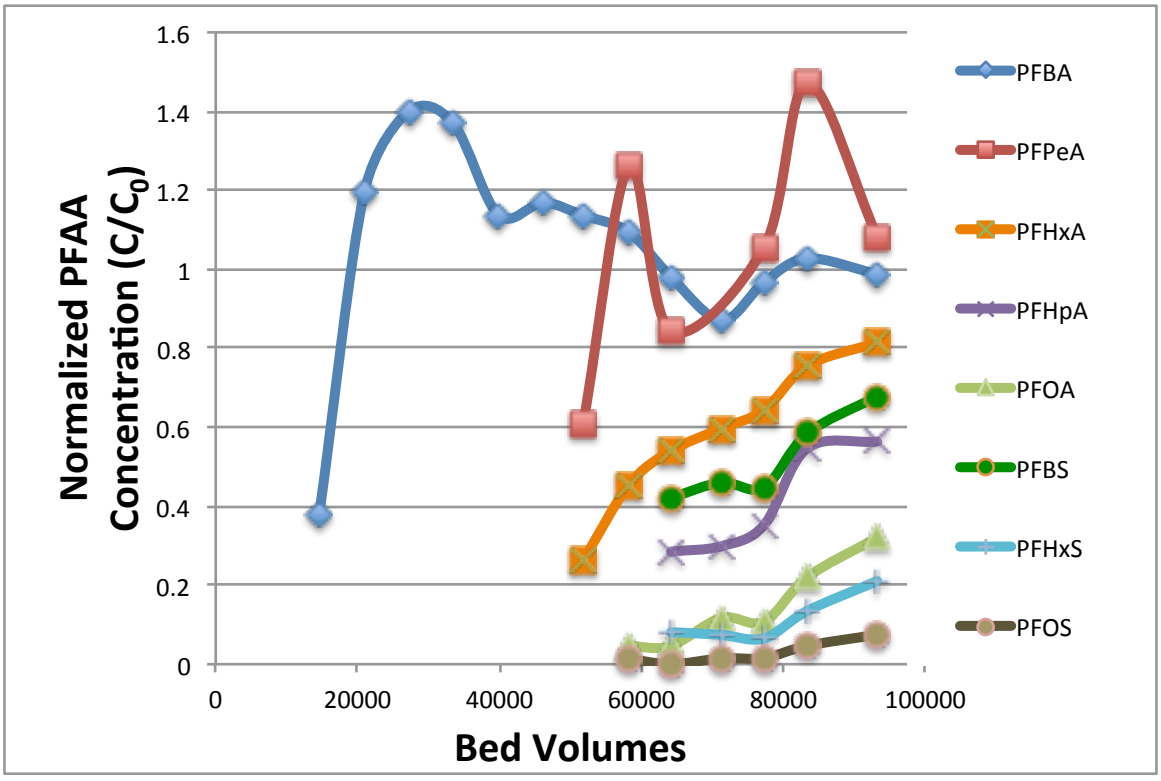

Figure 6.1 PFAA Breakthrough Curves from RSSCT; MN GW (TOC: 0.7 mg/L) EBCT: 13 min

The chromatographic effect is also observed in the RSSCT. This effect occurs as a more strongly adsorbing compound migrates through the adsorber and outcompetes a weaker compound for sorption sites causing the weaker compound to separate from the GAC and thereby result in an effluent concentration that exceeds the influent concentration. Both PFBA and PFPeA show this chromatographic effect with C/C0 values greater than 1. Previous work has shown the chromatographic effect occurring with PFBA and PFBS (Eschauzier et al., 2012),

phenolic compounds (Sontheimer et al., 1988), polymer sorption to mineral surfaces (Kawaguchi, 1990), and with cVOCs (earlier chapters of this effort).

Comparisons of both the RSSCT and full-scale adsorber performance at different EBCTs are shown in Figure 6.2 and Figure 6.3. The effect of EBCTs can manifest itself in three ways when treating waters containing DOM. On a theoretical basis, single solute breakthrough is not impacted by EBCT when expressed on a throughput basis, once a constant pattern mass transfer zone is established (Hand et al., 1989). However, increasing the EBCT has been shown to improve, reduce or not affect adsorber performance. Better performance occurs as the ratio of target organic mass transfer zone to the adsorber length decreases with increasing EBCT (Hand et al., 1989). This results in a more efficient use of GAC. In the presence of DOM deleterious effects on GAC's target organic capacity are also occurring. Intraparticle mass transfer, specifically pore diffusion, is the rate limiting phenomena occurring within typical GAC adsorbers (Hand et al., 1989). The diffusivity values of large humic components in DOM are 1-2 orders of magnitude slower than typical target organics (Sontheimer et al., 1988). This leads to a more distributed DOM MTZ and a situation where DOM has sorbed onto the GAC in the deeper portions of the adsorber before the target organic enters this portion of the bed. This phenomenon is termed "carbon fouling" and results in reduced GAC capacity. At some point, pre-loading of DOM onto GAC is comparable to the co-loading of DOM and target organic and no further efficiency gains are seen with increasing EBCT (Fotta, 2012; Hand et al., 1989). Further increases to the EBCT fouls the GAC to such an extent than overall adsorber efficiency is decreased (Knappe et al., 1997; Sontheimer et al., 1988; Summers et al., 2013).

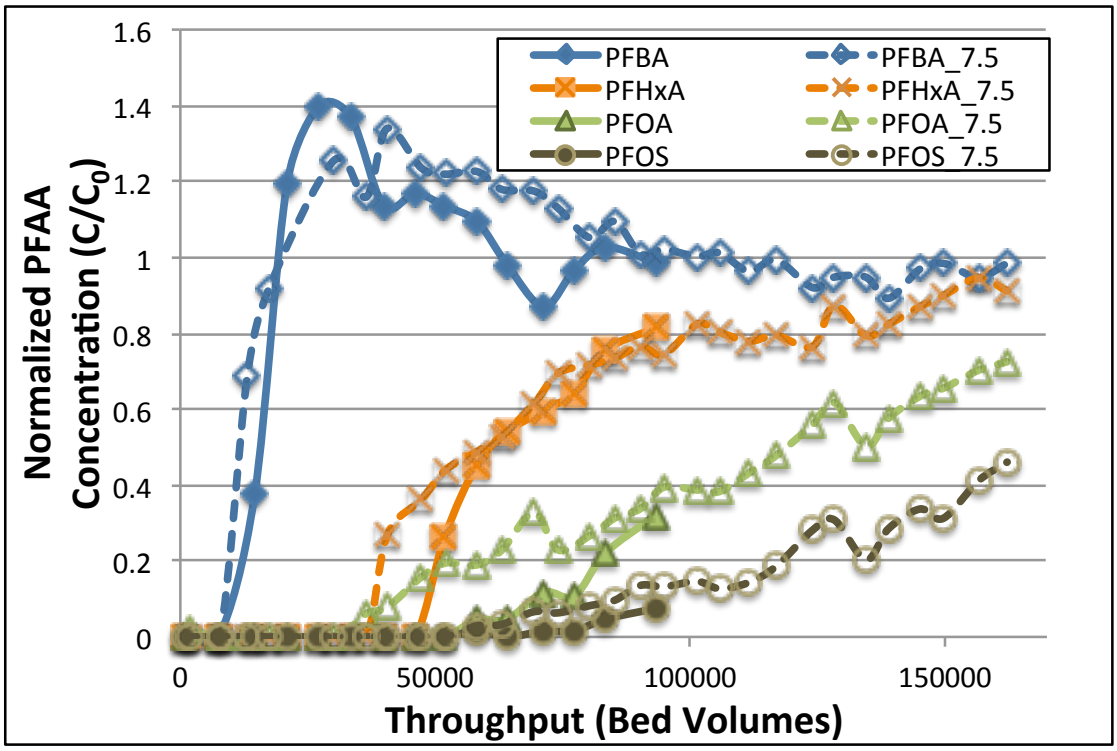

Figure 6.2 PFAA Capacity as a function of EBCT; RSSCT; Mn GW (TOC:0.7 mg/L); EBCT: 7.5 min and 13 min. Filled symbols are for an EBCT of 13 min.

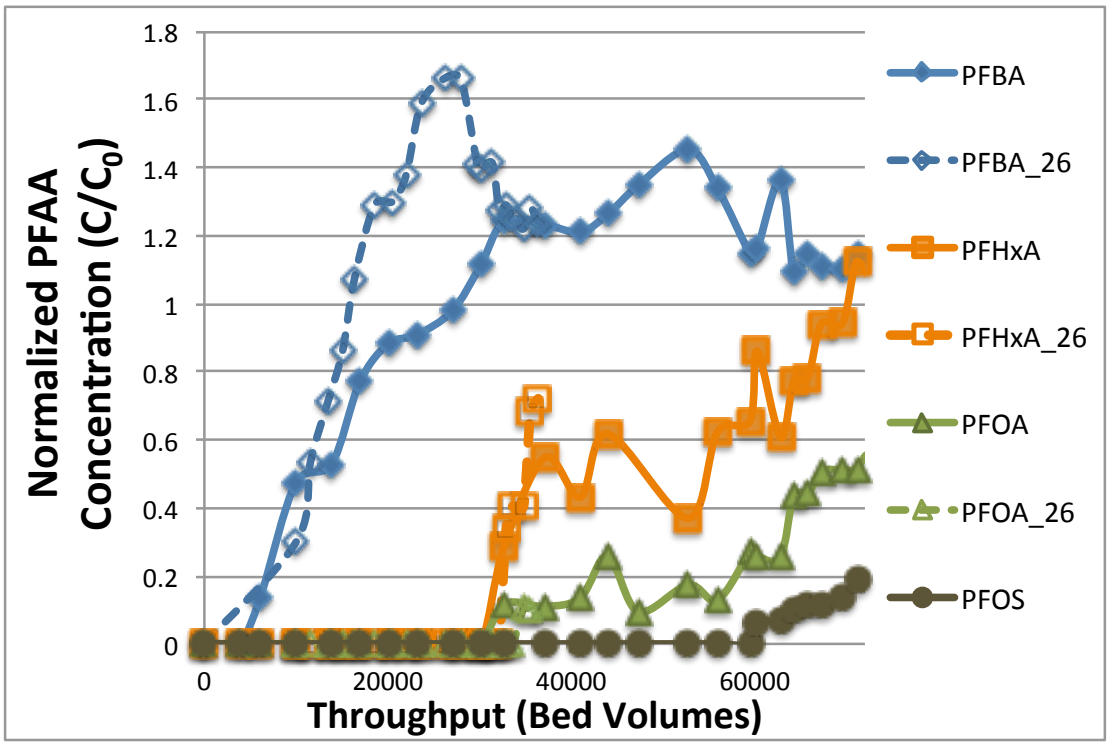

Figure 6.3 PFAA Capacity as a function of EBCT; Full-Scale; Mn GW (TOC:0.7 mg/L); EBCT: 13 min and 26 min. Filled symbols are for an EBCT of 13 min.

For the RSSCT, Figure 6.2 shows the initial breakthrough for the 13 minute EBCT column outperformed that of the 7.5 minute EBCT column by approximately 10-30% for PFBA, PFHxA and PFOS. The bed volume values for these capacities were taken at 10% and 20% breakthrough. The 13 minute PFOA column outperformed the 7.5 minute column by more than 50% using the same throughput markers. The efficiency gains with a longer EBCT are not as great with the other PFAAs or when using throughput to 50% breakthrough. The lack of decreasing performance with increasing EBCT shows an absence of significant DOM fouling with depth. The only compound that showed a decrease in capacity at the longer EBCT was PFBS. The reduced capacity at the higher EBCT for PFBS was attributed to the low influent concentration that was close to the analytical limit of quantification. Additionally, the capacity differences between EBCTs are diminished when considering throughput to 50% breakthrough. Throughput values for all eight different PFAAs for 10%, 20%, and 50% breakthrough are presented in Table 6.3. The lack of substantial capacity reduction with increasing EBCT can be expected for a groundwater. The TOC concentration of the MN background matrix was 0.7 mg/L. In addition to a lower quantitative value, groundwater DOM is more recalcitrant, less labile, and more hydrophilic than an equivalent surface water concentration, as indicated by the low SUVA value (Thurman, 1985). Both the quantitative and qualitative characteristics of groundwater DOM make carbon fouling with depth less likely to occur. Carbon fouling with adsorber depth was not observed in the full-scale adsorber either. The full-scale breakthrough curves can be seen in Figure 6.3.

Table 6.3 PFAA throughput values at different levels of breakthrough and EBCTs in RSSCT; Capacities measured in bed volumes to 10%, 20% and 50% of PFAA C_0. PFAA samples were analyzed in two batches with the second batch having higher influent concentrations; effluent results were normalized to the respective batch they were analyzed in.

Compound	Avg C_0 batch#1 (ng/L)*	Avg C_0 batch#2 (ng/L)*	BV_10 (7.5min)	BV_10 (13min)	BV_10 ratio (13min/7.5min)	BV_20 (7.5min)	BV_20 (13min)	BV_20 ratio (13min/7.5min)	BV_50 (7.5min)	BV_50 (13min)	BV_50 ratio (13min/7.5min)
PFBA	554	673	8855	10338	1.2	9703	12414	1.3	11573	15628	1.4
PFPeA	16	25	52913	52719	1.0	53537	53065	1.0	55853	54005	1.0
PFHxA	120	145	38228	48862	1.3	39296	50296	1.3	59857	60336	1.0
PFHpA	64	77	64910	60537	0.9	66228	61922	0.9	79883	81181	1.0
PFOA	505	690	42679	69040	1.6	56208	82242	1.5	118603	-	-
PFBS	16	23	91048	59898	0.7	91287	61026	0.7	92817	79518	0.9
PFHxS	48	60	91856	80384	0.9	92905	91627	1.0	143206	-	-
PFOS	508	532	86068	98219	1.1	120000	117844	1.0	165108	-	-

Another indicator of carbon efficiency is the CUR. Table 6.4 shows CURs for both the RSSCT and full-scale columns at 2 EBCTs each. The CURs reported in Table 6.4 were determined using the inverse of the effective Freundlich capacity parameter, K*, as described in equation 6.5. A CUR less than or equal to 0.20 lbs. GAC/1000 gallons water treated (24 mgGAC/Lwater) has been used to signify well adsorbed compounds while a CUR at or above 0.60 lbs GAC /1000 gallons water treated (72 mgGAC/Lwater) denotes weakly adsorbing compounds and unfeasibly high GAC costs (Knappe and Summers, 2012). From Table 6.4, PFBA is the only compound where GAC treatment is in the transition range between practical and unfeasible. All other compounds had CURs less than 20 mgGAC/Lwater indicating GAC is a viable treatment option at these PFAA concentrations in this water. Also seen in Table 6.4 are the similarities between CURs at the two EBCTs for both the RSSCT and the full-scale column. This reinforces a lack of fouling by DOM with increasing adsorber depth. As discussed in the later, compared to the full-scale adsorber, the breakthrough occurred later in the RSSCTS at the 13 minute EBCT for PFBA, PFPeX and PFHxA, thus the CURs are lower for the RSSCT.

Table Error! No text of specified style in document.**.1** Carbon Use Rates to 50% breakthrough for PFAAs.

Compound	RSSCT; EBCT 7.5 min			RSSCT EBCT: 13 min			Full-Scale EBCT: 13 min			Full-Scale EBCT: 26 min		
	K* (m^3/kg)	CUR (mg_{GAC}/L)	CUR ($\#_{GAC}$/1000 gal)	K* (m^3/kg)	CUR (mg_{GAC}/L)	CUR ($\#_{GAC}$/1000 gal)	K* (m^3/kg)	CUR (mg_{GAC}/L)	CUR ($\#_{GAC}$/1000 gal)	K* (m^3/kg)	CUR (mg_{GAC}/L)	CUR ($\#_{GAC}$/1000 gal)
PFBA	19	54	0.45	25	40	0.33	19	54	0.45	19	55	0.45
PFPeA	90	11	0.09	87	12	0.10	56	18	0.15	50	20	0.17
PFHxA	97	10	0.09	97	10	0.09	58	17	0.14	57	18	0.15
PFHpA	129	7.8	0.06	131	7.6	0.06	-	-	-	-	-	-
PFOA	191	5.2	0.04	-	-	-	108	9.3	0.08	-	-	-
PFBS	150	6.7	0.06	128	7.8	0.06	-	-	-	-	-	-
PFHxS	231	4.3	0.04	-	-	-	-	-	-	-	-	-
PFOS	266	3.8	0.03	-	-	-	-	-	-	-	-	-

RSSCT and full-scale breakthrough curves for four PFAAs are shown in Figure 6.4. Showing much of the same data, Table 6.5 presents the scale-up ratios between the RSSCT capacity and the full-scale capacity for five PFAAs at 10%, 20% and 50% breakthrough concentrations on a C/Co normalized basis. The RSSCT consistently over predicts GAC capacity by about 70% with a standard deviation of 20%. For the reasons stated above, over prediction by the RSSCT is expected. Previous research has shown that the RSSCT-PD over-predicts GAC capacity by a factor of 3.0 +/- 1.2 for 10% breakthrough of target organics (Kennedy, 2013). The lower over-prediction factor of 1.7 is thought to be due to the groundwater background matrix. The majority of the 101 data points used in the Kennedy study were from surface water background matrices with TOC measurements between 1.7 mg/L and 3.9 mg/L. The characteristics (both quantity and quality) of the groundwater DOM in this study did not compete or foul GAC to the same extent as surface water DOM and hence the closer prediction of the RSSCT results.

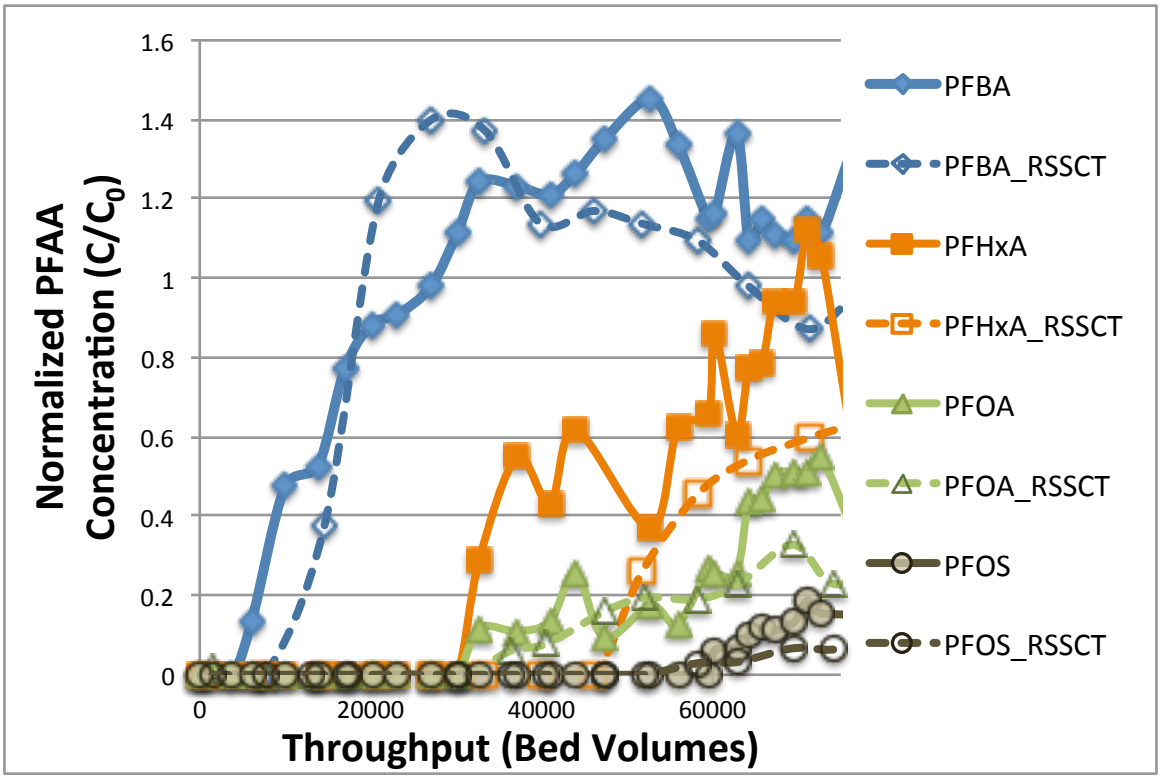

Figure 6.4 PFAA Capacities Differences between RSSCT and Full-Scale. EBCT: 13 min.

Table 6.5 Comparisons between RSSCT and Full-Scale Capacities for PFAAs. Capacities measured in bed volumes to 10%, 20% and 50% breakthrough

	Scale-Up		
Compound	**BV_10_RSSCT/ BV_10_FullScale (13min)**	**BV_20 RSSCT/ BV_20 FullScale (13min)**	**BV_50 RSSCT/ BV_50 FullScale (13min)**
PFBA	2.0	1.8	1.4
PFPeA	1.6	1.6	1.5
PFHxA	1.6	1.6	1.7
PFOA	2.1	1.6	-
PFOS	1.5	1.6	-
avg by column	1.8	1.6	1.5
std deviation by column	0.26	0.08	0.14
standard error by column	0.15	0.05	0.09
			overall avg = 1.7
			standard deviation for all data = 0.21
			standard error for all data = 0.12

To correct the overprediction of capacity by the RSSCT, Kennedy developed a regression equation using the RSSCT bed volumes at 10% breakthrough to predict full-scale throughput to 10% breakthrough. The regression is shown in equation 6.6.

$$lnBV_{10\%}^{full-scale} = (0.57 \pm 0.32) + (0.855 \pm 0.029) * lnBV_{10\%}^{PD-RSSCT} \qquad (eqn. 6.6)$$

Table 6.6 shows the predicted full-scale bed volumes to 10% breakthrough. Using equation 6.6, RSSCTs were consistently overcorrected resulting in underprediction of full-scale PFAA capacity. For example, PFOA and PFOS predicted full-scale capacities were 24.3K and 32.8K bed volumes, while the observed capacities were 32.1K and 64.2K bed volumes. Since Kennedy's regression is predicated on correcting RSSCT data that over-predicts full-scale capacity by a factor of 3.0 +/- 1.2, it is no surprise his regression overcompensates for scaling. However, full-scale capacities are within the range created when using Kennedy's mean prediction and the upper confidence limit. PFOS is the one exception, as the observed capacity is ~1K bed volumes greater than the Kennedy's upper confidence limit.

Table 6.6 Scale-Up; Predicted Full-Scale Bed Volumes to 10% Breakthrough Using RSSCT Bed Volumes to 10% Breakthrough (Kennedy, 2013).

Compound	RSSCT BV 10 (EBCT:13 min)	Kennedy FS Prediction BV 10	Kennedy FS Prediction (Upper CL) BV 10	Full Scale BV 10 (EBCT: 13 min)
PFBA	10300	4800	8600	5100
PFPeA	52700	19300	36400	33300
PFHxA	48900	18100	34000	31100
PFHpA	60600	21700	41100	-
PFOA	69000	24300	46200	32100
PFBS	59900	21500	40700	-
PFHxS	80400	27600	52800	-
PFOS	98200	32800	63000	64200

Another methodology to address the overprediction of the RSSCT capacity involves a fouling index (FI) (Corwin, 2010). A more thorough discussion of the FI is provided in chapter Five of this work but a brief overview is provided here.

The FI is based upon the scaling factor raised to some power 'Y' as shown in equation 6.7. The scaling factor is the ratio of the diameter of a GAC particle in the large column (LC) to the diameter of a GAC particle in the RSSCT.

$$FI = SF^{Y} = \left(\frac{d_{p,LC}}{d_{p,RSSCT}}\right) \qquad (eqn.\,6.7)$$

Equation 6.8 is used to adjust RSSCT capacity to more accurately reflect full-scale capacity.

$$Throughput_{\ LC} = \frac{Throughput_{RSSCT}}{FI} \qquad (eqn.\,6.8)$$

The RSSCT capacity correction process was visually applied to four PFAA compounds. This was accomplished by adjusting the fouling factor, Y, until the RSSCT capacity matched the full-scale capacity. When Y = 0, the FI becomes 1 (i.e, $SF^0 = 1$) and no correction of RSSCT throughput is needed. Greater values of Y, indicate greater correction and when Y = 1, a linear dependence on the scaling factor exists. For three of the four compounds, a Y of 0.2 resulted in a satisfactory full-scale capacity match. The fourth compound, PFOS, nearly matched full-scale results and only required a Y value of 0.05. The graphs for the PFBA and PFOS are presented in Figure 6.5 and Figure 6.6. Graphs for the other two PFAAs are included in the appendix.

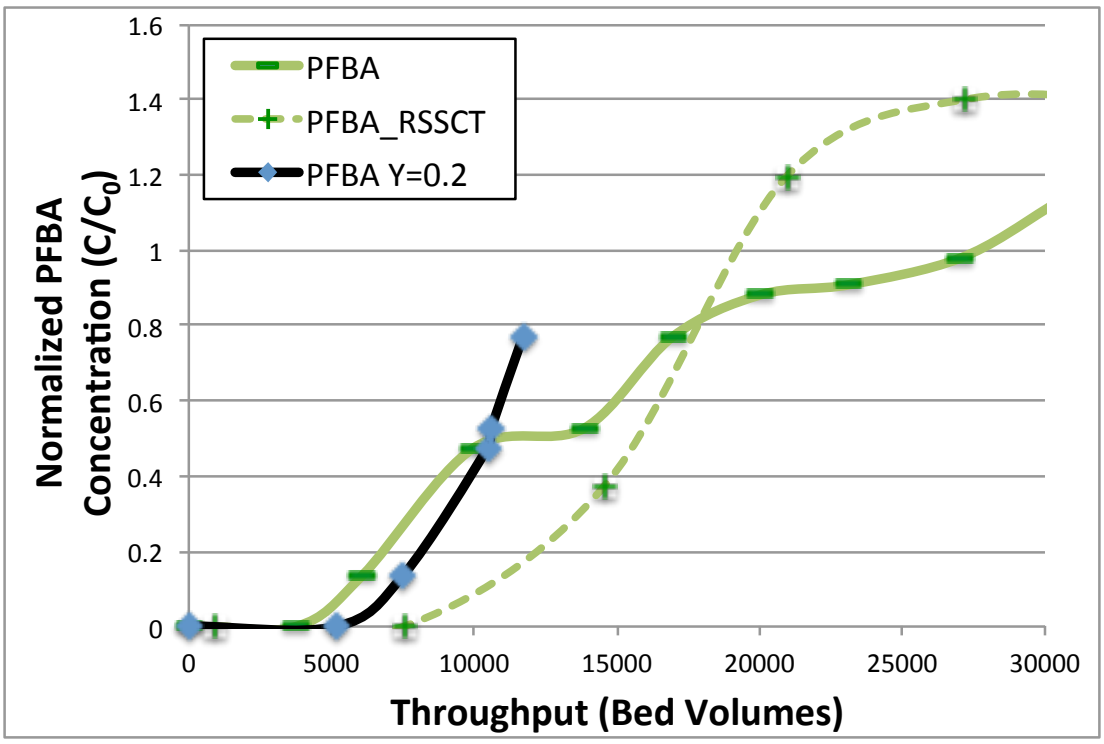

Figure 6.5 Scale-Up of RSSCT results to predict full-scale capacity for PFBA using Fouling Index. FI applied visually. EBCT: 13min

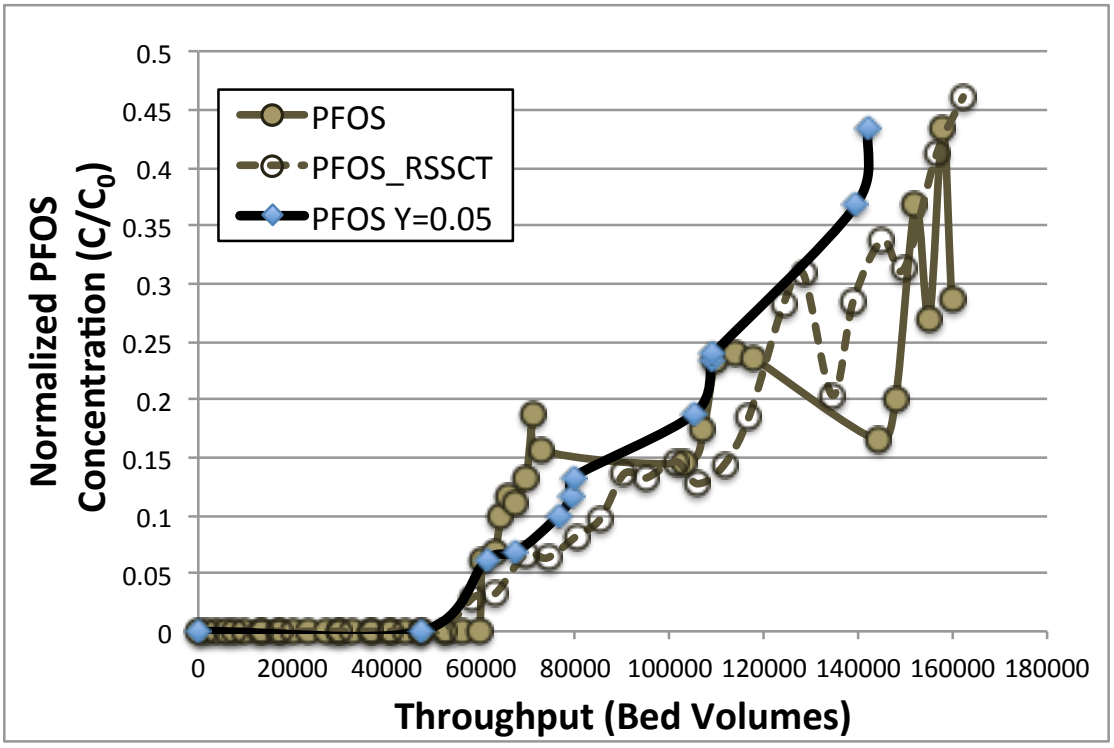

Figure 6.6 Scale-Up of RSSCT results to predict full-scale capacity for PFOS using Fouling Index. FI applied visually. EBCT: 13min

Visually correcting RSSCT results using the FI can assist with further adsorption work involving similar chemical classes in the same water. If significantly different conditions exist (e.g. increasing TOC load with spring run-off or algal blooms, significant changes to target organic concentrations, etc.) or a different background matrix is involved, two RSSCTs with different particle sizes are required to visually determine accurate fouling factors. Two other regressions have been developed to predict fouling factors without the use of multiple RSSCTs. One was developed by Kennedy and uses the ratio of the micropollutant (MP) concentration to the TOC concentration, the MP's pH dependent octonol-water partition coefficient (log D), and the RSSCT throughput to 10% breakthrough to predict Y. The regression is shown as equation 6.9.

$$Y = [2.59 + 3.94 * \frac{C_0^{MP}}{TOC_0} - 7.87 * BV_{10\%}^{PD-RSSCT} - 0.402 * logD +$$

$$4.2 * 10^{-4} * \left(\frac{C_0^{MP} * BV_{10\%}^{PD-RSSCT}}{TOC_0}\right) + 2.86 * 10^{-6} * BV_{10\%}^{PD-RSSCT} * logD]^{-1.47} \quad (eqn. 6.9)$$

A literature search for log D or log K_{ow} values for PFAAs was unproductive. As surfactants, perfluorinated compounds aggregate at the interface between octonol and water making the determination of log K_{ow} value difficult (Rahman et al., 2014). When values were located, often only one partition coefficient was provided for a wide range of carbon chain lengths. With these limitations in mind, the FI was applied to the RSSCT breakthrough data from PFOA using an estimate of the log K_{ow} of 6.3. Using such a large partition coefficient resulted in predicted Y value of 1.42 and an unreasonably large FI of 20.9. Applying this correction factor led to a drastic overcorrection and the scale-up effort using this regression was discontinued. More definitive determination of log D values should be made before this regression can be properly applied.

The second regression is shown as equation 6.10 and was developed during this effort. More explanation regarding its development is provided in chapter 5.

$$Y = 0.17 * \left(\frac{C_0}{TOC_0}\right)^{-0.12} \qquad (eqn. 6.10)$$

Scale-up graphs of four RSSCTs using the Y value predicted by equation 6.10 are included in the appendix. The regression resulted in overcorrection of all four RSSCT data sets analyzed. When applying the lower 95% confidence limit, mixed results were observed. Both full-scale breakthrough curves were captured for PFBA and PFOA when applying the 95% confidence limit; however, both PFPeA and PFHxA predictions were still overcorrected compared to the full-scale capacity. One possible explanation for this is the variability seen in the influent concentration to the full-scale column over the 4.8 year operation time. Also, although attempts were made to match full-scale and RSSCT influent concentrations, they were not equal. This surely contributes some degree of difficultly with scale-up.

6.6 Conclusions

Due to their ubiquitous presence in the environment and prolific use in industry, PFAAs are a class of compounds receiving increased attention. Conventional water treatment technologies have not shown the ability to substantially remove PFAAs. Using data from both RSSCT and full-scale adsorbers, this chapter investigated the use of GAC as a viable treatment technology.

Longer chained PFAAs and sulfonate-containing compounds broke through later than their shorter chained and carboxylic-containing counterparts. The increased capacity with chain length is due to an increase to the hydrophobic portion of the PFAA and thusly an increased

adsorption potential. Greater adsorption of PFAAs with sulfonate moieties is still undetermined. Explanations may include specific electron-donor interactions, hydrophobicity as a function of the moiety size, or HSAB theory. At different EBCTs, neither the RSSCT nor the full-scale adsorber showed significantly different capacity for a PFAA. This is indicative that significant fouling of the GAC by groundwater DOM with depth is not occurring. The RSSCT overpredicted full-scale capacity of PFAAs by about 70%. Past research has shown, the RSSCT overpredicts by a factor of 3.0+/-1.2 (Kennedy, 2013). The groundwater's lower TOC quantity and more recalcitrant character are believed to be the reason for the lack of fouling with longer EBCTs and the smaller capacity over-prediction. RSSCT scale-up efforts were applied to the data with mixed results. Visually, fouling factors were found to be 0.20 for three of four breakthrough curves. The fourth fouling factor was only 0.05. Three different regressions were used to predict full-scale adsorber performance without the use of multiple RSSCTs. Consistently, all three regressions overcorrected RSSCT capacities and thereby underpredicted capacity seen in the full-scale adsorber. Variable full-scale influent concentrations, and unequal influent concentrations between the RSSCT and the full-scale adsorber, are believed to be partially responsible for the scale-up difficulty. CURs were calculated for a total of 20 RSSCT and full-scale breakthrough curves. The four carbon-chained PFBA is the only compound where GAC treatment is in the transition range between practical and unfeasible – all other PFAAs had CURs below accepted thresholds, signifying GAC as a viable treatment technology.

Chapter 7 Final Conclusions and Future Research Needs

7.1 Remarks

The chief objective of this effort was to evaluate GAC's capacity to remove low concentrations of cVOCs and PFAAs from groundwater. Specifically the research focused on how competing target organics and DOM in the background matrix affected adsorption. Chapter 3 evaluated cVOC adsorption and Chapter 4 focused specifically on DOM and 1,2 DCA adsorption. Since a significant portion of this effort involved the use of the RSSCT, Chapter 5 addressed scale-up of RSSCT results to full-scale. Chapter 6 investigated PFAA adsorption onto GAC using both the RSSCT and a full-scale adsorber.

Overall conclusions are provided at the end of each respective chapter; to avoid redundancy, conclusions here are discussed in context of the hypotheses developed in Chapter 1, that broadly guided efforts throughout this research.

7.2 Hypotheses

7.2.1 H-1; GAC capacity for cVOCs is negatively affected by competition from both dissolved organic matter in groundwaters and co-solutes

Competition for adsorption sites between co-solutes was found in groundwater at the concentrations evaluated. Co-solutes with similar adsorptivities affected one another four to five times more than co-solutes with dissimilar adsorptivites. Groundwater DOM adversely affects GAC capacity for cVOCs to a greater extent than co-solutes. Experiments at two EBCTs in a low-TOC GW (TOC: 0.3 mg/L) consistently had less cVOC capacity, ~25%, than experiments conducted in organic-free water. The high TOC end member water (TOC: 1.5 mg/L) had greater

reductions in capacity, ~50%. Displacement of a weak adsorbing compound by a more strongly adsorbing compound resulted in effluent concentrations of the weak adsorbing compound exceeding that in the influent. Competing co-solutes and DOM are both believed to contribute to displacement with DOM being the larger contributor to this phenomenon. Often observed in surface waters, increased GAC fouling with adsorber depth and normalized breakthrough of target organic independent of influent concentration did not occur. The lower TOC concentration in GW and the more recalcitrant nature of the DOM are believed to be responsible for this behavior.

7.2.2 H-2; Characteristics of dissolved organic matter, other than concentration, can be used to predict cVOC adsorption

Using fluorescence spectroscopy, DOM characteristics were correlated to experimental RSSCT capacities for 1,2 DCA. Regressions combining three terms, including 1) a fluorescent indicator (e.g. FI, HIX, or peak C intensity), 2) a TOC mass term (e.g. TOC concentration or UV absorbance value) and 3) a target organic mass term (e.g. influent 1,2 DCA concentration), were created with coefficients of determination greater than 0.78. A correlation using only UV absorbance and influent 1,2 DCA concentration was also developed and had a coefficient of determination of 0.74.

7.2.3 H-3; Bench-scale breakthrough results can be scaled up to predict full-scale adsorber performance

Scale-up was accomplished in this effort using a variety of methods. Visually applying a FI provided good correlation between adsorption capacities of GACs at different sizes but requires two RSSCTs to be conducted and can only be considered valid for the particular water and concentration range being investigated. Existing regressions provided mixed results with

cVOCs. Application of existing scale-up methodology to PFAA adsorption was difficult because the molecular descriptor needed for the regression, log D, was not available. Using the data garnered in this effort, a scale-up correlation was created using the target organic influent concentration and the TOC concentration. This regression simulated the cVOC curves well but had mixed results with PFAA scale-up. Variable full-scale influent concentrations, and unequal influent concentrations between the RSSCT and the full-scale adsorber, are believed to be responsible for scale-up difficulty for PFAAs.

7.2.4 H-4; Adsorption of perfluoroalkyl acids from a groundwater using GAC behaves in a similar manner to cVOC adsorption.

Similar to cVOCs, GAC fouling as a function of adsorber depth was not seen to occur in with the groundwater matrix investigated in this study. The RSSCT over-predicted full-scale capacity by 1.7 times. Considering the larger scaling factor of GAC particle size in the PFAA effort, this is indicative of less over-prediction than observed in the cVOC work. Due to a smaller overprediction of capacity, visual scale-up work resulted in smaller fouling factors when compared to the cVOC effort (Y = 0.05 and 0.2 for PFAA and Y = 0.24 and 0.57 for cVOCs). Using the CUR as a metric of efficiency, three of four full-scale results (and seven of eight RSSCT results) indicate GAC is a viable treatment option to remove PFAA from the groundwater used in this study.

7.3 Future Work

The use of GAC to effectively remove cVOCs from groundwater is promising but additional effort is required to fully understand and optimize treatment processes. The definitive mechanisms competing co-solutes and DOM adversely affecting GAC adsorption of both cVOCs and PFAA compounds in groundwater is yet to be determined. Relating GAC

performance to the correlation between cVOC concentration and DOM concentration was developed for 1,2 DCA but needs to be expanded to include other cVOCs of interest. Prediction of target organic breakthrough with the use of DOM characteristics is promising; the data set employing the use of fluorescent and UV technologies should be expanded. Significant displacement of weaker adsorbing compounds was observed in this effort. To avoid regulatory violation and possible adverse health consequences, displacement of weakly adsorbing compounds in multi-solute systems could be investigated further. With minor adjustments the PSDM was accurate in scenarios involving single solutes in organic-free water and precise in predicting the order of elution in co-solute scenarios; however, the utility of the model could be enhanced significantly if multi-component *and* DOM fouling could be predicted accurately.

In order to realize the full advantages of the PD-RSSCT, which can be operated more economically than pilot columns, continued scale-up work between GAC particle sizes is warranted. The correlation between target organic and the influent DOM concentrations using only groundwaters and proportionally designed RSSCTs should be expanded. Relationships between DOM characteristics, through either the use of fluorescent metrics or size distribution metrics could be researched further. Methodology employing two RSSCTs with different particle sizes and a weakly adsorbing surrogate compound could be developed to quickly determine the FI for a water that could be applied to predict full-scale GAC performance stronger adsorbing compounds. Selecting a surrogate compound that broke through quickly, but not before DOM breakthrough, would have to be ensured if this was pursued.

Future work in the PFAA area could include a more focused approach on linear versus branched PFAAs. Preliminary observations have found that linear isomers are preferentially adsorbed onto GAC compared to their branched counterparts (Eschauzier et al., 2012).

Additional research is also needed with the earlier eluting, shorter chained compounds. As weaker adsorbing compounds, the shorter chained PFAA concentrations may be displaced by longer chained PFAAs and causing effluent concentrations to exceed influent concentrations. Weaker adsorbing PFAA compounds may dictate GAC change-out, influencing treatment costs. Also, as regulatory measures are enacted for the longer chained PFOA and PFOS, industry is expected to increase the use of shorter chained PFAAs (Appleman et al., 2013). The CURs determined apply only to the MN water; additional GWs should be investigated to determine if similar efficiencies exist in other waters. A more controlled scale-up effort focusing on equal influent concentrations between full- (or pilot-) and small-scale adsorbers should be attempted to determine the applicability of the RSSCT for PFAA adsorption.

Chapter 8 References

Ahrens, L., Taniyasu, S., Yeung, L.W.Y., Yamashita, N., Lam, P.K.S., Ebinghaus, R., 2010. Distribution of polyfluoroalkyl compounds in water, suspended particulate matter, adn sediment from Tokyo Bay, Japan. Chemosphere 79, 266–272. doi:10.1016/j.chemosphere.2010.01.045

Alfarra, A., Frackowiak, E., Béguin, F., 2004. The HSAB concept as a means to interpret the adsorption of metal ions onto activated carbons. Applied Surface Science 228, 84–92. doi:10.1016/j.apsusc.2003.12.033

Appleman, T.D., Dickenson, E.R.V., Bellona, C., Higgins, C.P., 2013. Nanofiltration and granular activated carbon treatment of perfluoroalkyl acids. Journal of Hazardous Materials 260, 740–746. doi:10.1016/j.jhazmat.2013.06.033

Appleman, T.D., Higgins, C.P., Quiñones, O., Vanderford, B.J., Kolstad, C., Zeigler-Holady, J.C., Dickenson, E.R., 2014. Treatment of poly-and perfluoroalkyl substances in US full-scale water treatment systems. Water Research 246–255.

AWWA, 2011a. Water Quality and Treatment, Sixth Edition. ed. American Water Works Association.

AWWA (Ed.), 2011b. AWWA Treatment Technology Workshop for Carcinogenic VOCs. AWWA, Washington, DC.

Baker, A., Genty, D., 1999. Fluorescence wavelength and intensity variations of cave waters [WWW Document]. Journal of Hydrology. URL https://cuvpn.colorado.edu/dana/home/index.cgi (accessed 5.25.14).

Baker, A., Tipping, E., Thacker, S.A., Gondar, D., 2008. Relating dissolved organic matter fluorescence and functional properties. Chemosphere 73, 1765–1772. doi:10.1016/j.chemosphere.2008.09.018

Bao, L.-J., Maruya, K.A., Snyder, S.A., Zeng, E.Y., 2012. China's water pollution by persistent organic pollutants. Environmental Pollution 163, 100–108. doi:10.1016/j.envpol.2011.12.022

Barnes, K.K., Kolpin, D.W., Furlong, E.T., Zaugg, S.D., Meyer, M.T., Barber, L.B., 2008. A national reconnaissance of pharmaceuticals and other organic wastewater contaminants in the United States — I) Groundwater. Science of The Total Environment 402, 192–200. doi:10.1016/j.scitotenv.2008.04.028

Benotti, M.J., Trenholm, R.A., Vanderford, B.J., Holady, J.C., Stanford, B.D., Snyder, S.A., 2009. Pharmaceuticals and Endocrine Disrupting Compounds in U.S. Drinking Water. Environ Sci Technol 43, 597–603. doi:10.1021/es801845a

Berrigan, J.K., 2004. Scale up of Rapid Small Scale Adsorption Tests to Field Scale Adsorbers: Theoretical and Experimental Basis 1–226.

Cai, M., Zhao, Z., Yang, H., Yin, Z., Hong, Q., Sturm, R., Ebinghaus, R., Ahrens, L., Cai, M., He, J., Xie, Z., 2012. Spatial distribution of per- and polyfluoroalkyl compounds in coastal waters from the East to South China Sea. Environmental Pollution 161, 162–169. doi:10.1016/j.envpol.2011.09.045

Cammack, W.K.L., Kalff, J., Prairie, Y.T., Smith, E.M., 2004. Fluorescent dissolved organic matter in lakes: Relationships with heterotrophic metabolism. Limnol. Oceanogr. 49, 2034–2045.

Carter, M.C., Weber, W.J., 1994. Modeling Adsorption of TCE by Activated Carbon Preloaded by Background Organic Matter - Environmental Science & Technology (ACS Publications). Environmental science & technology.
Cerminara, P.J., Sorial, G.A., Papadimas, S.P., Suidan, M.T., Moteleb, M.A., Speth, T.F., 1995. Effect of influent oxygen concentration on the GAC adsorption of VOCs in the presence of BOM. Water Research 29, 409–419.
Chowdhury, Z., Summers, R.S., Westerhoff, G.P., Leto, B.J., Nowack, K.O., Corwin, C.J., 2013. Activated Carbon - Solutions for Improving Water Quality. AWWA.
Coble, P.G., 1996. Characterization of marine and terrestrial DOM in seawater using excitation-emission matrix spectroscopy. Mar Chem 51, 325–346.
Coble, P.G., Green, S.A., Blough, N.V., Gagosian, R.B., 1990. Characterization of dissolved organic matter in the Black Sea by fluorescence spectroscopy.
Corwin, C., Summers, R.S., 2012. Controlling trace organic contaminants with GAC adsorption. Journal-American Water Works Association 104, E36–E47. doi:10.5942/jawwa.2012.104.0004
Corwin, C.J., 2010. Trace Organic Contaminant Removal from Drinking Waters by Granular Activated Carbon: Adsorption, Desorption, and the Effect of Background Organic Matter. PhD Thesis.
Corwin, C.J., 2012. Activated Carbon for Organic Contaminant Control, in: ACS Book Draft#3. pp. 1–28.
Corwin, C.J., Summers, R.S., 2010. Scaling Trace Organic Contaminant Adsorption Capacity by Granular Activated Carbon. Environ Sci Technol 44, 5403–5408. doi:10.1021/es9037462
Corwin, C.J., Summers, R.S., 2011. Adsorption and desorption of trace organic contaminants from granular activated carbon adsorbers after intermittent loading and throughout backwash cycles. Water Research 45, 417–426. doi:10.1016/j.watres.2010.08.039
Cory, R.M., Miller, M.P., McKnight, D.M., Guerard, J.J., Miller, P.L., 2010. Effect of instrument-specific response on the analysis of fulvic acid fluorescence spectra. Limnology and Oceanography: Methods 8, 67–78.
Crittenden, J.C., Berrigan, J.K., Hand, D.W., 1986a. Design of rapid small-scale adsorption tests for a constant diffusivity. Journal (Water Pollution Control Federation) 312–319.
Crittenden, J.C., Berrigan, J.K., Hand, D.W., Lykins, B., 1987. Design of Rapid Fixed-Bed Adsorption Tests for Nonconstant Diffusivities. Journal of Environmental Engineering - ASCE 113, 243–259.
Crittenden, J.C., Hutzler, N.J., Geyer, D.G., Oravitz, J.L., Friedman, G., 1986b. Transport of Organic Compounds With Saturated Groundwater Flow: Model Development and Parameter Sensitivity. Water Resour. Res. 22, 271–284. doi:10.1029/WR022i003p00271
Crittenden, J.C., Reddy, P.S., Arora, H., Trynoski, J., Hand, D.W., Perram, D.L., Summers, R.S., 1991. Predicting GAC performance with rapid small-scale column tests. Journal-American Water Works Association 83, 77–87.
Crittenden, J.C., Reddy, P.S., Hand, D.W., Arora, H., 1989. Prediction of GAC Performance Using Rapid Small-Scale Column Test (No. Rpt# 90549). American Water Works Association Research Foundation.
Crittenden, J.C., Wong, B.W., Thacker, W.E., Snoeyink, V.L., Hinrichs, R.L., 1980. Mathematical model of sequential loading in fixed-bed adsorbers. Journal (Water Pollution Control Federation) 2780–2795.
Cummings, L., Summers, R.S., 1994. Using RSSCTs to predict field-scale GAC control of DBP

formation. Journal of the American Water Works Association 86, 88–97.
EPA, U.S., 1996. ICR Manual for Bench and Pilot Scale Treatment Studies 1–388.
EPA, U.S., 2009. Water Treatment Technology Feasibility Support Document for Chemical Contaminants for the Second Six-Year Review ofNational Primary Drinking Water Regulations (No. EPA 815_B-09-007). U.S. E.P.A.
EPA, U.S., 2010. Drinking Water Strategy [WWW Document]. Water: Drinking Water Strategy. URL http://water.epa.gov/lawsregs/rulesregs/sdwa/dwstrategy/index.cfm (accessed 3.26.12).
EPA, U.S., 2011. National Primary Drinking Water Regulations: Group Regulation of Carcinogenic Volatile Organic Compound (VOCs) - Reg DaRRT | Laws & Regulations | US EPA [WWW Document]. yosemite.epa.gov. URL http://yosemite.epa.gov/opei/rulegate.nsf/byRIN/2040-AF29?opendocument (accessed 6.20.13).
Eschauzier, C., Beerendonk, E., Scholte-Veenendaal, P., De Voogt, P., 2012. Impact of Treatment Processes on the Removal of Perfluoroalkyl Acids from the Drinking Water Production Chain. Environ Sci Technol 46, 1708–1715. doi:10.1021/es201662b
Fellman, J.B., Hood, E., Spencer, R.G.M., 2010. Fluorescence spectroscopy opens new windows into dissolved organic matter dynamics in freshwater ecosystems: A review. Limnol. Oceangr. 55, 2452–2462. doi:10.4319/lo.2010.55.6.2452
Flores, C., Ventura, F., Martin-Alonso, J., Caixach, J., 2013. Occurrence of perfluorooctane sulfonate (PFOS) and perfluorooctanoate (PFOA) in N.E. Spanish surface waters and their removal in a drinking water treatment plant that combines conventional and advanced treatments in parallel lines. Science of the Total Environment, The 461-462, 618–626. doi:10.1016/j.scitotenv.2013.05.026
Focazio, M.J., Kolpin, D.W., Barnes, K.K., Furlong, E.T., Meyer, M.T., Zaugg, S.D., Barber, L.B., Thurman, M.E., 2008. A national reconnaissance for pharmaceuticals and other organic wastewater contaminants in the United States — II) Untreated drinking water sources. Science of The Total Environment 402, 201–216. doi:10.1016/j.scitotenv.2008.02.021
Fotta, M.E., 2012. Effect of Granular Activated Carbon Type on Adsorber Performance and Scale-Up Approaches for Volatile Organic Compound Removal 1–141.
Gillogly, T.E., Snoeyink, V.L., Elarde, J.R., Wilson, C.M., Royal, E.P., 1998. 14C-MIB adsorption on PAC in natural water. Journal of the American Water Works Association 90, 98–108.
Gnielinski, V., 1978. Gleichungen zur berechnung des warmeund stoffaustausches in durchstromten ruhenden kugelschuttungen bei mitteren und grossen pecletzahlen.
. Verf. Tech. 12, 363–366.
Graham, M.R., Summers, R.S., Simpson, M.R., Macleod, B.W., 2000. Modeling equilibrium adsorption of 2-methylisoborneol and geosmin in natural waters. Water Research 34, 2291–2300.
Grandjean, P., Andersen, E.W., Budtz-Jørgensen, E., Nielsen, F., Mølbak, K., Weihe, P., Heilmann, C., 2012. Serum vaccine antibody concentrations in children exposed to perfluorinated compounds. JAMA: the journal of the American Medical Association 307, 391–397.
Guelfo, J.L., Higgins, C.P., 2013. Subsurface Transport Potential of Perfluoroalkyl Acids at Aqueous Film-Forming Foam (AFFF)-Impacted Sites. Environ Sci Technol 47, 4164–4171. doi:10.1021/es3048043

Hand, D.W., Crittenden, J.C., Arora, H., Miller, J.M., Lykins, B.W., Jr, 1989. Designing fixed-bed adsorbers to remove mixtures of organics. Journal-American Water Works Association 67–77.
Hand, D.W., Mertz, K., 1999. AdDesignS User Manual 1–126.
Hayduk, W., Laudie, H., 1974. Prediction of diffusion coefficients for nonelecrolytes in dilute aqueous solutions. J. Amer. Inst. Chem. Eng 20, 611–615.
Henderson, T., Cannon, F., 2011. Tailored Granular Activated Carbon Treatment of Perchlorate in Drinking Water. ESTCP Cost and Performance Report.
Her, N., Amy, G., Foss, D., Cho, J., 2002. Variations of Molecular Weight Estimation by HP-Size Exclusion Chromatography with UVA versus Online DOC Detection. Environ Sci Technol 36, 3393–3399. doi:10.1021/es015649y
Higgins, C.P., Luthy, R.G., 2006. Sorption of Perfluorinated Surfactants on Sediments †. Environ Sci Technol 40, 7251–7256. doi:10.1021/es061000n
Hudson, N., Baker, A., Reynolds, D., 2007. Fluorescence analysis of dissolved organic matter in natural, waste and polluted waters—a review. River Res. Applic. 23, 631–649. doi:10.1002/rra.1005
Hudson, N., Baker, A., Ward, D., Reynolds, D.M., Brunsdon, C., Carliell-Marquet, C., Browning, S., 2008. Can fluorescence spectrometry be used as a surrogate for the Biochemical Oxygen Demand (BOD) test in water quality assessment? An example from South West England. Science of the Total Environment, The 391, 149–158. doi:10.1016/j.scitotenv.2007.10.054
Jarvie, M.E., Hand, D.W., Crittenden, J.C., Hokanson, D.R., 2005. Simulating The Performance of Fixed-Bed Granular Activated CArbon Adsorbers: Removal of Synthetic Organic Chemicals in th Presence of Background Organic Matter, in:. Michigan Technological University.
Jones-Lepp, T.L., Sanchez, C., Alvarez, D.A., Wilson, D.C., Taniguchi-Fu, R.-L., 2012. Point sources of emerging contaminants along the Colorado River Basin: Source water for the arid Southwestern United States. Science of the Total Environment, The 430, 237–245. doi:10.1016/j.scitotenv.2012.04.053
Kalbitz, K., Geyer, W., Geyer, S., 1999. Spectroscopic properties of dissolved humic substances - a reflection of land use history in a fen area. BIogeochemistry 47, 219–238.
Kawaguchi, M., 1990. Sequential polymer adsorption: competition and displacement process. Advances in colloid and interface science 32, 1–41.
Kennedy, A., 2013. Granular Activated Carbon Adsorption of Organic Micropollutants: Scale-Up and Effect of Background Dissolved Organic Matter. University of Colorado - Boulder.
Kilduff, J.E., Karanfil, T., Weber, W.J., 1998. Competitive effects of nondisplaceable organic compounds on trichloroethylene uptake by activated carbon. I. Thermodynamic predictions and model sensitivity analyses. Journal of Colloid And Interface Science 205, 271–279.
Kim, S.D., Cho, J., Kim, I.S., Vanderford, B.J., Snyder, S.A., 2007. Occurrence and removal of pharmaceuticals and endocrine disruptors in South Korean surface, drinking, and waste waters. Water Research 41, 1013–1021. doi:10.1016/j.watres.2006.06.034
Knappe, D., Matsui, Y., Snoeyink, V., 1998. Predicting the Capacity of Powdered Activated Carbon for Trace Organic Compounds in Natural Waters. Environ Sci Technol 32, 1694–1698.
Knappe, D., Summers, R.S., 2012. Evaluation of the Henry's Law Constant and Freundlich Adsorption Constant for VOCs (No. WRF/WFP #4462).
Knappe, D.R., Snoeyink, V.L., Roche, P., Prados, M.J., Bourbigot, M.-M., 1999. Atrazine

removal by preloaded GAC. Journal of the American Water Works Association 91, 97–109.
Knappe, D.R.U., Snoeyink, V.L., Roche, P., Prados, M.J., Bourbigot, M.-M., 1997. The effect of preloading on rapid small-scale column test predictions of atrazine removal by GAC adsorbers. Water Research 31, 2899–2909. doi:10.1016/S0043-1354(97)00148-6
Kolpin, D., 2002. Pharmaceuticals, Hormones, and Other Organic Wastewater Contaminants in U.S. Streams, 1999-2000: A National Reconnaissance. Environ Sci Technol 36, 1202–1211.
Korak, J.A., 2014. Use of Fluorescence Spectroscopy to Characterize Dissolved Organic Matter. University of Colorado - Boulder.
Korak, J.A., Dotson, A.D., Summers, R.S., Rosario-Ortiz, F.L., 2014. Critical analysis of commonly used fluorescence metrics to characterize dissolved organic matter. Water Research 49, 327–338. doi:10.1016/j.watres.2013.11.025
Krasner, S.W., Westrick, J.J., Regli, S., 1995. Bench and Pilot Testing under the ICR. Journal of the American Water Works Association 87, 60–68.
Li, Q., Mariñas, B.J., Snoeyink, V.L., Campos, C., 2003a. Three-Component Competitive Adsorption Model for Flow-Through PAC Systems. 2. Model Application to a PAC/Membrane System. Environ Sci Technol 37, 3005–3011. doi:10.1021/es020990j
Li, Q., Snoeyink, V.L., Mariãas, B.J., Campos, C., 2003b. Elucidating competitive adsorption mechanisms of atrazine and NOM using model compounds. Water Research 37, 773–784.
Loos, R., Gawlik, B.M., Locoro, G., Rimaviciute, E., Contini, S., Bidoglio, G., 2009. EU-wide survey of polar organic persistent pollutants in European river waters. Environmental Pollution 157, 561–568. doi:10.1016/j.envpol.2008.09.020
Mastropole, A.J., 2011. Evaluation of Available Scale-Up Approaches fro the Design of GAC Contactors. North Carolina State University.
Matsui, Y., Fukuda, Y., Inoue, T., Matsushita, T., 2003. Effect of natural organic matter on powdered activated carbon adsorption of trace contaminants: characteristics and mechanism of competitive adsorption. Water Research.
Matsui, Y., Knappe, D.R.U., Iwaki, K., Ohira, H., 2002a. Pesticide Adsorption by Granular Activated Carbon Adsorbers. 2. Effects of Pesticide and Natural Organic Matter Characteristics on Pesticide Breakthrough Curves. Environ Sci Technol 36, 3432–3438. doi:10.1021/es011366u
Matsui, Y., Knappe, D.R.U., Takagi, R., 2002b. Pesticide Adsorption by Granular Activated Carbon Adsorbers. 1. Effect of Natural Organic Matter Preloading on Removal Rates and Model Simplification. Environ Sci Technol 36, 3426–3431. doi:10.1021/es0113652
Mayer, L.M., Schick, L.L., Loder, T.C., 1999. Dissolved protein fluorescence in two Maine estuaries. Mar Chem 64, 171–179. doi:10.1016/S0304-4203(98)00072-3
McKnight, D.M., Boyer, E.W., Westerhoff, P.K., Doran, P.T., Kulbe, T., Andersen, D.T., 2001. Spectrofluorometric characterization of dissolved organic matter for indication of precursor organic material and aromaticity. Limnol. Oceangr. 38–48.
Merk, W., Fritz, W., Schlunder, E.U., 1981. Competitive Adsorption of Two Dissolved Organics onto Activated Carbon_III. Chem Eng Sci 36, 743–757.
Nguyen, M.-L., Westerhoff, P., Baker, L., Hu, Q., Esparza-Soto, M., Sommerfeld, M., 2005. Characteristics and Reactivity of Algae-Produced Dissolved Organic Carbon. J. Envir. Engrg. 131, 1574–1582. doi:10.1061/(ASCE)0733-9372(2005)131:11(1574)
Plumlee, M.H., Larabee, J., Reinhard, M., 2008. Perfluorochemicals in water reuse. Chemosphere 72, 1541–1547. doi:10.1016/j.chemosphere.2008.04.057
Post, G.B., Cohn, P.D., Cooper, K.R., 2012. Perfluorooctanoic acid (PFOA), an emerging

drinking water contaminant: A critical review of recent literature. Environmental Research 116, 93–117. doi:10.1016/j.envres.2012.03.007
Prieto-Rodriguez, L., Miralles-Cuevas, S., Oller, I., Agüera, A., Puma, G.L., Malato, S., 2012. Treatment of emerging contaminants in wastewater treatment plants (WWTP) effluents by solar photocatalysis using low TiO_2 concentrations. Journal of Hazardous Materials 211-212, 131–137. doi:10.1016/j.jhazmat.2011.09.008
Rahman, M.F., Peldszus, S., Anderson, W.B., 2014. Behavior and fate of perfluoroalkyl and polyfluoroalkyl substances (PFASs) in drinking water treatment: A review. Water Research 50, 318–340. doi:10.1016/j.watres.2013.10.045
Regulations, P.1.N.P.D.W., 1994. Code of Federal Regulations.
Rossner, A., Snyder, S.A., Knappe, D.R.U., 2009. Removal of emerging contaminants of concern by alternative adsorbents. Water Research 43, 3787–3796. doi:10.1016/j.watres.2009.06.009
Rowe, B.L., Toccalino, P.L., Moran, M.J., Zogorski, J.S., Price, C.V., 2007. Occurrence and Potential Human-Health Relevance of Volatile Organic Compounds in Drinking Water from Domestic Wells in the United States. Environ Health Perspect 115, 1539–1546. doi:10.1289/ehp.10253
Saikat, S., Kreis, I., Davies, B., Bridgman, S., Kamanyire, R., 2013. The impact of PFOS on health in the general population: a review. Environmental Science: Processes & Impacts 15, 329–335.
Schideman, L.C., Mariñas, B.J., Snoeyink, V.L., Campos, C., 2006. Three-Component Competitive Adsorption Model for Fixed-Bed and Moving-Bed Granular Activated Carbon Adsorbers. Part I. Model Development. Environ Sci Technol 40, 6805–6811. doi:10.1021/es060590m
Sontheimer, H., Crittenden, J., Summers, R., 1988. Activated Carbon for Water Treatment, Second Edition. ed. DVGW-Forschungsstelle, Kalsruhe.
Speth, T.F., 1991. Evaluating Capacities of GAC Preloaded with Natural Water. J. Envir. Engrg. 117, 66–79.
Speth, T.F., Miltner, R.J., 1989. Effect of preloading on the scale-up of GAC microcolumns. Journal of the American Water Works Association 81, 141–148.
Speth, T.F., Miltner, R.J., 1990. Technical Note: Adsorption Capacity of GAC for Synthetic Organics. Journal (American Water … 1–4.
Summers, R.S., Haist, B., Koehler, J., Ritz, J., Zimmer, G., Sontheimer, H., 1989. The influence of background organic matter on GAC adsorption. Journal-American Water Works Association 66–74.
Summers, R.S., Hooper, S.M., Solarik, G., Owen, D., Hong, S., 1995. Bench-scale evaluation of GAC for NOM control. Journal of American Water Works 87, 69–80.
Summers, R.S., Kim, S.M., Shimabuku, K., Chae, S.-H., Corwin, C.J., 2013. Granular activated carbon adsorption of MIB in the presence of dissolved organic matter. Water Research 1–7. doi:10.1016/j.watres.2013.03.054
Summers, R.S., Roberts, P.V., 1988. Activated carbon adsorption of humic substances: II. Size exclusion and electrostatic interactions. Journal of Colloid And Interface Science.
Sun, H., Li, F., Zhang, T., Zhang, X., He, N., Song, Q., Zhao, L., Sun, L., Sun, T., 2011. Perfluorinated compounds in surface waters and WWTPs in Shenyang, China: Mass flows and source analysis. Water Research 45, 4483–4490. doi:10.1016/j.watres.2011.05.036
Thacker, W.E., Snoeyink, V.L., Crittenden, J.C., 1983. Desorption of compounds during

operation of GAC adsorption systems. Journal of the American Water Works Association 75, 144–148.
Thurman, E.M., 1985. Humic Substances in Groundwater, in: Aiken, G.R., McKnight, D.M., Wershaw, R.L., MacCarthy, P. (Eds.), Humic Substances in Soil, Sediment, and Water. Wiley-Interscience, pp. 87–103.
Toccalino, P.L., Hopple, J.A., Interior, U.U.S.D.O.T., 2010. Quality of Water from Public-Supply Wells in the United States, 1993-2007 Overview of Major Findings. BiblioGov.
Vidic, R.D., Sorial, G.A., Papadimas, S.P., Suidan, M.T., Speth, T.F., 1992. Effect of molecular oxygen on the scaleup of GAC adsorbers. Journal-American Water Works Association 98–105.
Westerhoff, P., Yoon, Y., Snyder, S., Wert, E., 2005. Fate of Endocrine-Disruptor, Pharmaceutical, and Personal Care Product Chemicals during Simulated Drinking Water Treatment Processes. Environ Sci Technol 39, 6649–6663. doi:10.1021/es0484799
Xiao, F., Simcik, M.F., Gulliver, J.S., 2013. Mechanisms for removal of perfluorooctane sulfonate (PFOS) and perfluorooctanoate (PFOA) from drinking water by conventional and enhanced coagulation. Water Research 47, 49–56. doi:10.1016/j.watres.2012.09.024
Zachman, B.A., Summers, R.S., 2010. Modeling TOC Breakthrough in Granular Activated Carbon Adsorbers. J. Envir. Engrg. 136, 204–210. doi:10.1061/(ASCE)EE.1943-7870.0000145
Zhang, W., Chang, Q.-G., Liu, W.-D., Li, B.-J., Jiang, W.-X., Fu, L.-J., Ying, W.-C., 2007. Selecting activated carbon for water and wastewater treatability studies. Environ. Prog. 26, 289–298. doi:10.1002/ep.10222
Zhou, Z., Liang, Y., Shi, Y., Xu, L., Cai, Y., 2013. Occurrence and Transport of Perfluoroalkyl Acids (PFAAs), Including Short-Chain PFAAs in Tangxun Lake, China. Environ Sci Technol 47, 9249–9257. doi:10.1021/es402120y
Zimmer, G., 1988. Untersuchungen zur Adsorption organischer Spurenstoffe aus naturlichen Wassern.
Zogorski, J.S., Carter, J.M., Ivahnenko, T., Lapham, W.W., Moran, M.J., Rowe, B.L., Squillace, P.J., Toccalino, P.L., 2006. Volatile Organic Compounds in the Nation's Ground Water and Drinking-Water Supply Wells 1–112.

Appendix A – Analytical and Experimental Error

Table_A.1 Results of duplicate and triplicate samples collected over the experimental period to estimate analytical error. Results shown are for cVOC analysis only.

total # duplicate or triplicate sets	% difference		standard deviation		coefficient of variation	
	abs average	median	average	median	average	median
95	6.0%	2.8%	0.39	0.03	0.10	0.02

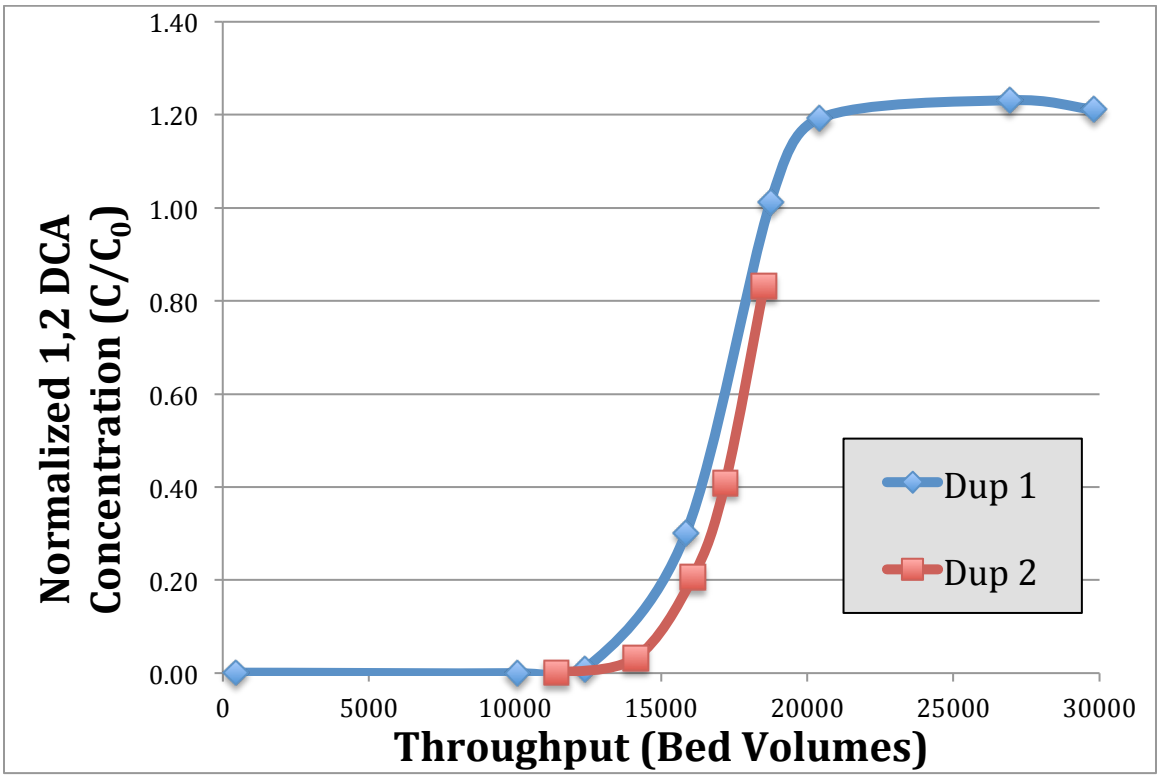

Figure_A.1 Results from duplicate columns run under identical conditions. Results used to estimate experimental error. Breakthrough curves represent 1,2 DCA breakthrough in CO GW II with influent concentration of ~ 5µg/L. Co-solutes were also included in column (data not shown) with influent concentrations of CT = 1. 4 µg/L and TCE = 1.8 µg/L.

Table_A.2 Detection limits for GC/MS using single ion mode (SIM) for analysis of cVOCs. Modified EPA method 524.3 (headspace modification instead of purge and trap); * Analyzed using SPME. ** May be analyzed using headspace or SPME. Compounds underlined were the analytes used in this research. MDL: method detection limit; LCMRL: Lowest Concentration Minimum Reporting Levels (the lowest spiking concentration such that the probability of spike recovery in the 50 – 150% range is at least 99%).

Compound	CAS	MDL (ng/L)	LCMRL (ng/L)
Benzene	71-43-2	23	24
Carbon Tetrachloride	56-23-5	21	21
1,2-Dichloroethane	107-06-2	7.9	20
1,2-Dichloropropane	78-87-5	16	25
Dichloromethane**	75-09-2	11	116
Tetrachloroethylene	127-18-4	30	30
Trichloroethylene	79-01-6	10	17
Vinyl Chloride*	75-01-4	3.2	11
1,3-Butadiene*	106-99-0	16	43
1,1-Dichloroethane	75-34-3	16	23
1,2,3-Trichloropropane	96-18-4	20	37
1,1,2,2-Tetrachloroethane	79-34-5	7.1	30
1,1,1,2-Tetrachloroethane	630-20-6	16	16

Appendix B – RSSCT Calculation Spreadsheet

Table_B.1 RSSCT Spreadsheet used in experimental design and set-up. Text in blue indicates data that is input by the user; black text is calculated by the governing design equations.

RSSCT Design		Column			
		1	2	units	design equation
Carbon	Manufacturer	Norit	Norit		
	Product	GAC 400	GAC400		
	Type	Bituminous	Bituminous		
	Dry Bed Density, ρ_b	0.43	0.43	g/cm^3	
	Bed Porosity, ε	0.38	0.38		
	Particle Porosity, ε_p	0.5	0.5		
	Approach	PD	PD		
	X	1.0	1.0		
Large Column	Upper Sieve Size (Large Scale)	12	12		
	Lower Sieve Size (Large Scale)	40	40		
	$d_{p\ LC}$	0.92	0.92	mm	
	$EBCT_{LC}$	7.5	15.0	min	
	Hydraulic Loading Rate, v	5.0	5.0	m/hr	
	Re_{LC}	3.6	3.6		
Small Column	Upper Sieve Size (Small Scale)	100	100		
	Lower Sieve Size (Small Scale)	200	200		
	$d_{p\ SC}$	0.11	0.11	mm	
	RSSCT column diameter	4.76	4.76	mm	
	Flow Rate	2.00	2.00	mL/min	
	Hydraulic Loading Rate, v_{SC}	6.74	6.74	m/hr	$v_{SC}=Q_{SC}/A$
	Minimum HLR	5.9	5.9	m/hr	
	Ideal HLR	43	43	m/hr	
	Temperature, T	23	23	°C	
	Kinematic Viscosity, kv	9.34E-07	9.34E-07	m^2/s	
	Density of Water, ρ_w	997.6	997.6	kg/m^3	

	Dynamic Viscosity, dv	9.32E-03	9.32E-03	$g \cdot cm^{-1} \cdot s^{-1}$	
	Column Area, A	0.178	0.178	cm^2	$A=\pi \cdot (DC_{SC})^2/4$
	Aspect Ratio, AR	44	44		$AR=d_{p\ SC}/DC$
	Scaling Factor, SF	8.50	8.50		$SF=d_{LC}/d_{SC}$
	$EBCT_{SC}$	0.88	1.76	min	$EBCT_{SC}=EBCT_{LC}/SF^{2-x}$
	Minimum Re_{SC}	0.5	0.5		
	Re_{SC}	0.6	0.6		
	Bed Volume, V	1.765	3.529	mL	$V=A \cdot l_{SC}$
	Bed Length, l_{SC}	9.91	19.81	cm	$l_{SC}=v_{SC} \cdot EBCT_{SC}$
	Mass GAC Required, M_{GAC}	0.759	1.518	g	$M_{GAC}=EBCT_{SC} \cdot Q_{SC} \cdot \rho_b$
	Total Throughput	60,000	30,000	#BVs	
	RSSCT Run Time	37	37	days	
	Volume Water Required	106	106	L	

Appendix C – SEC and UV absorbance data

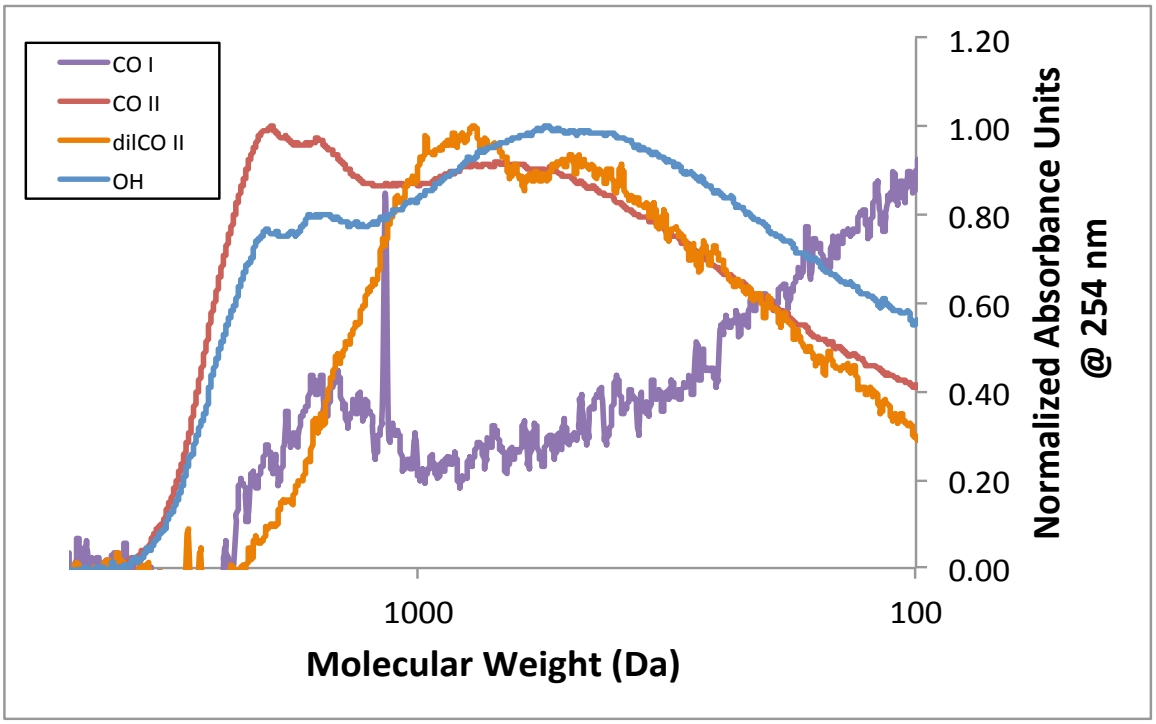

Figure_C.1 Graphical representation of Size Exclusion Chromatography (SEC) normalized to influent TOC concentration for four groundwaters.

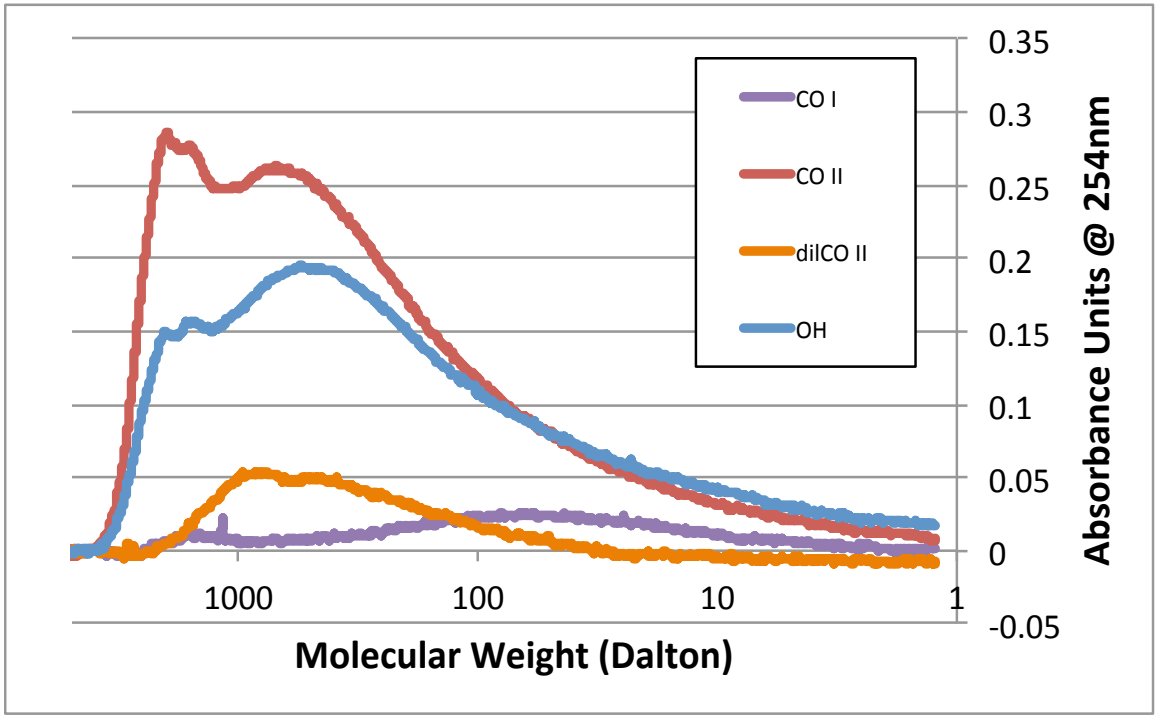

Figure_C.2 Graphical representation of Size Exclusion Chromatography (SEC) not normalized to TOC concentration for four groundwaters.

Table_C.1 UV adsorption data for four groundwaters used in this research.

Wavelength (nm)	CO GW I	CO GW II	dilCO II	OH
	Absorbance (cm^{-1})			
200	0.43724	0.82053	0.72200	0.44580
201	0.34716	0.77390	0.67590	0.41025
202	0.27539	0.73236	0.63659	0.38111
203	0.21956	0.69816	0.60280	0.35741
204	0.17546	0.66713	0.57561	0.33931
205	0.14173	0.63993	0.54734	0.32105
206	0.11332	0.61290	0.52330	0.30538
207	0.09187	0.58715	0.50008	0.29120
208	0.07463	0.56144	0.47771	0.27768
209	0.06072	0.53665	0.45477	0.26420
210	0.05022	0.51060	0.43235	0.25137
211	0.04188	0.48366	0.40894	0.23817
212	0.03524	0.45724	0.38552	0.22523
213	0.02984	0.42808	0.36080	0.21138
214	0.02552	0.40024	0.33679	0.19773
215	0.02245	0.37236	0.31203	0.18459
216	0.01975	0.34375	0.28743	0.17139
217	0.01769	0.31625	0.26385	0.15819
218	0.01538	0.28900	0.24019	0.14461
219	0.01422	0.26252	0.21792	0.13242
220	0.01317	0.23833	0.19663	0.12052
221	0.01241	0.21472	0.17650	0.10963
222	0.01162	0.19253	0.15751	0.09964
223	0.01116	0.17228	0.13975	0.08976
224	0.01052	0.15361	0.12396	0.08054
225	0.01048	0.13688	0.10953	0.07293
226	0.01039	0.12158	0.09655	0.06522
227	0.00918	0.10735	0.08456	0.05875
228	0.00922	0.09548	0.07458	0.05286
229	0.00842	0.08445	0.06498	0.04753
230	0.00861	0.07540	0.05709	0.04317
231	0.00834	0.06743	0.05042	0.03911
232	0.00781	0.06010	0.04378	0.03571
233	0.00775	0.05427	0.03929	0.03264
234	0.00754	0.04843	0.03499	0.03000
235	0.00738	0.04494	0.03138	0.02828
236	0.00680	0.04071	0.02770	0.02595
237	0.00654	0.03770	0.02551	0.02477
238	0.00657	0.03525	0.02341	0.02338
239	0.00660	0.03305	0.02164	0.02214
240	0.00629	0.03139	0.02055	0.02149
241	0.00604	0.02943	0.01884	0.02054
242	0.00605	0.02808	0.01780	0.01961
243	0.00599	0.02700	0.01748	0.01915
244	0.00570	0.02599	0.01673	0.01859
245	0.00559	0.02485	0.01568	0.01822

Wavelength (nm)	CO GW I	CO GW II	dilCO II	OH
246	0.00534	0.02408	0.01486	0.01766
247	0.00511	0.02351	0.01464	0.01754
248	0.00566	0.02334	0.01407	0.01742
249	0.00508	0.02256	0.01399	0.01681
250	0.00505	0.02172	0.01325	0.01639
251	0.00468	0.02154	0.01338	0.01653
252	0.00441	0.02073	0.01309	0.01599
253	0.00482	0.02042	0.01240	0.01576
254	0.00443	0.02020	0.01221	0.01552
255	0.00483	0.02019	0.01247	0.01561
256	0.00463	0.01949	0.01163	0.01478
257	0.00456	0.01943	0.01200	0.01482
258	0.00456	0.01920	0.01171	0.01473
259	0.00486	0.01909	0.01175	0.01534
260	0.00464	0.01855	0.01162	0.01435
261	0.00432	0.01823	0.01155	0.01441
262	0.00451	0.01838	0.01125	0.01371
263	0.00415	0.01788	0.01115	0.01398
264	0.00479	0.01801	0.01127	0.01403
265	0.00409	0.01783	0.01113	0.01358
266	0.00422	0.01747	0.01060	0.01409
267	0.00417	0.01729	0.01051	0.01335
268	0.00402	0.01737	0.01053	0.01330
269	0.00389	0.01643	0.01041	0.01311
270	0.00374	0.01673	0.01046	0.01291
271	0.00415	0.01655	0.01051	0.01286
272	0.00392	0.01646	0.01014	0.01295
273	0.00401	0.01620	0.01038	0.01280
274	0.00368	0.01532	0.00974	0.01232
275	0.00401	0.01552	0.00965	0.01221
276	0.00406	0.01527	0.00957	0.01225
277	0.00362	0.01531	0.00966	0.01187
278	0.00361	0.01510	0.00945	0.01208
279	0.00337	0.01438	0.00899	0.01142
280	0.00371	0.01481	0.00923	0.01164
281	0.00377	0.01428	0.00870	0.01107
282	0.00346	0.01410	0.00894	0.01106
283	0.00327	0.01386	0.00885	0.01063
284	0.00348	0.01401	0.00839	0.01092
285	0.00345	0.01336	0.00868	0.01059
286	0.00366	0.01334	0.00848	0.01043
287	0.00349	0.01339	0.00858	0.01028
288	0.00315	0.01291	0.00797	0.00972
289	0.00386	0.01259	0.00845	0.00985
290	0.00344	0.01265	0.00821	0.01004
291	0.00315	0.01247	0.00785	0.00957
292	0.00324	0.01198	0.00762	0.00928
293	0.00344	0.01174	0.00771	0.00930
294	0.00289	0.01145	0.00737	0.00902
295	0.00291	0.01152	0.00727	0.00866

Wavelength (nm)	CO GW I	CO GW II	dilCO II	OH
296	0.00286	0.01131	0.00699	0.00842
297	0.00313	0.01108	0.00733	0.00848
298	0.00289	0.01077	0.00691	0.00831
299	0.00292	0.01109	0.00723	0.00825
300	0.00335	0.01059	0.00677	0.00798
301	0.00312	0.01067	0.00649	0.00775
302	0.00257	0.01010	0.00631	0.00725
303	0.00322	0.00973	0.00634	0.00758
304	0.00268	0.01005	0.00624	0.00725
305	0.00250	0.01001	0.00640	0.00745
306	0.00246	0.00939	0.00586	0.00657
307	0.00286	0.00966	0.00588	0.00716
308	0.00296	0.00942	0.00605	0.00679
309	0.00230	0.00910	0.00589	0.00701
310	0.00240	0.00887	0.00550	0.00606
311	0.00210	0.00883	0.00556	0.00636
312	0.00238	0.00859	0.00517	0.00614
313	0.00253	0.00818	0.00534	0.00565
314	0.00210	0.00835	0.00505	0.00585
315	0.00225	0.00820	0.00539	0.00605
316	0.00258	0.00873	0.00513	0.00622
317	0.00249	0.00766	0.00504	0.00523
318	0.00216	0.00779	0.00456	0.00563
319	0.00220	0.00752	0.00461	0.00573
320	0.00270	0.00756	0.00466	0.00568
321	0.00280	0.00791	0.00492	0.00584
322	0.00244	0.00712	0.00484	0.00560
323	0.00229	0.00699	0.00489	0.00502
324	0.00227	0.00696	0.00475	0.00517
325	0.00207	0.00658	0.00419	0.00458
326	0.00230	0.00645	0.00366	0.00431
327	0.00183	0.00691	0.00406	0.00478
328	0.00215	0.00683	0.00419	0.00469
329	0.00180	0.00624	0.00395	0.00420
330	0.00208	0.00604	0.00397	0.00462
331	0.00217	0.00617	0.00388	0.00428
332	0.00177	0.00588	0.00348	0.00444
333	0.00256	0.00642	0.00439	0.00470
334	0.00209	0.00576	0.00346	0.00403
335	0.00182	0.00546	0.00334	0.00440
336	0.00198	0.00565	0.00358	0.00403
337	0.00132	0.00554	0.00339	0.00371
338	0.00178	0.00513	0.00331	0.00434
339	0.00227	0.00574	0.00397	0.00403
340	0.00203	0.00568	0.00364	0.00402
341	0.00227	0.00531	0.00353	0.00396
342	0.00281	0.00557	0.00362	0.00376
343	0.00128	0.00448	0.00264	0.00320
344	0.00198	0.00534	0.00320	0.00377
345	0.00164	0.00455	0.00304	0.00390

Wavelength (nm)	CO GW I	CO GW II	dilCO II	OH
346	0.00157	0.00510	0.00307	0.00388
347	0.00180	0.00481	0.00333	0.00375
348	0.00171	0.00461	0.00323	0.00367
349	0.00059	0.00432	0.00293	0.00337
350	0.00076	0.00351	0.00273	0.00268
351	0.00157	0.00372	0.00271	0.00253
352	-0.00111	0.00158	0.00038	0.00028
353	0.00273	0.00530	0.00393	0.00415
354	0.00121	0.00408	0.00269	0.00296
355	0.00131	0.00379	0.00240	0.00295
356	-0.00091	0.00205	0.00098	0.00074
357	0.00251	0.00488	0.00382	0.00372
358	0.00161	0.00392	0.00260	0.00279
359	0.00139	0.00377	0.00244	0.00297
360	0.00152	0.00382	0.00262	0.00269
361	0.00125	0.00367	0.00233	0.00293
362	0.00145	0.00373	0.00234	0.00256
363	0.00131	0.00347	0.00214	0.00250
364	0.00134	0.00355	0.00228	0.00238
365	0.00157	0.00366	0.00222	0.00262
366	0.00138	0.00362	0.00219	0.00263
367	0.00143	0.00341	0.00229	0.00248
368	0.00107	0.00320	0.00192	0.00202
369	0.00130	0.00310	0.00225	0.00231
370	0.00126	0.00284	0.00234	0.00223
371	0.00170	0.00365	0.00121	0.00251
372	0.00123	0.00309	0.00182	0.00203
373	0.00114	0.00290	0.00183	0.00224
374	0.00118	0.00283	0.00197	0.00222
375	0.00128	0.00290	0.00193	0.00206
376	0.00111	0.00298	0.00308	0.00198
377	0.00167	0.00342	0.00242	0.00261
378	0.00085	0.00231	0.00187	0.00185
379	0.00122	0.00288	0.00194	0.00181
380	0.00120	0.00286	0.00195	0.00213
381	0.00138	0.00281	0.00211	0.00202
382	0.00112	0.00279	0.00131	0.00202
383	0.00114	0.00270	0.00154	0.00171
384	0.00117	0.00267	0.00168	0.00184
385	0.00113	0.00284	0.00181	0.00200
386	0.00116	0.00264	0.00168	0.00145
387	0.00124	0.00282	0.00203	0.00191
388	0.00108	0.00281	0.00183	0.00184
389	0.00103	0.00241	0.00166	0.00156
390	0.00138	0.00268	0.00217	0.00185
391	0.00138	0.00258	0.00209	0.00177
392	0.00076	0.00226	0.00187	0.00137
393	0.00125	0.00242	0.00175	0.00171
394	0.00114	0.00238	0.00186	0.00181
395	0.00115	0.00225	0.00177	0.00181

Wavelength (nm)	CO GW I	CO GW II	dilCO II	OH
396	0.00118	0.00257	0.00186	0.00170
397	0.00100	0.00229	0.00167	0.00169
398	0.00122	0.00263	0.00169	0.00173
399	0.00125	0.00238	0.00176	0.00162
400	0.00083	0.00205	0.00128	0.00129
401	0.00131	0.00260	0.00169	0.00180
402	0.00120	0.00237	0.00177	0.00167
403	0.00091	0.00223	0.00170	0.00149
404	0.00109	0.00222	0.00130	0.00163
405	0.00107	0.00225	0.00134	0.00150
406	0.00093	0.00221	0.00091	0.00144
407	0.00109	0.00219	0.00127	0.00143
408	0.00111	0.00238	0.00145	0.00145
409	0.00108	0.00206	0.00144	0.00134
410	0.00091	0.00211	0.00147	0.00136
411	0.00121	0.00208	0.00145	0.00145
412	0.00109	0.00235	0.00145	0.00156
413	0.00109	0.00213	0.00155	0.00136
414	0.00096	0.00191	0.00130	0.00125
415	0.00109	0.00207	0.00146	0.00126
416	0.00117	0.00209	0.00162	0.00149
417	0.00104	0.00211	0.00137	0.00138
418	0.00076	0.00199	0.00137	0.00104
419	0.00112	0.00222	0.00133	0.00152
420	0.00087	0.00190	0.00132	0.00113
421	0.00114	0.00231	0.00146	0.00135
422	0.00111	0.00199	0.00144	0.00136
423	0.00103	0.00197	0.00141	0.00124
424	0.00103	0.00207	0.00148	0.00145
425	0.00102	0.00208	0.00165	0.00128
426	0.00098	0.00198	0.00143	0.00131
427	0.00119	0.00205	0.00133	0.00144
428	0.00102	0.00191	0.00127	0.00108
429	0.00085	0.00183	0.00116	0.00108
430	0.00087	0.00177	0.00125	0.00124
431	0.00144	0.00210	0.00167	0.00147
432	0.00144	0.00236	0.00182	0.00160
433	0.00126	0.00197	0.00171	0.00127
434	0.00091	0.00197	0.00174	0.00125
435	0.00124	0.00179	0.00182	0.00131
436	0.00098	0.00191	0.00154	0.00109
437	0.00093	0.00166	0.00162	0.00099
438	0.00093	0.00183	0.00173	0.00132
439	0.00071	0.00182	0.00141	0.00099
440	0.00076	0.00147	0.00120	0.00080
441	0.00062	0.00125	0.00129	0.00069
442	0.00083	0.00140	0.00155	0.00086
443	0.00070	0.00173	0.00121	0.00101
444	0.00091	0.00178	0.00122	0.00105
445	0.00101	0.00188	0.00143	0.00121

Wavelength (nm)	CO GW I	CO GW II	dilCO II	OH
446	0.00100	0.00176	0.00115	0.00115
447	0.00100	0.00174	0.00118	0.00104
448	0.00094	0.00178	0.00095	0.00106
449	0.00103	0.00172	0.00120	0.00102
450	0.00074	0.00141	0.00123	0.00093
451	0.00102	0.00175	0.00126	0.00125
452	0.00099	0.00171	0.00107	0.00093
453	0.00101	0.00185	0.00123	0.00099
454	0.00079	0.00165	0.00111	0.00097
455	0.00089	0.00170	0.00113	0.00086
456	0.00082	0.00162	0.00115	0.00093
457	0.00089	0.00161	0.00115	0.00096
458	0.00099	0.00168	0.00122	0.00120
459	0.00084	0.00160	0.00102	0.00066
460	0.00096	0.00161	0.00123	0.00094
461	0.00119	0.00169	0.00122	0.00116
462	0.00087	0.00175	0.00132	0.00102
463	0.00083	0.00138	0.00117	0.00075
464	0.00113	0.00173	0.00122	0.00110
465	0.00088	0.00163	0.00118	0.00090
466	0.00064	0.00145	0.00080	0.00090
467	0.00083	0.00151	0.00112	0.00096
468	0.00100	0.00171	0.00118	0.00094
469	0.00102	0.00157	0.00114	0.00088
470	0.00098	0.00159	0.00129	0.00108
471	0.00086	0.00175	0.00130	0.00096
472	0.00085	0.00152	0.00122	0.00086
473	0.00091	0.00174	0.00110	0.00095
474	0.00077	0.00155	0.00124	0.00082
475	0.00087	0.00141	0.00103	0.00066
476	0.00079	0.00160	0.00103	0.00083
477	0.00105	0.00159	0.00092	0.00106
478	0.00109	0.00179	0.00123	0.00126
479	0.00084	0.00157	0.00116	0.00078
480	0.00072	0.00147	0.00101	0.00080
481	0.00094	0.00143	0.00116	0.00093
482	0.00091	0.00172	0.00122	0.00104
483	0.00089	0.00151	0.00103	0.00089
484	0.00099	0.00152	0.00117	0.00086
485	0.00117	0.00175	0.00114	0.00088
486	0.00099	0.00159	0.00085	0.00092
487	0.00089	0.00150	0.00104	0.00085
488	0.00096	0.00148	0.00102	0.00084
489	0.00107	0.00142	0.00097	0.00081
490	0.00090	0.00152	0.00088	0.00066
491	0.00093	0.00159	0.00124	0.00086
492	0.00085	0.00155	0.00094	0.00072
493	0.00092	0.00153	0.00114	0.00092
494	0.00082	0.00139	0.00100	0.00082
495	0.00078	0.00151	0.00105	0.00078

Wavelength (nm)	CO GW I	CO GW II	dilCO II	OH
496	0.00095	0.00146	0.00105	0.00079
497	0.00091	0.00141	0.00095	0.00091
498	0.00088	0.00155	0.00115	0.00085
499	0.00094	0.00149	0.00092	0.00082
500	0.00077	0.00132	0.00101	0.00079
501	0.00077	0.00142	0.00117	0.00099
502	0.00085	0.00146	0.00115	0.00104
503	0.00095	0.00159	0.00109	0.00090
504	0.00069	0.00129	0.00091	0.00053
505	0.00110	0.00161	0.00090	0.00085
506	0.00101	0.00166	0.00102	0.00104
507	0.00079	0.00138	0.00106	0.00077
508	0.00072	0.00149	0.00093	0.00088
509	0.00085	0.00159	0.00095	0.00075
510	0.00102	0.00156	0.00102	0.00080
511	0.00105	0.00156	0.00127	0.00090
512	0.00084	0.00138	0.00090	0.00064
513	0.00093	0.00143	0.00104	0.00076
514	0.00099	0.00147	0.00125	0.00094
515	0.00084	0.00146	0.00117	0.00094
516	0.00099	0.00162	0.00118	0.00089
517	0.00067	0.00136	0.00091	0.00073
518	0.00064	0.00125	0.00076	0.00076
519	0.00129	0.00183	0.00133	0.00129
520	0.00110	0.00172	0.00122	0.00094
521	0.00121	0.00173	0.00131	0.00117
522	0.00097	0.00153	0.00097	0.00085
523	0.00092	0.00152	0.00109	0.00081
524	0.00091	0.00158	0.00123	0.00110
525	0.00084	0.00138	0.00103	0.00093
526	0.00082	0.00136	0.00084	0.00078
527	0.00060	0.00124	0.00081	0.00075
528	0.00057	0.00117	0.00074	0.00058
529	0.00096	0.00151	0.00109	0.00080
530	0.00086	0.00146	0.00090	0.00073
531	0.00101	0.00140	0.00097	0.00092
532	0.00068	0.00136	0.00095	0.00063
533	0.00102	0.00158	0.00117	0.00094
534	0.00092	0.00151	0.00111	0.00088
535	0.00078	0.00121	0.00094	0.00069
536	0.00105	0.00141	0.00105	0.00093
537	0.00100	0.00153	0.00105	0.00072
538	0.00089	0.00137	0.00110	0.00085
539	0.00083	0.00139	0.00094	0.00071
540	0.00103	0.00152	0.00112	0.00102
541	0.00072	0.00118	0.00090	0.00071
542	0.00091	0.00132	0.00087	0.00088
543	0.00093	0.00148	0.00100	0.00088
544	0.00089	0.00144	0.00104	0.00083
545	0.00087	0.00144	0.00088	0.00071

Wavelength (nm)	CO GW I	CO GW II	dilCO II	OH
546	0.00070	0.00123	0.00078	0.00061
547	0.00090	0.00140	0.00113	0.00072
548	0.00088	0.00128	0.00081	0.00061
549	0.00078	0.00142	0.00102	0.00087
550	0.00083	0.00141	0.00106	0.00067
551	0.00105	0.00146	0.00107	0.00089
552	0.00090	0.00151	0.00103	0.00085
553	0.00075	0.00135	0.00084	0.00072
554	0.00073	0.00120	0.00080	0.00060
555	0.00093	0.00120	0.00093	0.00061
556	0.00068	0.00105	0.00090	0.00075
557	0.00092	0.00137	0.00094	0.00084
558	0.00098	0.00141	0.00100	0.00099
559	0.00067	0.00108	0.00083	0.00080
560	0.00092	0.00135	0.00103	0.00074
561	0.00099	0.00151	0.00113	0.00085
562	0.00089	0.00116	0.00101	0.00066
563	0.00087	0.00148	0.00112	0.00103
564	0.00085	0.00153	0.00080	0.00081
565	0.00062	0.00133	0.00077	0.00064
566	0.00096	0.00151	0.00114	0.00087
567	0.00067	0.00117	0.00071	0.00047
568	0.00079	0.00133	0.00088	0.00088
569	0.00120	0.00133	0.00103	0.00094
570	0.00054	0.00112	0.00068	0.00062
571	0.00076	0.00128	0.00079	0.00052
572	0.00074	0.00119	0.00094	0.00066
573	0.00082	0.00110	0.00094	0.00047
574	0.00063	0.00123	0.00083	0.00056
575	0.00086	0.00140	0.00098	0.00078
576	0.00064	0.00108	0.00075	0.00062
577	0.00088	0.00113	0.00075	0.00060
578	0.00058	0.00094	0.00073	0.00056
579	0.00083	0.00125	0.00101	0.00075
580	0.00074	0.00115	0.00086	0.00068
581	0.00087	0.00124	0.00091	0.00071
582	0.00086	0.00119	0.00077	0.00048
583	0.00086	0.00117	0.00087	0.00078
584	0.00098	0.00145	0.00106	0.00075
585	0.00093	0.00137	0.00096	0.00071
586	0.00090	0.00133	0.00082	0.00072
587	0.00074	0.00118	0.00089	0.00068
588	0.00067	0.00128	0.00077	0.00055
589	0.00078	0.00123	0.00091	0.00063
590	0.00095	0.00128	0.00096	0.00073
591	0.00074	0.00108	0.00062	0.00034
592	0.00063	0.00102	0.00077	0.00066
593	0.00053	0.00107	0.00054	0.00062
594	0.00079	0.00131	0.00089	0.00063
595	0.00075	0.00117	0.00081	0.00065

Wavelength (nm)	CO GW I	CO GW II	dilCO II	OH
596	0.00048	0.00118	0.00063	0.00052
597	0.00085	0.00125	0.00088	0.00054
598	0.00079	0.00116	0.00079	0.00066
599	0.00067	0.00094	0.00055	0.00037
600	0.00084	0.00115	0.00084	0.00055

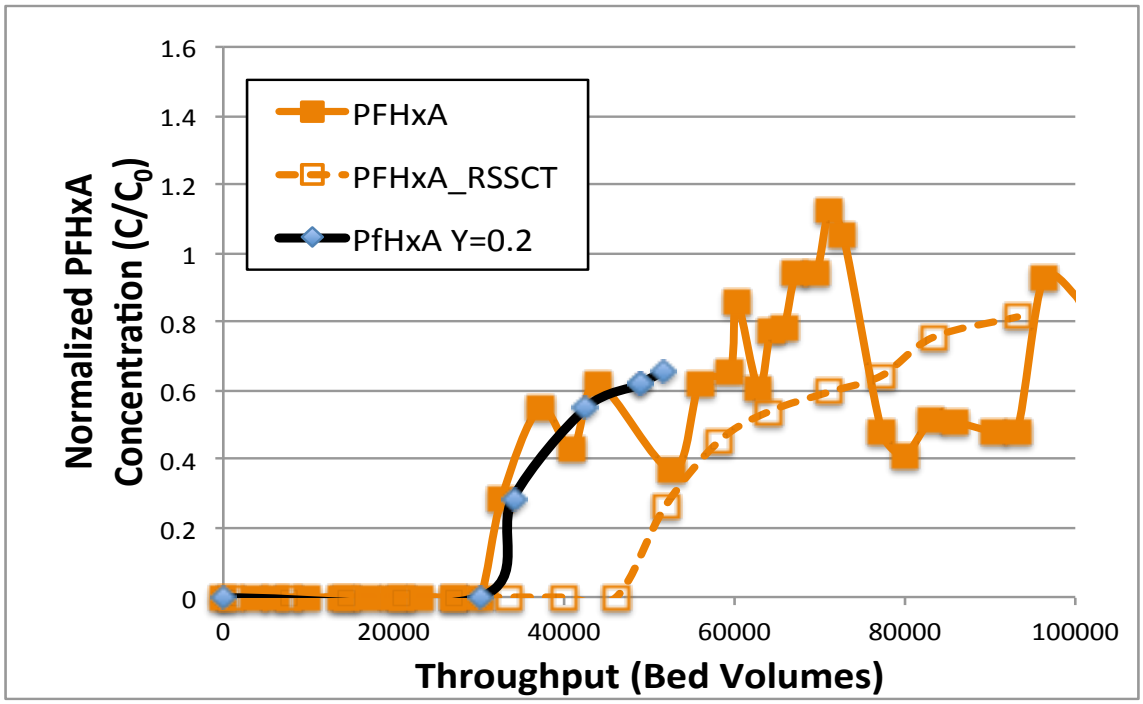

Figure_D.1 Visual FI applied to PFHxA RSSCT breakthrough curve. Y = 0.2. FI used to match full-scale capacity at 50% breakthrough. EBCT: 13 min.

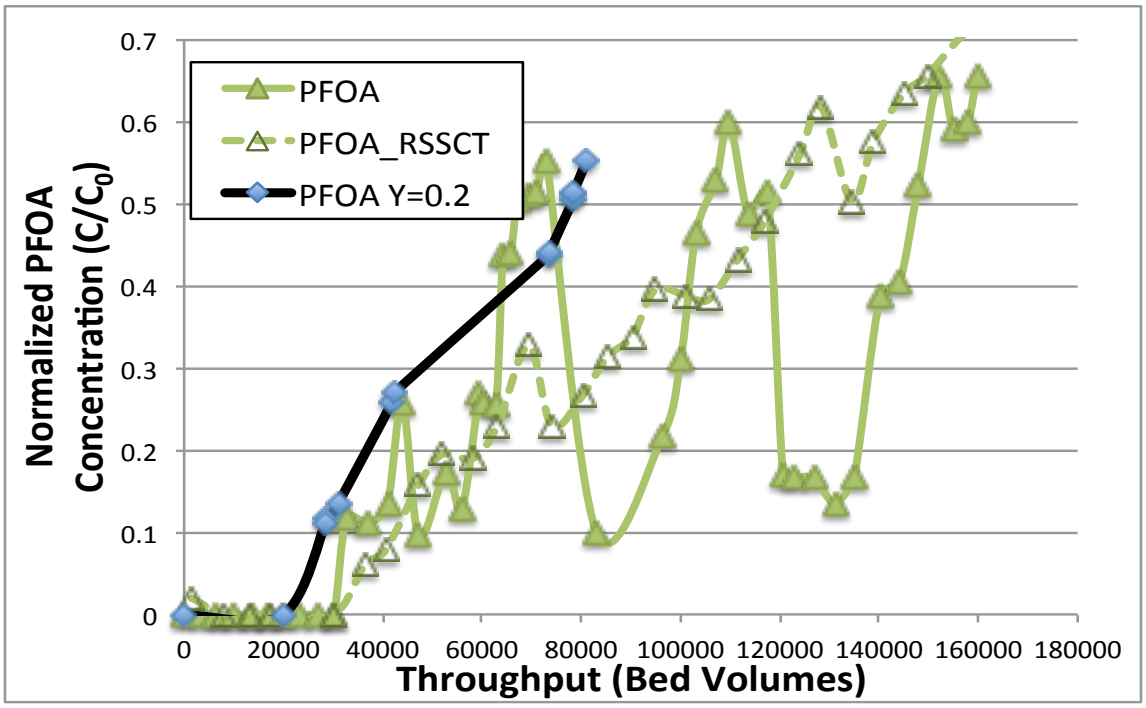

Figure_D.2 Visual FI applied to PFOA RSSCT breakthrough curve. Y = 0.2. FI used to match full-scale capacity at 50% breakthrough. EBCT: 13 min.

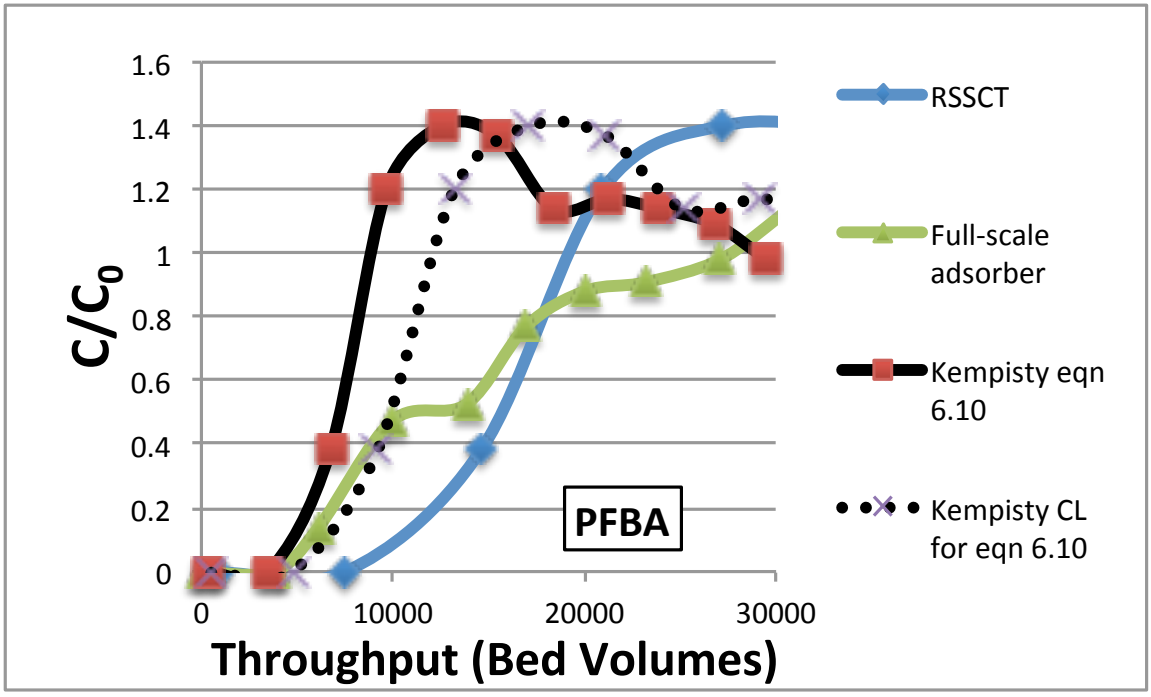

Figure_D.3 Fouling index applied to PFBA RSSCT using Y value predicted from C_0/TOC_0 regression (equation 6.10); EBCT:13 min.

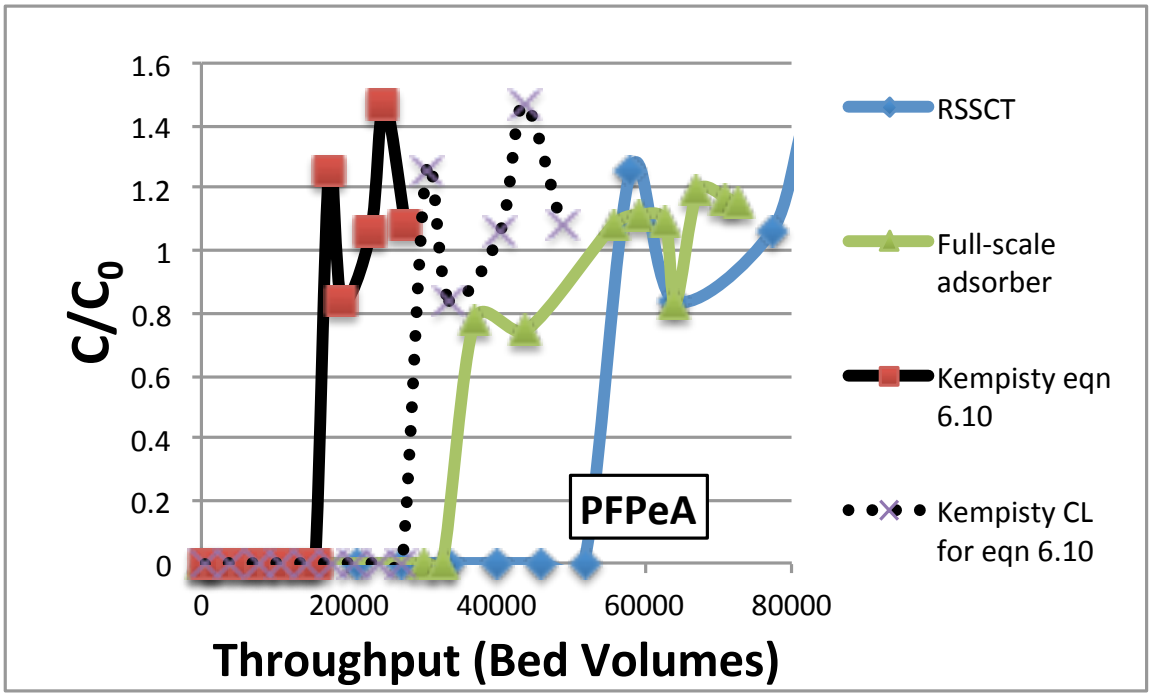

Figure_D.4 Fouling index applied to PFPeA RSSCT using Y value predicted from C_0/TOC_0 regression (equation 6.10); EBCT:13 min.

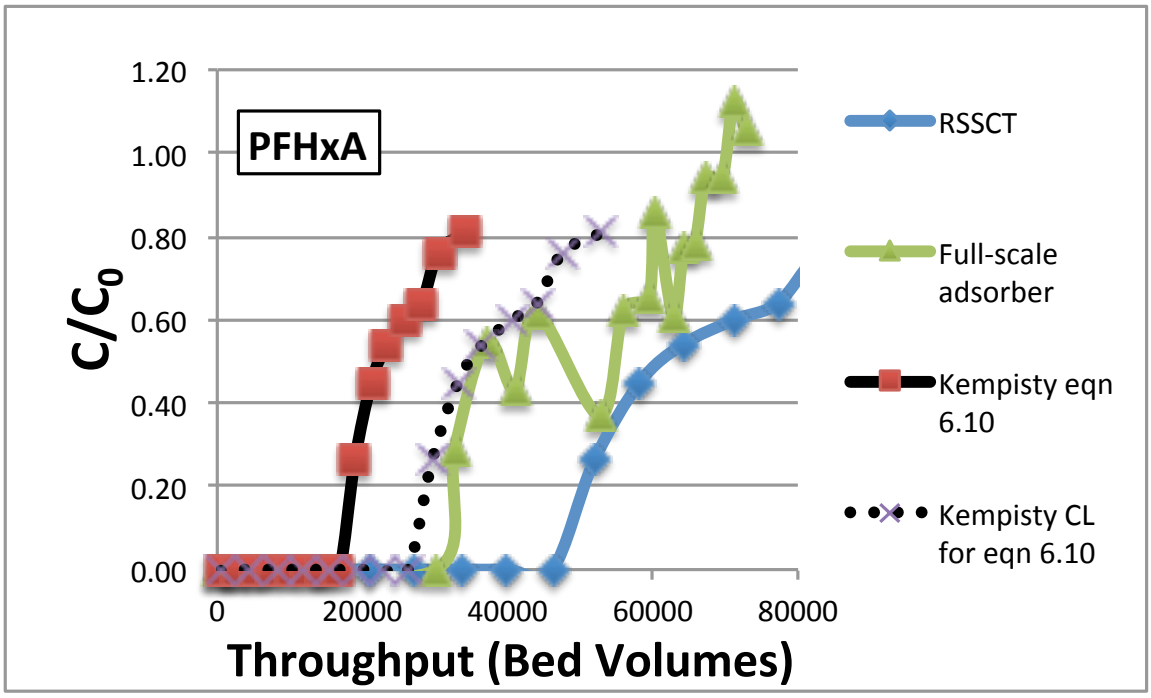

Figure_D.5 Fouling index applied to PFHxA RSSCT using Y value predicted from C_0/TOC_0 regression (equation 6.10); EBCT:13 min.

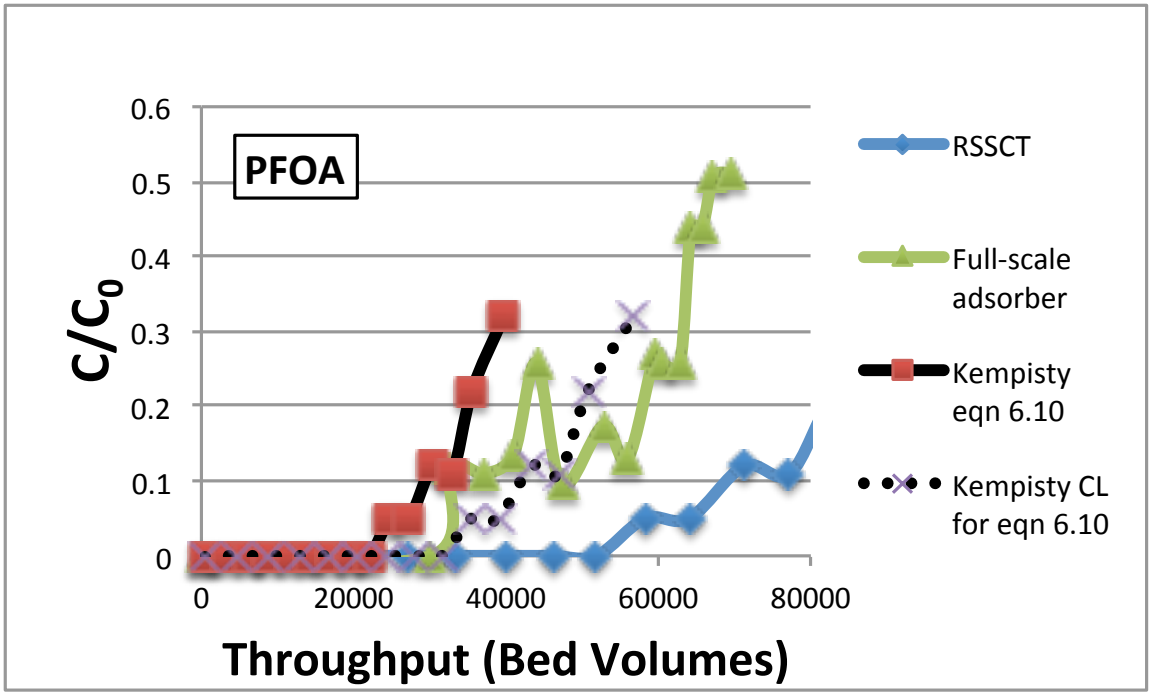

Figure_D.6 Fouling index applied to PFOA RSSCT using Y value predicted from C_0/TOC_0 regression (equation 6.10); EBCT:13 min.